Faculty of Biology, Ludwig-Maximilians University of Munich

In vivo modulation of integrin linked kinase

using transgenic mice

Thesis for the attainment of the doctoral degree

From the Faculty of Biology, Ludwig-Maximilans University, Munich

By

Chiraz El-Aouni

Tunesia, 2006

Fakultät für Biologie der Ludwig-Maximilian-Universität

München

In vivo modulation of integrin linked kinase
using transgenic mice

Dissertation der Fakultät für Biologie der Ludwig-Maximilians-Universität

München Zur Erlangung des Dr.rer.nat.

Vorgelegt von

Chiraz El-Aouni

Tunesien, 2006

Erklärung

Diese Dissertation wurde im Sinne von § 13 Abs. 3 bzw. 4 der Promotionsordnung vom 29. Januar 1998 von Herrn Prof. Dr. Matthias betreut.

Ehrenwörtliche Versicherung

Ich versichere hiermit ehrenwörtlich, dass die Dissertation von mir selbstständig, ohne unerlaubte Hilfe angefertigt ist.

München, am   20.03.2006

Chiraz El-Aouni

Dedicated to my mama

Table of contents

<u>Abbreviations</u>

AP	alkaline phosphatase
APS	ammonium persulfate
bp	base pair
BSA	bovine serum albumin
cDNA	complementary deoxyribonucleic acid
cm	centimeter
CRE	cyclization recombination
DMEM	dulbecco's modified eagle's medium
DNA	deoxyribonucleic acid
dNTP	deoxyribonucleoside triphosphate
ECM	extracellular matrix
E. coli	*Escherichia coli*
ELISA	enzyme linked immunosorbent assay
ES cells	embryonic stem cells
FCS	foetal calf serum
g	gram
GFP	green fluorescent protein
GH	growth hormone
GSK3	glycogen synthase kinase 3
h	hour
HE	hematoxylin-eosin
HRP	horseradish peroxidase
IHC	immunohistochemistry
IgG	immunoglobin G
kDa	kilo dalton
kb	kilo base
l	liter
LB	Luria Broth
M	molar
mA	milliampere
mg	milligram
min	minute
ml	millimeter
mM	millimolar
mRNA	messenger ribonucleic acid
nm	nanometer

ng	nanogram
PAGE	polyacrylamide gel electrophoresis
PAS	periodic-acid-schiff
PBS	phosphate buffered saline
PFA	paraformaldehyde
PCR	polymerase chain reaction
pg	picogram
RNA	ribonucleic acid
rpm	revolution per minute
RT	room temperature
RT-PCR	reverse transcription polymerase chain reaction
s	second
SD	standard deviation
SlD	slit diaphragm
SDS	sodium dodecyl sulphate
SEM	scanning electron microscopy
TBS	Tris-buffered saline
TBE	Tris- Boric acid- EDTA
TEM	transmission electron microscopy
UV	ultraviolet
μg	microgram
μl	microliter
μm	micrometer
WT	wild-type
WT-1	Wilms tumor-1 antigene

Introduction

1. <u>Introduction</u>

1.1. <u>The kidney</u>

The kidneys are a pair of bean-shaped organs in the paravertebral retroperitoneum. They are protected by three layers of connective tissue: the renal fascia, a fibrous membrane, surrounds the kidney and binds the organ to the abdominal wall; the adipose capsule, a layer of fat, cushions the kidney; and the renal capsule, a fibrous sac, surrounds the kidney and protects it from trauma and infection.

The kidney has three critical functions: (1) to clear the blood of nitrogenous and other waste metabolic products by filtration and excretion; (2) to balance the concentration of body fluids and electrolytes; (3) to recover by reabsorption small molecules (amino acids, glucose, and peptides), ions (Na+, Cl-, Ca2+, PO-), and water, in order to maintain blood homeostasis by producing urine. The urine is produced glomerular filtration followed by tubular reabsorption and secretion (Kierszenbaum, 2002).

The urinary system consists of paired kidneys and ureters and a single urinary bladder and urethra. Each kidney has an external cortex and an internal medulla. The cortex is divided into inner and outer regions. The medulla is formed by conical masses, the medullary pyramids. A medullary pyramid together with the associated covering cortical region, constitutes a renal lobe.

The renal artery enters the kidney and the renal vein emerges from the kidney at an indentation in the middle of the organ called the hilum. The renal artery supplies oxygen and blood to the kidney. The blood flows from the kidney through the renal vein after waste products have been removed.

The kidneys receive about 20% of the cardiac output per minute and filter about 1.25 l of blood per minute. Essentially, all the blood of the body passes through the kidneys every 5 minutes. About 180 l of glomerular ultrafiltrate are produced in 24 hours and transported through the uriniferous tubules. Of this amount, 178.5 l are recovered by the tubular cells and returned to the blood circulation, whereas only 1.5 l are excreted as urine (Tisher *et al.*, 1991).
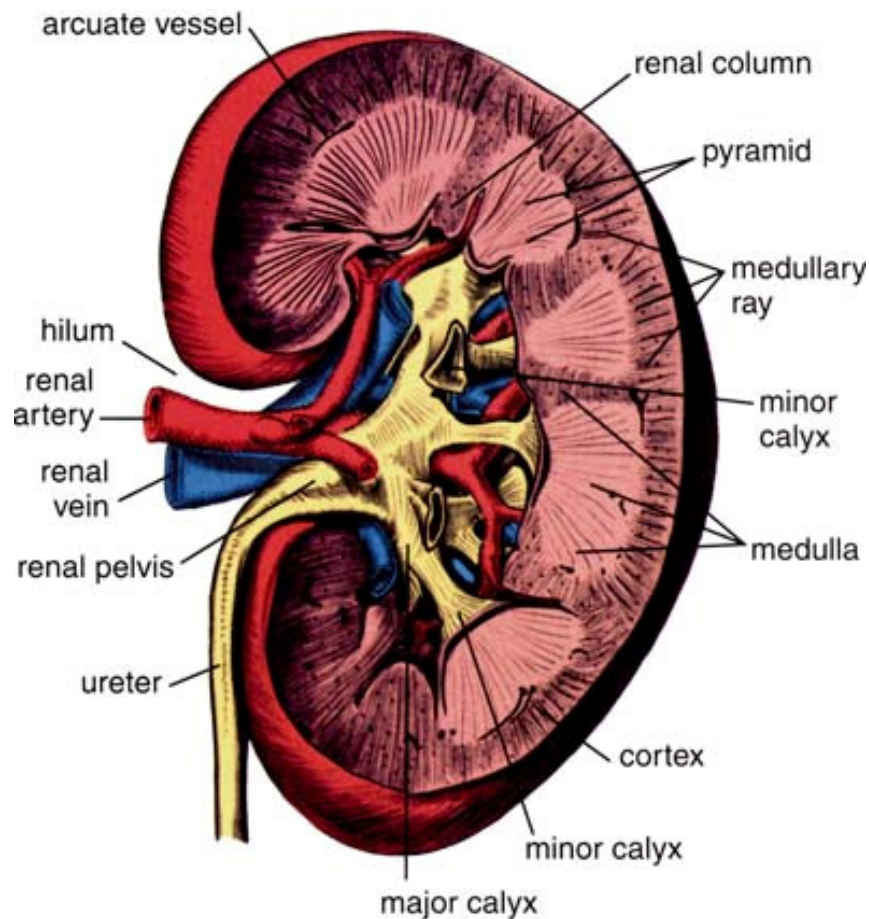
Figure 1 : Cross section of the kidney.

This normal adult kidney demonstrates the lighter outer cortex and the darker medulla, with the renal pyramids into which the collecting ducts coalesce and drain into the calyces and central pelvis. (Source: anatomy.iupui.edu/courses/histo_D502/D502f04/lecture.f04/urinaryf04/urinaryf04.html).

The generation of urine occurs in the basic units of the kidney, called nephrons. Each human kidney contains over 1 million nephrons. Nephrons consist of a network of capillaries, a glomerulus, a renal tubule, and a membrane that surrounds the glomerulus and functions as filter, called Bowman's capsule. The glomeruli are where urine production begins with the ultrafiltration of plasma. Urine formation occurs in the renal tubules, which travel from the outer tissue of the kidney, the cortex, to the inner tissue, the medulla, and return to the cortex.

Detailed structure of a nephron

Bowman's capsule
Glomerulus
Proximal tubule
Arteriole from renal artery
Distal tubule
Arteriole from glomerulus
Branch of renal vein
From another nephron
Collecting duct
Loop of Henle with capillary network
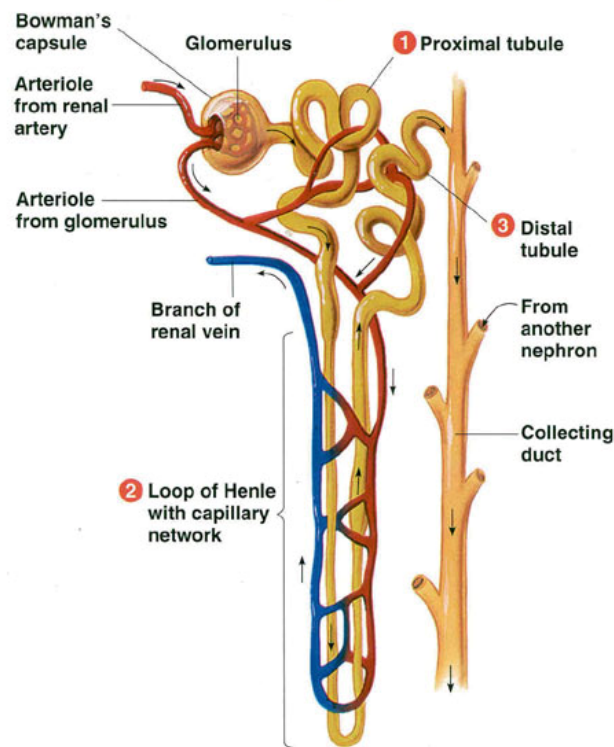
Figure 2: the nephron.

It is a tiny tubule consisting of a cluster of capillaries called the glomerulus, surrounded by a hollow bulb known as Bowman's capsule. Bowman's capsule leads into a long, convoluted tubule consisting of four sections: the proximal tubule, loop of Henle, distal tubule, and collecting duct. The collecting ducts empty into the central cavity of the kidney, the renal pelvis, which connects to the ureter. Each human kidney has about a million nephrons. (Source: forum.myspace.com).

1.1.1. <u>The glomerular filtration barrier</u>

The glomerulus is a specialized filtration unit of the kidney. Its function is to provide a molecular sieve for blood plasma so that low molecular waste products are excreted into the urine, while essential macromolecules, such as plasma proteins, are retained in the blood. About 150-180 L plasma are filtered every day in the kidney. Most of the primary urine is reabsorbed. Since less than 40 mg albumin is normally excreted with urine each day. Golmeruli are efficient filters in restricting protein transfer into the primary urine.
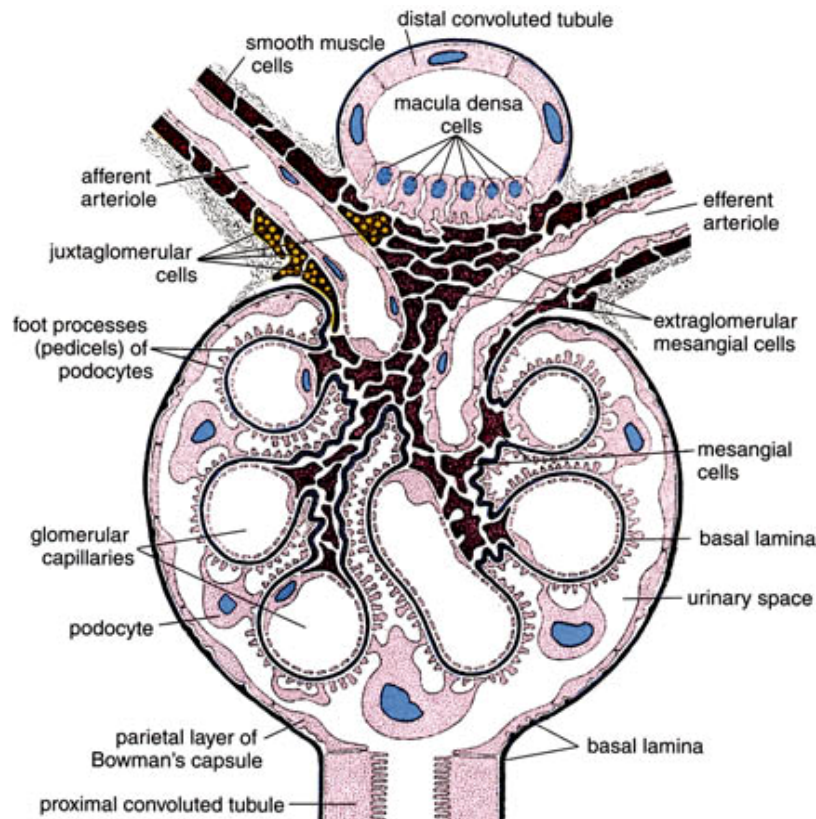
Figure 3: Glomerulus.

The capillaries are fenestrated without diaphragms, the thick basal lamina are produced by both endothelial cells of capillaries and podocytes that wrap around 10-20 capillary loops. The blood enters glomerulus at the afferent arteriole, passes through glomeruli capillaries then exits at the efferent arteriole. Both afferent and efferent arteriole are located at the vascular pole of the renal corpuscle. (Source: anatomy.iupui.edu/courses/histo_D502/ D502f04/lecture.f04/urinaryf04/urinaryf04.html).

The glomerular filtration barrier of the capillary walls is comprised of a complex structural arrangement of three elements: a fenestrated endothelium, the glomerular basement membrane (GBM), and highly specialized visceral epithelial cells, named podocytes, where the foot processes cover the outer surface of the GBM (Kritz *et al.*, 1996a, 1996b).

In the human kidney, the diameter of the endothelial fenestrae ranges from 70 to 100 nm which permits direct contact between blood plasma and the GBM, so the endothelium does not seem to represent a direct passage of macromolecules.

1.1.2. <u>Glomerular basement membrane</u>

The GBM is composed of a unique combination of laminins (laminin 11, α5, β2, γ1 chains), collagen IV (α3, α4 and α5), entactin/ perlecan and proteoglycans (Miner, 1999). These components provide the GBM with unique compositional and functional characteristics found nowhere else in the body. The complex inter- and intramolecular interactions of these molecules make the GBM a unique permeable scaffold that provides the capillary wall with tension strength and flexibility. Detachment of podocyte foot processes from the GBM is a key step in foot process retraction and podocyte loss, leading eventually to glomerulosclerosis. Attachment of the podocyte to the GBM is mediated by molecules that include α3 β1- integrin heterodimers and β-dystroglycan. These molecules provide a dynamic link between cell and matrix, which allows both a link to the actin cytoskeleton in the foot process.
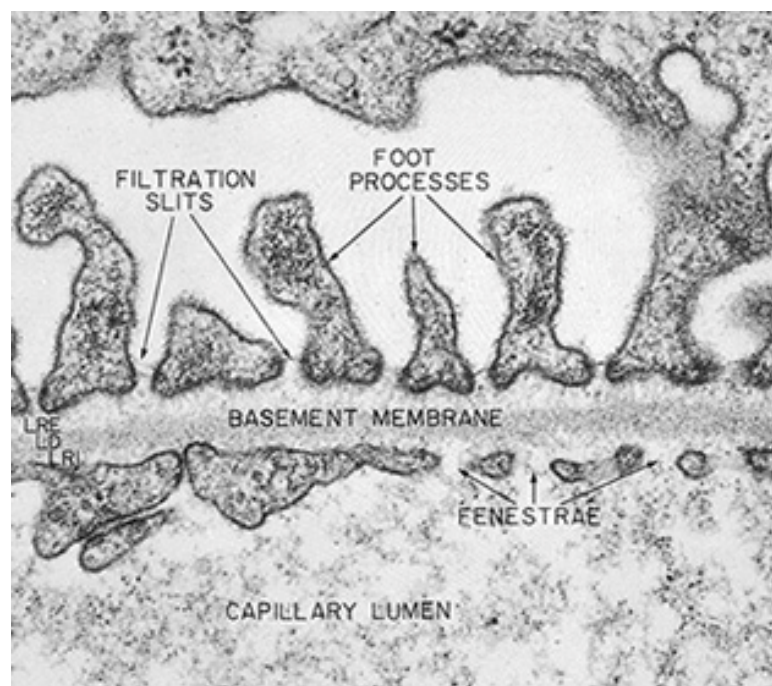
Figure 4: Transmission electron micrograph of the glomerular filtration barrier.

Detail of end feet of podocyte on the basement membrane. The basement membrane (basal lamina) is continuous, but the fenestrated capillary endothelium has pores. Glomerular filtrate passes from the capillary lumen, through the layers seen here, into the lumen of Bowman's capsule (where the foot processes are lying). Between the foot processes are thin slit membranes. (Source: cmm.ucsd.edu)**.**

1.1.3. <u>Podocyte</u>

Podocytes are unique cells with a complex cellular organization and cytoarchitecture. Podocytes or visceral glomerular epithelial cells are attached to the outer aspect of the glomerular basement membrane. They are highly differentiated and divided structurally and functionally into three differents segments: cell body, major processes, and foot processes.

Figure 5: Scanning electron microscope (SEM) micrograph of a glomerular podocyte as seen from the urinary space.

The large cell body sends out thick primary processes that futher ramify into fine secondary (foot) processes that interdigitate with foot processes from adjacent podocytes. Under the foot processes is the glomerular basement membrane that surrounds the glomerular capillary (not visible in this view, source: Benninghof: Lehrbuch der Anatomie: W. Kriz: Die Niere).

The cell bodies and major processes are generally not directly attached to the GBM, but are rather "free floating" in the filtrate in Bowman's space. In contrast, the foot processes cover the outer aspect of the GBM and interdigitate with foot processes of neighboring cells (Mundel and Kriz, 1995). The latter are connected by a specialized cell-cell junction, the glomerular slit diaphragm, which represents the main size-selective filter barrier in the kidney (Endlich *et al.*, 2001).
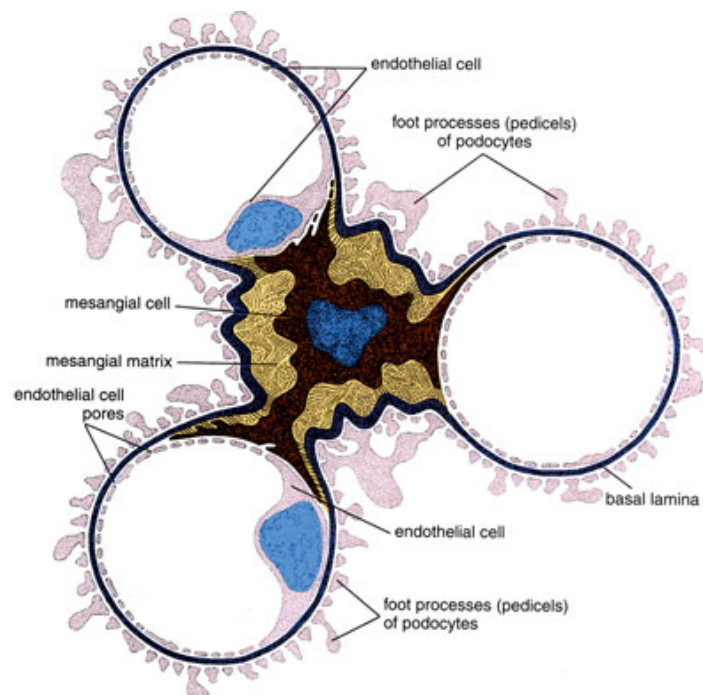
Figure 6: The renal glomerulus.

The glomerular filtration barrier consists of podocytes and fenestrated endothelium. Mesangial cells sit between capillary loops. Poodcytes are the largest cells in the glomerulus, possessing long cytoplasmic processes which in turn divide into numerous secondary foot processes that cover the outer aspect of the GBM. Normal Podocyte Structure. (Source: anatomy.iupui.edu/courses/histo_D502/D502f04/lecture.f04/urinaryf04/urinaryf04.html).

Podocytes are injured in many forms of human and experimental glomerular disease, including minimal-change disease (MCD), focal segmental glomerulosclerosis (FSGS), collapsing glomerulopathy, diabetic nephropathy, membranous glomerulopathy, crescentic glomerulonephritis, and lupus nephritis (Eddy and Schnaper, 1998; Somlo and Mundel, 2000). The early events are characterized by alterations in foot process and slit diaphragm configuration, with loss of foot processes and loss of slit diaphragm integrity. Foot process effacement and fusion are associated with the onset of proteinuria (Whiteside *et al.*, 1993) and are accompanied by a reorganization of the actin cytoskeleton into a dense network (Shirato *et al.*, 1996). However, the molecular mechanisms causing these morphological alterations of podocyte foot processes are poorly understood and remain an active area of ongoing research (Smoyer *et al.*, 1997).

1.1.3.1. The sole of the podocyte foot process

The basal membrane domain of foot processes contains several adhesion proteins that link podocytes to the extracellular matrix. These proteins encountered at this domain also form specialized, interconnected complex. The integrin $\alpha3\beta1$ localized to the soles of foot processes (Kerjaschki *et al.*, 1989), is essential for the maturation of podocyte.

Dystroglycan is also found at the sole of the podocyte's foot. Dystroglycan is heterodimeric protein composed of a transmembrane component, the beta subunit, and an extracellular component, the alpha subunit. Dystroclycans are connected to the actin-based cytoskeleton through utrophin. Both integrins and dystroglycans are coupled to the podocyte actin cytoskeleton (Barisoni and Mundel, 2003).

1.1.3.2. Podocyte proteins

Several podocyte proteins are located in the foot process. Foot processes contain an elaborate and dynamic actin-based cytoskeleton. This structure maintains the normal architecture of foot processes, including the proper positioning of transmembrane proteins and the slit diaphragms. The major molecular components of the podocyte are actin, α-actinin-4, podocin, ZO-1(Andrews, 1981; Akhtar and Al Mana, 2004), and synaptopodin (Mundel *et al.*, 1997).

CD2-associated protein (CD2AP) is an 80-kDa cytoplasmic protein expressed in all tissues. The protein has been localized by immunoelectron microscopy to the lateral wall of the foot process in close proximity to the insertion of nephrin (Yuan *et al.*, 2002a). Several recent studies reveal a direct interaction between podocin, nephrin, and CD2AP; moreover, CD2AP interacts with actin, indicating a close relationship between the cytoskeletal structure and the configuration of the slit diaphragm (Yuan *et al.*, 2002b).

Podocin is a protein that is exclusively expressed in the podocyte and seems to play a role in controlling the permeability of the filtration barrier, at the level of the slit diaphragm. Podocin localizes to the podocyte foot process membrane, at the insertion site of the slit diaphragm where it binds to the cytoplasmic tail of nephrin and CD2AP (Barisoni and Mundel, 2003).

Alpha-actinin-4 is another podocyte protein that binds with cytoskeleton proteins, especially filamentous actin. It is a widely expressed protein, and only one of four isoforms is significantly

expressed in podocytes. It interacts with a large number of cytoskeletal cell surfaces and signaling. One important podocyte marker is WT1, a tumor-suppressor gene that is widely expressed in epithelial cells of early nephron and is restricted to podocytes in the mature glomeruli (Akhtar and Al Mana, 2004).
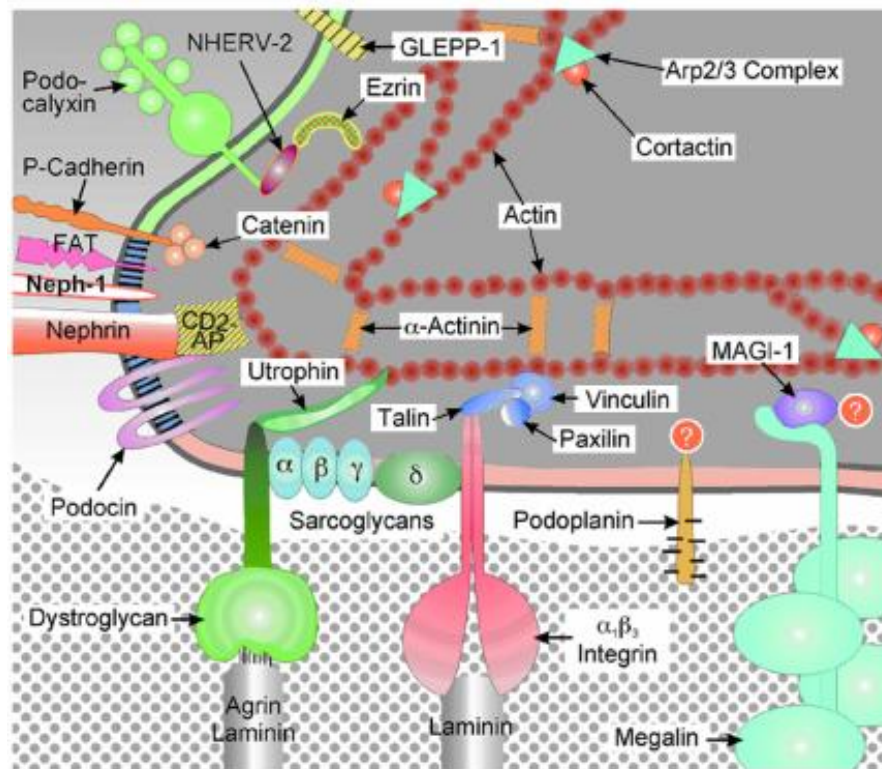
Figure 7: Schematic drawing of a latero-basel portion of a podocyte.

In this greatly simplified graph, molecules are not draw to a correct scale or shape. Intracellulary, nephrin interacts directly with CD2AP and possibly also podocin. Actin filaments are cross-linked and stabilized by α-actinin-4. Mutations in nephrin, CD2AP or podocin lead to proteinuria and nephritic syndrome, while mutations in α-actinin-4 lead to focal segmental glomerulorsclerosis (Kerjaschki, 2001).

Zona occludens (ZO) 1 is located on foot process at the point of insertion of slit diaphragms (Schnabel *et al.*, 1990). ZO-1 interacts with the actin-based cytoskeleton and may also have an important role in regulating the function of the slit diaphragm (Reiser *et al.*, 2000a).

Synaptopodin is an actin-associated protein of glomerular podocytes and telencephalic dendrites (Mundel *et al.*, 1991) without significant homology to any known protein. In both brain and kidney, *in vivo* and *in vitro*, synaptopodin gene expression is differentiation-dependent (Mundel *et al.*, 1997).

1.1.3.3. The slit diaphragm

The slit diaphragms are thin structures connecting interdigitated podocyte foot processes along the glomerular basement membrane. The slit diaphragm is a complex of proteins located in the extracellular space, and measuring 30- 40 nm in lengh (Tryggvason and Wartiovaara, 2001). Rodewald and Karnovsky showed 30 years ago that the slit diaphragm is made up of rod-like units connected in the center to a linear bar, forming zipper-like pattern. Several novel podocyte proteins and their mutation analysis, including mFat1 (Ciani *et al.*, 2003), the nephrin homologue Neph1 (Donoviel *et al.*, 2001), nephrin (Kestila *et al.*, 1998), CD2-associated protein (CD2AP) (Shih *et al.*, 1999), and podocin (Boute *et al.*, 2000), have emphasized the critical role of the slit diaphragm in maintaining the normal function of the glomerular filtration barrier.

1.2. <u>Glomerular disease and podocyte</u>

Glomerular diseases damage the glomeruli, letting protein and sometimes red blood cells leak into the urine. Sometimes a glomerular disease also interferes with the clearance of waste products by the kidney, so they begin to build up in the blood. Furthermore, loss of blood proteins like albumin in the urine can result in a fall in their serum level.

A number of different diseases can result in glomerular disease. It may be the direct effect of an infection or a drug toxic to the kidneys, or it may be the result from a disease that affects the entire body, like diabetes or lupus. Many different kinds of diseases can cause swelling or scarring of the nephron or glomerulus.

A number of glomerular disorders that may lead to chronic kidney disease are characterized by simplification and retraction of podocyte foot processes (FP) (Reiser *et al.*, 2002). FP effacement requires a precise interplay of multiple cellular functions including structural alterations of the cytoskeleton, movement of FP over the basement membrane, and reconstruction of the slit diaphragm (Somlo and Mundel, 2000). Podocytes are injured in many forms of human and experimental glomerular disease, including minimal change disease, focal segmental glomeruloschlerosis, diabetes mellitus and lupus nephritis (Somlo and Mundel, 2000; Endlich *et al.*, 2001; Kerjaschki, 2001).

Podocyte injury leads to severe progressive glomerular disease (Mundel and Shankland, 1999). Early podocyte manifestations of injury include vacuolization, pseudocyst formation, and detachment from the GBM, resulting in podocyte depletion (Barisoni and Mundel, 2003). The

discovery of several novel podocyte proteins and their mutation analysis including nephrin (Kestila *et al.*, 1998), CD2AP (Shih *et al.*, 1999), α-actinin-4 (Kaplan *et al.*, 2000) and podocin (Boute *et al.*, 2000) have shed light on the pathogenesis of FP effacement and proteinuria and emphasized the critical role of podocyte FP and the slit diaphragm in maintaining the function of the glomerular filtration barrier (Reiser *et al.*, 2004).

As discussed above, the form of acquired glomerular disease in which podocyte dysfunction is most clearly implicated is minimal change and FSGS. Other causes of renal diseases excluding those that involve altered podocyte function are reviewed below.

1.2.1. <u>IgA nephropathy</u>

IgA nephropathy is an inflammatory glomerular disease with immunoglobulin A (IgA) deposition in the glomeruli. The most common symptom of IgA nephropathy is hematuria, but it is often a silent disease that may go undetected for many years. It appears to affect men more often than women. Although IgA nephropathy is found in all age groups, young people rarely display signs of kidney failure because the disease usually takes several years to progress to the stage where it causes detectable complications.

1.2.2. <u>Hereditary nephritis- Alport syndrome</u>

The primary indicator of Alport syndrome is a family history of chronic glomerular diseases, but it may also involve hearing or vision impairment. Alport syndrome is characterized by irregular thinning, thickening and splitting of the glomerular basal lamina. The X-linked dominant version of the syndrome affects only men, the autosomal disease both men and women. Men with Alport syndrome usually first show evidence of renal insufficiency while in their twenties and reach the end stage renal disease by age 40. Autosomal disease course can vary with many women rarely showing significant renal impairment, and hearing loss may be so slight that can be detected only through testing with special equipment.

1.2.3. <u>Diabetic nephropathy</u>

Diabetic nephropathy is the leading cause of end stage renal disease in the Western world. Kidney disease is one of several problems caused by prolonged elevation in blood glucose, the central feature of diabetes. Diabetic nephropathy is typically defined by either macroalbuminuria

or by abnormal renal function as represented by an abnormality in serum creatinine or glomerular filtration rate. Renal disease is suspected to be secondary to diabetes in the clinical setting of long-standing diabetes. The natural history of diabetic nephropathy is a process that progresses gradually over years. Early diabetes is heralded by glomerular hyperfiltration and an increase in glomerular filtration rate. This is thought to be related to increased cell growth and expansion in the kidney, possibly mediated by hyperglycemia itself. In addition to directly damaging the kidney, elevated glucose levels appear to increase the renal blood flow, putting an additional strain on the filtering glomeruli.

1.2.4. <u>Glomerulosclerosis and Focal Segmental Glomerulosclerosis</u>

Glomerulosclerosis refers to scarring (sclerosis) of the glomeruli in the kidneys. This scarring impairs kidney function and may lead to kidney failure. In several sclerotic conditions, a systematic disease like lupus or diabetes mellitus is responsible. Glomerulosclerosis is caused by the activation of glomerular cells. This may be stimulated by growth factors, which may be produced by glomerular cells themselves or may be brought the glomerulus by the circulating blood. Early stages of glomerulosclerosis may not cause any symptoms. The most important warning sign of glomerular disease is proteinuria. However, the loss of large amounts of protein can result in the nephrotic syndrome with systemic edema formation.

In Focal segmental glomerulosclerosis (FSGS), segments of some glomeruli are affected initially. FSGS is the most frequent cause of intractable proteinuria in children and adults and is emerging as a major glomerular cause of chronic kidney disease in the US (Braden *et al.*, 2000). FSGS describes scarring initially in scattered regions of the kidney, typically limited to one part of the glomerulus and to a minority of glomeruli in the affected region. Recent advances in molecular genetics of FSGS led to the identification of several genes responsible for familial forms. In general, they code for proteins of the podocyte and are associated with the glomerular slit-diaphragm where they play a critical role in the control of glomerular permeability (Ghiggeri *et al.*, 2004).

1.2.5. <u>Minimal change disease</u>

Minimal change disease (MCD) is the diagnosis given when a patient has the nephrotic syndrome and the kidney biopsy reveals little or no change to the structure of glomeruli or surrounding tissues when examined by light microscopy. MCD is the most common cause of nephrotic

syndrome in children and accounts for 10 to 15 percent of cases in adults. There is no evidence of immune deposits and the only ultrastructural abnormality is fusion of the podocytes foot processes, which is common to proteinuric states. The underlying molecular defect has not been identified. The nephrotic syndrome and podocyte damage can be reversible spontaneously or in response to systemic steroid therapy (Barisoni and Mundel, 2003).

1.2.6. Conginital nephrotic syndrome

Conginital nephrotic syndrome (CNF) is an autosomal-recessive disease found in the Finnish population with an incidence of about 1 in 10 000 newborns, but it is less frequent in other population (Huttunen, 1976). CNF is characterized by massive nonselective proteinuria already in utero, and development of nephrosis immediately after birth. The disorder commonly results in infection, malnutrition, kidney failure and, prior to renal transplantation, death. The disease is known for the defect on NPHS1 gene. The NPHS1 gene product, termed nephrin, is a 180 kD type-1 transmembrane glycoprotein belonging to the immunoglobulin superfamily (Kestila *et al.*, 1998).

1.3. Integrins

Integrins are heterodimeric cell surface adhesion receptors that mediate cell adhesion and migration by providing a physical link between the extracellular matrix and the cytoskeleton (Hynes, 1992). They are composed of two subunits, α and β and each αβ combination have its own binding specificity and signaling properties. To date these proteins are formed from 18 α and 8β subunits, which dimerize to yield at least 24 different integrin heterodimers, each with distinct ligand binding and signaling properties (Brakebusch *et al.*, 2002).

Integrin can bind to different extracellular matrix molecules, such as collagens and laminins, or to cellular receptors, such as VCAM-1, which constitute the ligand binding domains. On the another hand the cytoplasmic domains play a critical role in the promotion of the cell anchorage as they interact with the cytoskeleton and provide a physical connection between the internal and external environment. A number of intracellular proteins have recently been identified, which directly interact with the cytoplasmic tails of β1, β2 and β3 integrin subunit. In addition to their anchoring function, integrins also mediate cell signaling by transducing multiple pathways through their cytoplasmic tails following activation by ligands ("outside-in" signaling) (Schwartz

et al., 1995). The cytoplasmic domains also modulate integrin affinity for their ligands by changing the conformation of the extracellular domains via a process called integrin activation, or "inside-out" signal transduction. Integrins are, therefore, signaling receptors that transmit information in both directions across the plasma membrane and provide an intersection where mechanical forces, cytoskeletal organization and biochemical signals meet (Pozzi and Zent, 2003).This binding results in the activation of intracellular signal processes regulating cell growth, differentiation, anoikis and cell survival (Attwell *et al.*, 2000). Integrin signaling occurs via the interaction of integrin cytoplasmic tails with intracellular regulatory or signaling molecules known to be involved in focal adhesion kinase (FAK) and mitogen-activated protein (MAP) kinase signaling cascades (Juliano, 1994).

1.3.1. <u>Signaling machinery of Integrins</u>

Integrins transduce signals by associating with adapter proteins that connect the integrin to the cytoskeleton, cytoplasmic kinases, and transmembrane growth factor receptors.

Integrin signaling and assembly of the cytoskeleton are intimately linked. As integrins bind to the ECM, they become clustered in the plane of the cell membrane and associate with a cytoskeletal and signaling complex that promotes the assembly of actin filaments. The reorganization of actin filaments into larger stress fibers, in turn, causes more integrin clustering, thus enhancing the matrix binding and organization by integrins in a positive feedback system.

Integrins activate various protein tyrosine kinases, including focal adhesion kinase (FAK), Src-family kinases, and a serine-threonine kinase, integrin-linked kinase (ILK) (Delcommenne *et al.*, 1998).

1.4. <u>The extracellular matrix</u>

The extracellular matrix (ECM) is the material found around cells. The ECM is a biologically active tissue composed of a complex mixture of macromolecules, that in addition to serving a structural function, also profoundly affects the cellular physiology of an organism. Eukaryotic cell adhesion, migration, proliferation and differentiation are examples of biological processes influenced by the composition and structural organization of surrounding extracellular matrices. The ECM not only affects the behavior of cells of the host organism, but also can serve as a substrate for the attachment and colonization of pathogenic microorganisms.

The extracellular matrix is made up of two classes of macromolecules. The first class is called glycosaminoglycans, which are polysaccharide chains. Members of this class are usually found to be covalently linked to proteins in the form of proteoglycans. The second class is made up by fibrous proteins. There are two functional types of fibrous proteins: the ones that are mainly structural, like collagen and elastin for example, and the ones that are mainly adhesive, like fibronectin and laminin. Members of both classes come in a great variety of shapes and sizes.

The members of the glycosaminoglycans form a highly hydrated, gel-like substance, in which the members of the fibrous proteins are embedded. Collagen fibers strengthen and help to organize the matrix, while elastin fibers give it resilience. The adhesive proteins help cells to attach to the extracellular matrix. Fibronectin for example promotes the attachment of fibroblasts and other cells to the matrix in connective tissues via the extracellular parts of some members of the integrin family, while laminin promotes the attachment of epithelial cells to the basal lamina, again via the extracellular domains of some members of integrins.

1.5. <u>The cytoskeleton</u>

The cytoskeleton is unique to eukaryotic cells. It is a dynamic three-dimensional structure that fills the cytoplasm. This structure acts as both muscle and skeleton, for movement and stability. The long fibers of the cytoskeleton are polymers of subunits. The primary types of fibers comprising the cytoskeleton are microfilaments, microtubules, and intermediate filaments.

The three cytoskeletal components have distinct sub-cellular localizations. Microfilaments are enriched in a layer known as the cell cortex, immediately beneath the plasma membrane, and in cell projections such as microvilli. Microtubules extend from the perinucleus towards the cell periphery. The plus ends of microtubules point to the cell periphery. Intermediate filaments are distributed in a similar pattern to microtubules.

The cytoskeleton perceives gravity or any force through special proteins known as integrins, which poke through the cell's surface membrane (Ingber *et al.*, 1994). Inside the cell, they are hooked to the cytoskeleton. Outside, they latch onto a framework known as the extracellular matrix. Ingber and his collegues have shown that when integrins move, the cytoskeleton stiffens with corresponding increase in stress.

1.6. <u>Integrin linked kinase (ILK)</u>

The human ILK was initially identified in a yeast two-hybrid screen using a "bait" plasmid expressing the cytoplasmic domain of β1 integrin subunit. It encodes a polypeptide of 451 amino acids with a molecular mass of 59 kDa (Dedhar *et al.*, 1999). The ILK orthologue gene was isolated from mice by cDNA library screening using a human ILK probe (Li *et al.*, 1997). The coding regions of these two ILK genes share 91.5% identity of nucleotide acid sequences and 99.1% of deduced amino acid sequences. ILK is highly conserved evolutionarily, with homologues identified in human, mouse, rat, Drosophila, and Caenorhabditis elegans. The gene encoding human ILK has been localized to human chromosome 11p15.5-p15.4 (Dedhar *et al.*, 1999). Regional loss of heterozygosity indicates that this part of chromosome 11 is strongly associated with tumorgenesis in a manner that might involve genomic imprinting (Yoganathan *et al.*, 2002).

1.6.1. <u>ILK structure</u>

ILK is a serine-threonine kinase that is ubiquitously expressed in mammalian cells as a major transcript of 1.8 kb, with strongest expression of the human ILK gene in heart, skeletal muscle and pancreas and of the mouse ILK in heart, lung, liver and kidney. ILK was first identified based on its interaction with the cytoplasmic domain of β1 integrin subunit using a yeast two-hybrid screen.However, ILK can also interact with the cytoplasmic tail of β3-integrin subunit (Li *et al.*, 1997; Dedhar *et al.*, 1999).

ILK is composed of three highly conserved structurally and functionally distinct domains: (1) the N- terminus domain; (2) the plekstrin homology domain; (3) the C-terminal domain and an integrin binding site (Dedhar *et al.*, 1999).

The ankyrin repeats: the N-terminus of ILK contains four ankyrin repeats (ANK) (amino acid residues 33-164), which allow its interaction directly to PINCH, an intracellular protein containing five LIM domains (Huttunen, 1976). The LIM domain is a protein-binding motif consisting of a cysteine-rich consensus sequence of approximately 50 residues that form two separate zinc fingers (Dawid *et al.*, 1998). PINCH appears to regulate the localization of ILK to focal adhesion plaques where ILK transduces downstream signaling via its Ser/Thr protein kinase activity (Li *et al.*, 1999). PINCH was initially identified by Rearden (Rearden, 1994) screening a human cDNA library with antibodies recognizing senescent erythrocytes. Yeast two-hybrid

screens using the N-terminal ANK-repeat domain of ILK as bait reveal that PINCH binds to ILK. The interaction between ILK and PINCH occurs in mammalian cells as well as *in vitro* (Huttunen, 1976). A series of mutational studies have defined the structural basis underlying the ILK-PINCH interaction. The PINCH-binding activity requires all four ANK repeats of ILK (Li *et al.*, 1999).

Figure 8: Functional domains of integrin linked kinase (ILK).

ILK is an intracellular serine/threonine protein kinase with a C-terminal kinase catalytic domain. There are four ankyrin repeats in the N-terminus (residues 33-164) and a phosphoinositide-binding motif between the ankyrin domain and the catalytic domain (residues 180-212). The integrin-binding site is in the extreme C-terminus of the kinase domain (residues 293-451) (Dedhar *et al.*, 1999).

The pleckstrin homology: the pleckstrin homology (PH) domain containing a consensus sequence is present in the center of ILK (residues 180-212) (Delcommenne *et al.*, 1998). PH domains have been implicated in interactions with other proteins and lipids (Haslam *et al.*, 1993; Mayer *et al.*, 1993).

The kinase catalytic domain: the C-terminal domain is homologous to the catalytic domain of a large number of protein kinase containing twelve subdomains and an integrin binding site (Lux *et al.*, 1990; Hanks and Quinn, 1991). Evolutionary, ILK appears to be highly conserved and ILK homologues have been found in humans, mice, and drosophila and C. elegans. However, subdomains I, VI and VII are less conserved between ILK and other known protein kinases (Dedhar *et al.*, 1999). Furthermore, *in vitro* kinase assays revealed that a single point mutation at position 359 within subdomain VIII resulted in the complete kinase deficiency (Novak *et al.*, 1998), which indicates subdomain VIII is critical for the ILK activity.

The integrin binding site: the binding site of the cytoplasmic domain of β1 integrin subunit was initially mapped to the C-terminus with the protein kinase catalytic domain (Dedhar *et al.*, 1999). Several studies suggest that ILK may also interact with the cytoplasmic domains of the β2 and β3 integrin subunits (Delcommenne *et al.*, 1998).

1.7. <u>The kinase activity of ILK</u>

ILK has a low kinase activity, which is stimulated transiently by cell-ECM interactions and by certain growth factors (Dedhar *et al.*, 1992). The activity of ILK is stimulated in a phosphatidylinositol (PI) 3-kinase-dependent manner and likely involves binding of the phosphoinositide phosopholipid product of PI 3-kinase, PI 3,4,5-triphosphate, to the PH-like domain of ILK (Dedhar *et al.*, 1992).
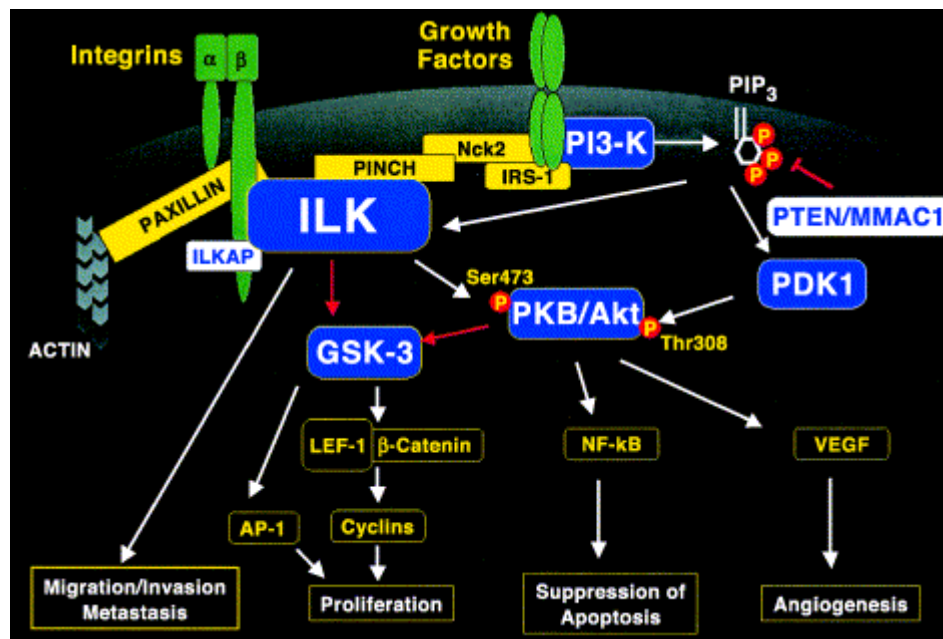
Figure 9: Schematic representation of the signal transduction pathways from integrins and growth factor receptors through ILK.

ILK interacts with the cytoplasmic domains of β1 or β3 integrins, and with the first LIM domain of PINCH via its N-terminal ankyrin repeats. ILK phosphorylates PKB/Akt on Ser 473. ILK phosphorylates and inhibits the activity of GSK-3 β (Yoganathan *et al.*, 2002).

Inhibition of ILK kinase activity suppresses cell growth in culture as well as growth of human colon carcinoma cells in SCID mice (Tan *et al.*, 2001). Several lines of experimental evidence suggest that these phenotypes are largely attributed to enhanced ILK kinase activity and phosphorylation of glycogen synthase kinase 3 (GSK 3β) on Serine 9 and PKB/Akt on Serine 473 (Delcommenne *et al.*, 1998; Persad *et al.*, 2001), two key proteins involved in a diverse array of cell functions including cell proliferation, survival and insulin responses (Cohen and Frame, 2001; Lawlor and Alessi, 2001). The ILK phosphorylation of PKB on Ser473 is positively regulated by the activity of PI3-kinase and negatively regulated by the tumor suppressor gene

PTEN that encodes a lipid phosphatase (Morimoto *et al.*, 2000). PTEN encodes a 3´-phosphatase that converts phosphatidylinositol 3, 4-bisphosphate into phosohatidylinositol-4-phosphate and phosphatidylinositol-3, 4, 5-triphosphate. ILK-dependent phosphorylation of GSK 3β in epithelial cells down regulates GSK 3β kinase activity (Delcommenne *et al.*, 1998). This in turn is associated with reduced E-cadherin expression, enhanced AP1 activity and increased β-catenin-Lef/Tcf activity (Novak *et al.*, 1998), which induces the expression of cell-cycle-promoting genes such as cyclins and c-myc (Radeva *et al.*, 1997).

Other targets of the ILK kinase activity are β-parvin (Yamaji *et al.*, 2001), the regulatory myosin light chain (MLC) (Deng *et al.*, 2001), and MLC phosphatase (Kiss *et al.*, 2002; Muranyi *et al.*, 2002), and its regulators CPI-17 (protein-kinase-C-dependent phosphatase inhibitor of 17 kDa) and PHI-1 (phosphatase holoenzyme inhibitor 1) (Deng *et al.*, 2001). The significance of their phosphorylation, however, is not clear.

1.7.1. <u>ILK expression in human cancers</u>

Recent findings in a number of cancers indicate that ILK expression is increased in tumors, and that higher-grade tumors express higher levels of ILK protein. Analysis of ILK expression in human prostate cancer biopsy samples demonstrated that ILK expression levels increased with tumor grade (Graff *et al.*, 2001). ILK expression levels are also increased in human colon adenocarcinomas (Bravou *et al.*, 2003), ILK expression is also increased in gastric cancers, with higher levels in higher-grade cancers and in metastases (Ninomiya *et al.*, 1995). In ovarian cancers, ILK expression is increased relative to benign tumours and normal ovarian epithelium. Increased expression of ILK has been reported in malignant melanomas relative to benign lesions and melanocytes. Again, higher levels of ILK were correlated with the depth of the melanoma lesions and with metastases, and an inverse correlation between the level of ILK expression and patient survival was demonstrated (Dai *et al.*, 2003). These findings that ILK protein levels are increased in several types of cancer indicate that ILK gene transcription, translation or protein stability could be dysregulated in cancer cells. At present, little is known about the mechanisms of regulation of ILK transcription.

1.7.2. <u>Role of ILK in relevance to nephrophathy</u>

To identify novel molecules activated in proteinuria, Kretzler and his colleagues undertook an expression screen on glomeruli from children with the congenital nephrotic syndrom of the Finish

type (CNF). Displaying 5800 mRNAs, 37 differentially regulated PCR products were isolated and 12 were further characterized (Haltia *et al.*, 1999). One cDNA with induction in the nephrotic glomeruli was identical to ILK (Kretzler *et al.*, 2001). ILK a serine threonine kinase, appeared to be a good candidate for regulating podocyte matrix interaction in proteinuria. ILK induction was found in glomeruli of three different renal diseases, all with severe alterations of the filtration barrier (Kretzler *et al.*, 2001).

In CNF, a mutation of a single molecule in the slit diaphragm, nephrin, causes a severe disturbance of the glomerular filtration unit (Haltia *et al.*, 1999; Kawachi *et al.*, 2000). In the murine model of nephrotoxic serum nephritis the acute inflammatory insult of the anti-GBM antibodies induces the rapid onset of a severe nephrotic syndrome (Schadde *et al.*, 2000). In the chronic progressive glomerulosclerosis of mice transgenic for growth hormone (GH), glomerular hypertrophy induces slowly progressive podocyte failure (Wanke *et al.*, 1992). These results are the first indications that changes in ILK expression occur in the damaged glomerulus and may play a role in the disturbed filtration barrier on proteinuria, irrespective of the initial insult (Kretzler, 2002). A significant increase of ILK mRNA was confirmed in podocytes from proteinuric mice compared to wild-type littermates using the real-time RT-PCR.

1.7.3. <u>ILK in kidney disease</u>

Recent studies have implicated ILK dysregulation in the development of several chronic glomerular diseases. Kretzler et al. identified ILK as a candidate downstream effector in proteinuria in patients with congenital nephritic syndrome (Kretzler *et al.*, 2001). An induction and disruption of ILK was also observed in mesangial matrix expansion by hyperglycemia in diabetic nephropathy (Hammes *et al.*, 2001). Li and al. have shown a tubule-specific induction of ILK in mouse kidney after both obstructive and diabetic injury, this induction is consistent with a role for ephithel to mesenchymal transition (EMT) (Sakai *et al.*, 2003).

Induction of ILK activity was found in podocytes cell culture grown on plastic or collagen I compared to collagen IV and fibronectin matrix molecules found in the normal glomerulus. ILK activity was assessed after *in vitro* challenge of podocytes with the polycation protamine sulfate (Reiser *et al.*, 2000b). Protamine induces foot process effacement probably via alteration of the luminal podocyte surface charge (Kerjaschki *et al.*, 1989). This result indicates ILK as a downstream effector of podocyte damage (Kretzler, 2002).

1.8. <u>Transgenic mice</u>

A transgenic mouse is an organism that had artificially DNA introduced into one or more of its cells. Transgenic mice are developed into a useful research tools in biological sciences. The mouse is an excellent experimental model for defining human gene function because of its anatomic, physiologic, and genetic similarity to humans (van der Weyden *et al.*, 2002). The mouse is also a popular model because of its relatively short life cycle and because its genome can be readily manipulated by molecular means.

In the last few years, a number of significant technological advances have dramatically increased our ability to create mouse models of human disease. Techniques including viral transgenics, pronuclear microinjection, and microinjection of genetically altered embryonic stem (ES) cells have been used to either add gene copies or disrupt genes ("knockout") in the mouse genome. Studies of normal gene function, altered gene expression, gene regulation, as well as the generation of mice with specific mutant genes and the production of mouse models for human diseases are some of the important types of studies to which transgenic mouse technology has made a significant impact (Cuthbertson and Klintworth, 1988; Denny and Justice, 2000; Malakoff, 2000).

1.8.1. <u>Conventional transgenic mice</u>

1.8.1.1. Pronuclear injection

Pronuclear injection results in random integration of the injected DNA into the genome and relies on the overexpression of the transgene to produce a phenotype. In most cases, the transgene can be defined as an expression cassette consisting of a gene driven by a promoter of choice (Brinster and Palmiter, 1984). To this end, the DNA containing the transgene is microinjected into the male pronucleus of fertilized mouse oocytes. Subsequently, viable embryos are implanted into pseudo-pregnant surrogate mothers. On average, 10-30 % of the resulting littermates bear the transgene in their genome. In general, a transgenic mouse line is established when the transgene is effectively transmitted to the following generations in a mendelian way. Although the transgenic DNA is present in all cells, transgene expression is dependent on many factors such as the chosen promoter and enhancer elements, the number of incorporated copies, and the locus of integration (Gassmann and Hennet, 1998).

The main limitation of the pronuclear injection is linked to the uncontrolled integration of the

transgene into the host genome. This random integration may influence the expression of genes situated close to the transgene, and the locus of integration may affect the expression of the transgene itself. Therefore, it is mandatory to generate several transgenic mouse lines with comparable transgene expression patterns that show identical phenotypes. This cumbersome drawback became obsolete with the emergence of targeted mutagenesis techniques.

1.8.1.2. Gene targeting

One of the most common uses of targeted insertion of DNA is to generate "knockout mice". The underlying mechanistic principle of this technology is homologous recombination. When an exogenous DNA sequence is integrated into the mouse genome, there is an extremely small but finite probability that it recombines itself at the site where the native sequence is similar to that of the exogenous sequence. For the homologous recombination to occur, the two sequences must be as close to identical as possible. Homologous genes from even closely related mammalian species may not be similar enough, particularly in the intron sequence. The probability of homologous recombination can be dramatically greater when the gene used to disrupt the endogenous gene is derived from the same strain of mouse as that of the recipient cells.

Targeted insertion is accomplished by introducing the DNA into embryonic stem (ES) cells. These are undifferentiated multipotent cells from mouse blastocysts which can develop into any type of cell and organ in the body. Under certain specific culture conditions, they can be maintained in the multipotent status. To increase the usefulness of recombinant ES cells, a mechanism for selection is usually constructed into the exogenously introduced DNA sequence. A selection marker, like the neomycin resistance gene, is normally added to targeting vectors to allow selection of ES cells that have integrated the vector into their genome. The exogenous DNA sequence is introduced into the ES cells most commonly by electroporation. Cells in which the introduced sequence is integrated into the homologous sequence in the host genome are selected and injected into the cavity of a mouse embryo at the blastocyst stage. The injected blastocyst is returned to a pseudo-pregnant host female mouse. Thus, the embryo consists of two types of cell, each with different genetic makeup; the native cells of the blastocyst and the injected ES cells. Since both are multipotent, the embryo develops to a whole animal which is chimeric, consisting of varying proportions of both cells. Male mice showing a high percentage of chimerism are then mated with wild type mice to check for germ-line transmission of the targeted allele in the F1 offspring.

1.8.2. <u>Conditional transgenic mice</u>

Conventional transgenic technologies are invaluable for modeling genetic disorders and answering specific questions in relation to developmental biology. However, this all or nothing approach is inflexible and cannot be used to answer more subtle questions about gene function. Furthermore, conventional knockout strategies affect every cell in an animal, so that it is often impossible to distinguish primary and secondary changes in a complex phenotype. In order to tease out more precise information about the role of a gene in a specific cell type at a critical stage of disease or development, a more sophisticated approach is required. Building on conventional transgenic techniques, conditional technologies allow flexible spacio-temporal control of gene expression. In these systems the switching on or off of a particular gene is conditional on a specific stimulus (Ryding *et al.*, 2001).

1.8.2.1. Conditional knockout

To overcome the limitation of conventional knockout animals, conventional genome modifications have been combined with site-specific recombination systems that rely on recombinases that promote the reciprocal exchange between two short DNA recognition sequences (Kwan, 2002). Currently there are two recombinase systems that have been applied in mouse gene targeting: Cre and Flp.

Cre is the 38-kDa product of the cre (cyclization recombination) gene of bacteriophage P1 and is a site specific DNA recombinase of the Int family (Sternberg *et al.*, 1986) which efficiently catalyzes reciprocal conservative DNA recombination between pairs of *loxP* (locus of X-over of P1) sites (Hoess *et al.*, 1990). In a similar manner the Flp from the budding yeast *Saccharomyces cerevisiae* (Dymecki, 1996) mediates recombination between FRT (FLP recombination target) sites.

Each of these recombinases (Cre or Flp) recognizes a 34-bp DNA sequence. Both *loxP* and FRT sites consists of two 13-bp inverted repeats flanking an 8-bp non-palindromic core region. One molecule of this recombinase binds per inverted repeat or two molecules line up at one (*loxP* or FRT) site. The recombination occurs in the asymmetric core region. These 8 bases are also responsible for the directionality of the site. Two site (*loxP* or FRT) sequences in opposite orientation to each other invert the inverting piece of DNA; two sites in direct orientation dictate excision of the inverting DNA between the sites leaving one site behind (Ryding *et al.*, 2001). This precise removal of DNA can be used to eliminate an endogenous gene or transgene and to activate a transgene.

1.8.2.1.1 The Cre/LoxP system

The Cre /loxP system is a tool for tissue-specific knockout of such genes which cannot be investigated in differentiated tissues because of their early embryonic lethality in mice after conventional knockouts. Modification of a specific gene with loxP sites flanking the region of interest is achieved using standard gene targeting vectors in ES cells (Gubler *et al.*, 1993). Mice derived from these targeted ES cells can be bred to produce homozygotes for the floxed allele. This mouse line is than crossed to a conventional transgenic mouse line with Cre targeted to a specific tissue or cell type. Recombination, excision and consequent inactivation of the target gene occurs only in those cells expressing Cre recombinase. Hence, the target gene remains active in all cells and tissues which do not express Cre.

Figure 10: Structure and sequence of the recombinase recognition loxP sites.

A) Each site consists of two 13-bp inverted repeats flanking an asymmetric 8-bp core region which define the orientation of the recognition site indicated by the red arrow in the loxP sequence.

B) Recombinase- mediated recombination between two recognition sites in forward orientation.

1.8.2.1.2 The Flp/FRT system

The FLP-FRT system, becoming more frequently used in mouse research, is similar to Cre-lox in many ways. It involves the use of flippase (FLP) recombinase, derived from *Saccharomyces cerevisiae* (yeast). In lieu of *loxP* sites, FLP recognizes a pair of FLP recombinase target (FRT) sequences flanking the genomic region of interest. As with *loxP* sites, orientation of the FRT sequences dictates inversion or deletion events in the presence of FLP. The use of Flp in transgenic mice is at a less advanced stage than that of Cre and a direct comparison between the two is not possible at this time (Ryding *et al.*, 2001). The recombination efficiency of Flp is inferior to that of Cre (Buchholz *et al.*, 1998). One of the disadvantages of Flp compared with Cre is that no ubiquitously expressing reporter for Flp is available.

2. <u>Aim of the study</u>

The integrin linked kinase is a serine threonine kinase, which has been shown to be involved in a wide variety of regulatory processes associated with cell function. Recently, our group identified an ILK induction in glomerular disease by an expression screening on glomeruli from children with congenital nephritic syndrome of the Finnish type. These data suggested that ILK plays a central role in the podocytes damage.

The aim of this study was to elucidate the functional role of ILK in the glomerular filtration barrier *in vivo* using transgenic mice. To address this issue ILK deletion was carried out using a podocyte specific cre/Lox system. Further, a mouse line overexpressing ILK was developed using transgenic mouse technology. The phenotypic characterization of the mouse lines was used to characterize the role of ILK *in vivo* in podocyte function.

Material and Methods

3. <u>Materials and Methods</u>

3.1. <u>Animals experimentation</u>

Transgenic mice expressing Cre recombinase specifically in podocytes were obtained from L.B.Holzmann. The podocin-cre strain was engineered by subcloning the Cre-recombinase cassette under the regulation of the human NPHS2 promoter. (University of Michigan, Ann Arbor, USA) (Moeller *et al.*, 2002). 129/ILK$^{flox+/+}$ mice were provided by S.Dedhar (University of British Columbia, Vancouver, Canada) (Terpstra *et al.*, 2003). For this study wild type mice were obtain from Charles River, Sulzfeld Germany.

Mice were maintained on a 12-h light, 12-h dark cycle and fed standard rodent chow and tap water. Mice used in expression studies and for phenotypic analysis were weaned at an age of three weeks, marked by ear piercing and housed in cages separated by sex. At the time of weaning, tail tips were clipped and kept at –20°C for genotypic analysis. All experiments were carried out according to the German Animal Protection Law (Tierschutzgesetz; Genehmigungsaktenzeichen: 211-2531-31/96).

Composition of the feed	Normal feed	Breeder feed
Protein %	19	22.5
Fat %	4	5
Fiber %	6	4.5
Ashes %	7	6.5
Calcium %	0.9	0.9
Phosphor %	0.7	0.7

3.2. <u>Generation of ILK deficient mice in podocyte</u>

To selectively delete ILK from glomerular podocytes, transgenic mice expressing Cre recombinase specifically in podocytes were bred with mice in which exon 5 to 12 of the ILK gene were flanked by lox sites. These mice were crossed with 2.5P-Cre-mice (podocin$^{Cre+/+}$) with the Cre-recombinase cassette under the regulation of the human NPHS2 promoter of the podocin

gene. The podocin^{Cre} mice were bred with homozygous floxed ILK mice. The F1 podocin$^{Cre+/-}$/ ILK$^{flox+/-}$ bitransgenic mice were backcrossed to homozygous ILK$^{flox+/+}$/ podocin$^{-/-}$ mice generating homozygous ILK$^{flox+/+}$-podocin$^{Cre+/-}$ mice (podoILK -/-). Mice of all genotypes were born at the expected Mendelian frequency.

3.3. Identification of transgenic mice

3.3.1. Polymerase chain reaction (PCR)

3.3.1.1. Proteinase K digest of mouse tails

Tail tips were clipped at weaning and frozen at −80 °C. fragments of 3-5 mm were cut and incubated at 56 °C overnight in 1.5 ml centrifuge tubes containing 200 μl of Kawasaki buffer and 10 μl proteinase K (Siegma, 20 mg/ml in bidistilled water).

Kawasaki buffer (pH 8.3):　　　20 mM Tris-HCL, pH 8.3

　　　　　　　　　　　　　　1.5 mM MgCl$_2$

　　　　　　　　　　　　　　25 mM KCl

The buffer was autoclaved. Tween-20 was added to an end concentration of 0.5% (w/v) after the solution had cooled to RT. The resulting buffer was kept at RT.

After the overnight digest, the samples were heated at 95 °C for 15 min to inactivate the proteinase K, centrifuged at 15.000 xg at 4 °C for 5 min. After that, the supernatant was transferred to a new tube. 1 μl of the supernatant were used as template for the PCR.

3.3.1.2. PCR conditions

For genotyping, the isolated genomic DNA from tails of three week old mice was used to detect the transgenicity. The following oligonucleotide primers were used for the Polymerase chain reaction (PCR); for the floxed ILK-locus: Fr-Lox: 5'-CCAGGTGGCAGAGGTAAGTA-3' and Rv-Lox: 5′-CAAGGAATAAGTGAGCTCAGAA-3'. The presence of the transgene for the podocin-specific Cre-recombinase was detected using the PCR primer: Fr-Cre: 5-GCATAACCA GTAAACAGCATTGCTG-3` and Rv-Cre: 5′-GGACATGTTCAGGGATCGCC AGGCG -3′ (Moeller *et al.*, 2002). The reaction was prepared in 0.5 ml PCR tubes on ice. The PCR was carried out with Taq DNA polymerase (5 units/ μl; Qiagen) in a total volume of 25 μl:

DNA sample (template)	1.0 μl
10 x PCR buffer	2.5 μl
1 mM dNTPs	4.0 μl
10 pmol forword primer	1.0 μl
10 pmol reverse primer	1.0 μl
Taq DNA polymerase	0.2 μl
Bidistilled water	15.3 μl

The reaction was performed as following in a Gene Amp 9700 thermoblock cycler (Applied Biosystems, Darmstadt, Germany). The PCR condition was as follows:

CRE			Lox-ILK		
94 °C	3 min		94 °C	3 min	
94 °C	45 sec		94 °C	2 min	
56 °C	45 sec	30 x	61 °C	45 sec	35 x
72 °C	45 sec		72 °C	3 min	
72 °C	7 min		72 °C	7 min	
4 °C	∞		4 °C	∞	

Amplified DNA fragments were loaded on agarose gels for electrophoresis.

3.3.2. <u>Agarose gel electrophoresis</u>

Agarose	Gibco BRL Invitrogen, Karlsruhe	
10 x TBE-buffer	121.1 g	Tris
	51.35 g	boric acid
	3.72 g	EDTA
	ad 1000 ml	bidistilled water
6x loading buffer	0.025 g	Xylene
	0.025	bromphenol blue

7 ml	ddH$_2$O
1.4 ml	0.5 M EDTA
3.6 ml	glycerol

500 bp DNA ladder	Peqlab, Erlangen
1 KB DNA ladder	Gibco BRL Invitrogen, Karlsruhe

Agarose gels (0.6 to 2 % depending on the length of the DNA fragment) were prepared by dissolving agarose in 0.5 TBE-buffer by boiling the buffer in a microwave. After the solution had cooled, 6 µl ethidium bromide were added and the mixture was transferred into the appropriate gel chamber for solidation. The gel was then covered with TBE buffer and 2µl of 6x loading buffer was added to each DNA samples. Then samples and DNA ladder marker were loaded onto the gel. The gel was run under for the first 10 min by 70 V, and then under constant voltage 120V in order to separate DNA fragments. After the electrophoresis, the gel was visualised under the UV-light and photographed with a video processor (P67E, Mitsubishi).

3.3.3. <u>Isolation and elution of DNA fragments from agarose gel</u>

DNA fragments were separated in an agarose gel cast with Ethidium bromide. After running the band was visualised on a UV light-box. The band of interest was carefully cut using a scalpel and placed in a 1.5 ml microfuge tube. The DNA extraction was done using Qiagen Kit. The gel slice was weighed and 3x volumes of buffer QG were added to 1 volume of gel. The microfuge tube was than incubated at 50°C for 10 min. to dissolve the gel by vortexing every 2-3 min during the incubation. After the gel slice dissolved completely, 1 volume of isopropanol was added to the sample and was mixed. To bind the DNA, the contents of the tube was applied to the Qiaquick column and centrifuged for 1 min. The flow-through was discarded and 750 µl of buffer PE was added to the column and centrifuged for 1 min. The flow-through was discarded and the centrifugation step was repeated. The Qiaquick column was than placed into a clean 1.5 ml microcentrifuge tube and 50 µl of buffer TE or H$_2$O was added to the center of the Qiaquick membrane and centrifuged for 1 min. at maximum speed to elute the DNA.

3.3.4. <u>Quantification of DNA</u>

2 µl of the sample was added to 100 µl TE in microfuge tube, was mixed well and read in a spectrophotometer by OD 260 and OD 280 to determine the purity of the DNA.

The ratio OD_{260}/ OD_{280} should be determined in order to assess the purity of the sample. The ratio should be between 1.8 –2.0. A ratio less than 1.8 indicates that there may be proteins or other UV absorbers in the sample, and a ratio higher than 2.0 indicates the samples may be contaminated.

3.3.5. <u>Enzymatic digestion of DNA</u>

Restriction endonucleases   Roche, Mannheim

10x reaction buffer   Roche, Mannheim

Restriction enzymes were used for DNA digestion applying the recommended buffers in a 50 or 100 µl final volume. 1-3 µg DNA were usually digested with at least 10 units of the required enzyme, either for 1h or over night at the prescribed temperature.

3.3.6. <u>DNA dephosphorylation</u>

Treatment of digested DNA with alkaline phosphatase (calf intestinal phosphatase, CIP, NEB) which catalyses the removal of 5´ phosphate groups was carried out in order to prevent self-recirculation of the plasmid vector. The following components were added to the purified DNA:

10 x CIAP reaction buffer   10 µl

CIAP (0.01 unit/ pmol of ends)*   1- 2 µl

Bidistilled water   ad 100 µl

* A general formula for calculating the picomoles of ends of linear double-stranded DNA is: (µg DNA/ kb size of DNA) x 3.04 = pmol of ends.

The reaction mixture was incubated at 37 °C for 30 min. The reaction was stopped by heating at 85 °C for 15 min.

3.3.7. <u>DNA ligation</u>

DNA fragment and vector were ligated with a molecular ratio of 1:3 using the T4 DNA ligase (Boehringer, Mannheim, Germany). For ligation with T4-ligase, the 10x ligation buffer and 1 unit of the ligase were used in a total volume of 20 µl and the reaction mixture was incubated over night at 16°C. Linearised, dephosphorylated vector in the absence of the insert was ligated for the negative control.

3.3.8. <u>Electroporation of *E. coli*</u>

The electrocompetent *E. coli* DH5α was thawed on ice and the plasmid of interest was diluted in TE or H_2O and placed on ice. 15 ml tube containing LB medium without antibiotics was prepared. Then, 1 µl of plasmid DNA was pipetted into the electrocompetent cells and 2/ 3 times for mixing. Immediately, the contents were transferred into the bottom of the cuvette and electroporated at 1.8 kV and 1 ml of SOC medium was then added immediately to the cells. The contents of the cuvette were transfered into 1.5 ml Eppendorf tube and incubated at 37°C for 1-2 hrs. 200 µl of the transformed cell suspension was plated onto LB plate with the appropriate antibiotic for selection. The suspension was gently spread over the surface of the agar plate. At the end, the plate was placed in 37°C bacterial incubator for 16-24 hrs until colonies appeared.

SOC medium:

Bacto-tryptone peptone	20 g
Bacto-yeast extract	5 g
NaCl	0.5 g
ddH_2O	ad 950 ml

The mixture was shaken until the solutes had dissolved. 10 ml of a 0.25 M KCl solution was added and the pH value was adjusted to 7.0, then the medium was autoclaved. The final medium additionally contained 100 mM $MgCl_2$ and 20 mM glucose.

Luria-Bertani (LB) medium:

Bacto-tryptone	10 g
Bacto-yeast extract	5 g
NaCl	10 g

        ddH$_2$O   ad 1000 ml

The mixture was shaken until the solutes were dissolved, the pH value was adjusted to 7.0 with 5 M NaOH and then the medium was autoclaved.

Agar-LB plates:

        LB-medium   1000 ml

        Agar, granulated   15 g

After autoclaving, the solution was left at RT, till the temperature dropped to 50 °C, than the antibiotic was added and the medium was directly poured in 90 mm Petri dishes. After the medium had hardened completely, the plates were inverted and stored at 4 °C.

After incubation at 37 °C, a single colony was picked up from the agar plate and put in 50 or 200 ml LB medium supplemented with the specific antibiotic, for Mini, Midi preparations. The bacteria respectively were incubated to grow overnight at 37 °C with shaking. The next day, the medium was centrifuged, the supernatant was discarded and the precipitate was treated following the Qiagen Mini/ Midii Kit protocol (provided by the manufacture).

3.4. <u>DNA extraction and purification</u>

3.4.1. <u>Mini preparation</u>

The mini preparation was done by using Qiagen kit. The cells were harvest by centrifugation at 80000 rpm for 10 minutes. The supernatant was decanted and the pellet bacterial cells was resuspended in 250 µl of buffer P1 and transferred to a 1.5 ml tubes. A 250 µl of buffer P2 was added in each tube and the tubes were gently inverted to avoide shearing of the genomic DNA. Further, 350 µl of buffer N3 was added and again the tubes were inverted. A centrifugation step was followed for 10 minutes at maximum speed. The supernatant was applied to the wells of the Qiaprep column. The Qiaprep column was centrifuged for 1 min. and 750 µl of buffer PE was added for washing and then centrifuged for 1 minute. The flow-through was discarded and the tubes were again centrifuged for 1 minute to remove residual wash buffer. In the end the Qiaprep column were placed in a clean 1.5 ml tubes and 50 µl of H$_2$O was added to the center of each Qiaprep column, to elute the DNA. After 5 minutes incubation, the tubes were centrifugated.

3.4.2. <u>Midi preparation</u>

The midi preparation was done by using Qiagen kit. A single bacterial colony was picked into 3 ml of LB medium containing the appropriate antibiotic and the culture was incubated at 37°C with shaking for 8-9 hours. The content of the tube was transfered to 50 ml LB medium and incubated as above for 11-14 hours. The cells were harvested by transferring into a 50 ml sterile conical tube and spinning at 4000 rpm for 20 minutes at 4°C. The supernatant was decanted, and the pellet was resuspended in 10 ml of buffer P1. 10 ml of buffer P2 was added to each tube and mixed by gently inverting 4-6 times. Next, 10 ml of buffer P3 was added to the tube and mixed gently then incubated on ice for 20 minutes. The suspension was centrifuged at 4000 rpm for 20 min. and the supernatant was removed to a fresh tube. The Qiagen-tip 100 was equilibrated by applying 4 ml of buffer QBT, and allowing the column to empty by gravity flow. Next, the supernatant was applied to the column and allowed to enter the resin by gravity flow. The Qiagen-tip was washed twice with 10 ml buffer QC and the DNA was eluted with 5 ml buffer QF. The eluted DNA was precipitated by adding 3.5 ml isopropanol. The tube was vortexed and centrifuged at 4000 rpm for 30 min. at 4°C. The supernatant was decanted and the DNA pellet was washed with 2 ml 70 % ethanol, and centrifuged at 4000 rpm for 10 min. The pellet of DNA was air-dried for 10 min. and redissolved in a suitable volume of TE.

Buffer QBT (equilibration buffer)

750 mM	NaCl
50 mM	MOPS, pH 7.0
15 %	isopropanol
0.15 %	Triton X-100

3.5. <u>Protein analysis</u>

3.5.1. <u>Extraction of protein from cells</u>

Medium was aspirated and cells were rinsed with PBS. Approximately 10^6 cells were resuspended in 500 μl lysis buffer and lysed on ice for 20 min. Then cells were scraped. The cellular extracts were transferred to a microcentrifuge tube. Cell debris were removed by centrifugation at 10 000 rpm for 15 min at 4°C. The protein concentration of the supernatant was

determined using the BioRad reagent.

Lysis buffer:

50 mM	Tris, pH 8
0.25 %	Sodium deoxycolate
1 %	Nonidet P-40
1 %	SDS
150 mM	NaCl

3.5.2. Extraction of proteins from tissues

Tissues samples stored at - 80°C were weighed, placed in 1.5 ml centrifuge tubes to which 100 µl protein extraction buffer was added and homogenized with a tissue homogenizer for 3 min. It is imperative that the tissues stay cold so that protease does not have time to act on the protein. After homogenization 400 µl extraction buffer was added and the samples were stored on ice for 15 minutes.

Protein extraction buffer :

10 mM	Tris-HCl, pH 7.5
1 %	Nonidet P-40
0.25 %	Sodium deoxycolate
150 mM	NaCl
1 mM	NaF
1 mM	EGTA
1 mM	Na_3VO_4
1 µg/ ml	Aprotinin
1 µg/ ml	Leupeptin
1 µg/ ml	Pepstatin

The samples were centrifuged at 14000 rpm at 4°C for 5 minutes. The supernatant was removed and an aliquot was removed for the measurement of protein concentration and samples were stored at –20 °C.

3.5.3. Measurement of protein concentration by Lowry

A set of protein standards of known concentrations was prepared by serially diluting a bovine serum albumin (BSA) stock solution (5 mg/ml) in PBS. Samples were diluted such that their concentration would fall within the BSA standard range. 5 µl of the standards and samples were pipetted into 96-well plates containing. A mixture of 20 µl of reagent S and 1 ml of Reagent A was prepared. From this mixture 25 µl was then added to the samples. 200 µl of Reagnet B was added and mixed thoroughly with repeated pipetting. The plate was then allowed to incubate at room temperature for 15 minutes and the absorbance was measured at 650 nm. A standard curve was prepared by plotting the absorbance of the standards versus protein concentrations. The protein concentration of the samples was determined using the standard curve.

Dc Protein Assay (Bio-Rad, München):

> Reagent A, alkaline copper tartrate solution
>
> Reagent B, dilute Folin reagent
>
> Reagent S, surfactant

3.5.4. Creatinine measurement

To determine the content of creatinine in urine, the Jaffé method was used. 50 µl of samples, standard (3) and diluted urine 1:50, was added into a 96-well polystyrene plate. The standard solution was diluted 3 times to determine the standard curve. Next 100 µl of buffer solution (1) was added to each sample. The latter were mixed and tempered to a constant preselected temperature for 5 minutes. 100 µl of picric acid solution (2) was added, and mixed. Then the plate was immediately placed in the ELISA plate reader. After 1 minute the plate was read at 490 nm. This process was done again after 5 minute premeasurement.

Buffer solution (1)

> Phospate buffer   12.5 mmol/ l

| | NaOH | 313 mmol/ l |

Picric acid solution

| | Picric acid | 8.73 mmol/ l |

| | Standard solution (3) | |

Creatinine

| | 1 mg/ dl | (88.4 μmol/ l) |

The reagents were provided by Merckotest Creatinine Test (Diagnostika MERCK, Darmstadt).

3.5.5. <u>Biochemical analysis</u>

To investigate the potential effect of transgene expression on the immune function, the following assays were carried out at the Institute of Medical Microbiology, Immunology and Hygiene, Technical University of Munich. Blood (400-600 μl) of 12 week-old mice was collected by bleeding from the retroorbital sinus in a 1-ml lithium-heparin tube (Kabe Labortechnik GmbH, Nümbrecht-Elsenroth, Germany), centrifuged at 2000 rpm for 5 min, and urea nitrogen, total protein, albumin and cholesterol was determined in plasma using a Hitachi autoanalyzer (Hitachi, Tokyo, Japan).

3.5.6. <u>Enzyme linked immunosorbent assay (ELISA)</u>

This technique (Engvall and perlmann, 1971) allows the detection of antibodies that bind to a plate-bound antigen or antibody by an enzymatic reaction and was used to determine serum antibody titers and specificities.

96-well ELISA plates (polystyrene plate) were coated for 1h at RT with 5 μg/ml antigen in coating buffer (50 μl/ well). The plates were washed 3 x with wash solution and unspecific binding sites on the plate were blocked with 100 μl/ well blocking buffer for at least 1 h at RT. After this, the plates were washed again and 50 μl of mice urine were added to each well at an appropriate dilution in sample/ conjugate buffer and incubated at least 1 h at RT, followed by a washing step. Bound antibodies were then detected using 50 μl/ well Goat anti-Mouse Albuminaffinity purified (1h, RT), which were either directly coupled to Goat anti-Mouse Albumin-HRP conjugate, which were diluted 1/10000- 1/200000 in coating buffer. Plates were washed 3 times.

To develop a colored reaction, ABTS.development solution was used as substrate for the alkaline phosphatase. 50 μl substrate buffers were added in each well and reaction was developed for 5 to 30 min. The plate was read at 405 nm in a spectrophotometer (Geniosplus, Switzerland) at different time points.

Coating Buffer:

0.05 M carbonate-bicarbonate, pH 9.6

Wash solution:

50 mM Tris

0.14 M NaCl

0.05% Tween 20

Ad 1000 ml Aqua dest, pH 8.0

Blocking (Postcoat) solution:

50 mM Tris

0.14 M NaCl

1% BSA

Ad 1000 ml Aqua dest, pH 8.0

Sample/ Conjugate solution

50 mM Tris

0.14 M NaCl

1% BSA

0.05% Tween 20

Ad 1000 ml Aqua dest, pH 8.0

ABTS (Invitrogen:

5 ml ABTS- buffer

1 ABTS- tablet

Ad 50 ml Aqua dest

3.6. <u>SDS-polyacrylamide gel electrophoresis (SDS-PAGE)</u>

Sodium dodecyl sulphate (SDS) is an anionic detergent which denatures proteins by wrapping around the polypeptide backbone. In doing so, SDS confers a negative charge to the polypeptide in proportion to its length. The negative charges on SDS destroy most of the complex structure of proteins, and are strongly attracted toward an anode in an electric field.

A polyacrylamide gel with acrylamide content above a critical density restrains larger molecules from migrating as fast as smaller molecules. Because the charge-to-mass ratio is nearly the same among SDS- denatured polypeptides, the final separation of proteins is dependent almost entirely on the differences in molecular weight (MW).

Running gel 10 %

1.5 M Tris/ HCl pH 8.8	5 ml
30 % Acrylamide/ Bis	6.7 ml
10 % SDS	200 μl
H_2O (Aqua bidest)	7.9 ml
10 % APS (ammonium persulfate)	200 μl
TEMED (Tetraethylethylenediamine)	8 μl

Stacking gel

0.5 M Tris/ HCl pH 6.8	2.5 ml
30 % Acrylamide/ Bis	1.7 ml
10 % SDS	100 μl
H_2O (Aqua bidest)	5.6 ml
10 % APS (ammonium persulfate)	100 μl
TEMED (Tetraethylethylenediamine)	10 μl

Running buffer (stock) 10 x

Tris base (Roth, Germany)	30.3 g
Glycine (Merck, Germany)	144 g
ad 1 l distilled water	

Running buffer (ready to use)

Stock solution	40 ml
SDS 10 %	4 ml
Distilled water	ad 400 ml

Loading buffer, 2 x

1.25 M Tris/ HCl, pH 6.8	2.5 ml
Glycerol (87 %)	5.8 ml
Bromphenol blue	5 mg
SDS	1 g
β-Mercaptoethanol	2.5 ml
Aqua bidest	35 ml

3.7. <u>Western Blot</u>

Samples were diluted with 2x Loading buffer and heated at 95°C for 10 min. Samples were loaded and the electrophoresis was performed initially at 80 V for a few minutes and then at 130 V. A molecular weight standard (Low molecular weight range, Biorad, MA, USA) was loaded in the first slot for estimation or the protein size. The SDS-PAGE is stopped few minutes after the dye front had reached the end of the gel.

Then the whole setup was dismantled and the stacking gels were discarded. The gel was removed from the electrophoresis chamber and the separated proteins were transferred to an Immobilon-P PVDF membrane (Millipore, Bradford, MA, USA) by semidry electrophoretic blotting in a MilliBlot-Graphite Electroblotter (Biorad, München, Germany). Twelve sheets of gel blotting paper cut to the same sizes as the gel (8,3 cm x 5,5 cm) and were soaked in anode buffer I, anode buffer II or the cathode buffer.

After the transfer, the membrane was stained with Ponceau red for 8 min while shaking. Then, the membrane was washed with distilled water, the molecular weight standard bands were marked and photographed. The membrane was incubated in blocking solution using in phosphate-buffered saline PBS supplemented with 5% skimmed milk powder for 1h at room temperature to block unspecific binding of the antibody. The primary antibody was then applied

to the membrane and incubated overnight at 4°C by gently shaking. The dilution of the antibody was mostly varied between 1:1000 to 1:3000 in TBS-T or in milk. After incubation, the membrane was washed 3 times for 10 min. with TBS-T. Following washing, the secondary antibody diluted to 1:5000 -1:10 000 was applied to the membrane and incubated for 1 hr at room temperature with gently shaking. After that, the membrane was washed 3 times for 10 min. with TBS-T.

For the detection of proteins the following detection system was used: The enhanced chemiluminescence (ECL). ECL is a non-radioactive immunoassay technology; it's defined as the emission of light resulting from the dissipation of energy from substance in an excited state. In chemiluminescence the excitation is effected by luminol. The HRP/ hydrogen peroxide catalysed oxidation of luminol in alkaline condition. Following oxidation, the luminol is in an excited state which then decays to ground state via light emitting pathway. Enhanced chemiluminescence is achieved by performing the oxidation of luminol by the HRP in the presence of chemical enhancers such as phenols. This has the effect of increasing light output approximately 1000 fold and also extending the time of light emission.The light produced by the ECL reaction peaks after 5-20 min and decays slowly thereafter with a half life of approximately 60 min.

 2ml of the solution from bottle 1 and bottle 2 was mixed and then given to the membrane for 1 min at room temperature. The membrane was shortly drained and placed and covered with a transparency foil. Immediately, the membrane and a film were transferred in a cassette, for an exposure of 15 seconds to 10 minutes. The exposure time was varied from 15 seconds to 20 minutes till an optimal detection was reached.

Anode buffer I

1 M Tris pH 10.4	150 ml (0.3 M)
Methanol 20 %	100 ml
Aqua bidest	ad 500 ml

Anode Buffer II

1 M Tris pH 10.4	12.5 ml (25 mM)
Methanol 20 %	100 ml
Aqua bidest	ad 500 ml

Cathode buffer

1 M Tris pH 9.4	12.5 ml (25 mM)
1 M 6-Aminohexanacid	20 ml (40 mM)
Methanol 20 %	100 ml
Aqua bidest	ad 500 ml

Blotting buffer

Tris base (Roth, Germany)	25 mM (3.03 g)
Glycine (Merck, Germany)	190 mM (14.4 g)
SDS	0.1 % (w/ v)
Methanol (Merck, Germany)	200 ml
Distilled water	800 ml

Wash buffer (TBS) 10* stock solution

Tris base (Roth, Germany)	60.6 g
Sodium chloride (Merck, Germany)	87.6 g

ad 1 l distilled water, adjust pH 7,5 using 1N HCL (Merck, Germany)

Wash buffer (TBS-T)

1*TBS (10* TBS stock solution diluted 1:10)

0.05% Tween (Sigma, Germany)

Blocking buffer

dried milk powder	5 % (w/ n) in TBS-T

Ponceau red

Ponceau S (Roth)	0.2 g
glacial acetic acid	1 ml
distilled water	ad 100 ml

3.7.1. <u>Coomassie blue staining of protein gels</u>

Polyacrylamide gels were stained for approximately 15 minutes with Coomassie staining solution (0.025 %Coomassie Blue in 10 % Acetic acid). To visualize proteins, gels were destained in destaining solution with shaking. After destaining, the blue protein bands appeared against a clear background. The gel could be stored in water or directly photographed and dried to maintain a permanent record.

Coomassie blue solution

Coomassie R 250	1 g
Methanol	200 ml
Acetic acid	100 ml
Distilled water	700 ml

Destaining solution

Methanol	300 ml
Acetic acid	100 ml
Distilled water	600 ml

3.7.2. <u>Drying of SDS-PAGE gels</u>

The DryEaseTM Mini-Gel Drying system, Novex, Germany was used for drying polyacrylamide gels. The stained gels are washed in distilled water 3 times for 3 minutes. The gels were then equilibrated in Gel-dry solution for 15-20 minutes in a rotary shaker. 2 Pre-wet pieces of cellophane were incubated in Gel-Drying Solution for 15-20 seconds. After that the DryEase gel drying frame was placed on the gel dryer base and was covered with a piece of cellophane. The gel was placed in the center of the cellophane sheet with no air trapped between gel and cellophane. The gel was covered with a second layer of cellophane. The remaining frame was aligned so that its corner pins fit into the holes on the bottom frame. The plastic clamps are pushed onto the four edges of the frame. At the end, the assembly was put upright on a benchtop and the gel was dried for 12-36 hours. After drying the gel/ cellophane sandwich was removed and the excess cellophane was trimmed off. The dried gels were pressed between pages of a book for approximately 2 days.

3.8. <u>Mice Perfusion</u>

For perfusion, mice were killed by ether inhalation. They were placed on their back on a small surgical platform rack and fixed with needle. The animals were swapped with 70% alcohol to wet the fur. The abdominal skin was cut by a longitudinal incision. The skin and the gut were removed to expose abdominal aorta and vena cava and connective tissue and fat were cleaned. The left kidney was clamped. The left ventricle was fixed with a tweezers. A needle to which the perfusion tubes were attached was inserted into the left ventricle of the heart and immediately the vena cava was cut. The perfusion was started with PBS (pH 7.4, 37°C) for 20 seconds and then the perfusion valve was switched to a 3% glutaraldehyde solution at 37°C. The animals were perfused for five minutes. The kidney were cut and post-fixed in situ by immersion in 3% glutaraldehyde for 24 hours.

3.9. <u>Histological techniques</u>

3.9.1. <u>Paraffin section</u>

Mice were perfused with 3% glutaraldehyde in PBS. The kidney was separated from the body, cut and a portion were placed in tissue cassettes and then fixed in 3% PBS-buffered formalin for 24 hours. The fixed tissues were dehydrated in an ascending ethanol series in a Histomaster 2050/DI (Bavimed, Germany) and embedded in paraffin. Approximately 3-5 µm thick sections were cut using a HM 315 microtome (Micron GmbH, Germany). Sections were transferred into a water bath and mounted on glass slides (Marienfeld, Germany).

3.9.2. <u>Frozen sections</u>

Kidney tissue was placed on a thin layer of OCT (optimum cutting temperature). More OCT was added until the tissue was completely covered and placed onto a dry ice container. After a few minutes the OCT was completely solidified, and the tissue can be stored in a -80°C freezer. Frozen section was then cut in a microtome of the desired thickness 4 – 8 µm. The sections were placed on gelatin-coated slides and stored at -20°C until immunostaining.

3.9.3. <u>Immunohistochemistry</u>

Immunohistochemistry is the localization of antigens in tissue sections by the use of labeled antibodies as specific reagents through antigen-antibody interactions. Antibodies are visualized by a marker such as fluorescent dye, enzyme, radioactive elements or colloidal gold. IHC makes it possible to visualize the distribution and localization of specific cellular components within a cell or tissue.

The principle of immunohistochemistry has existed since the 1930's, but it was not until 1942 that the first immunohistochemistry study was reported. Coons and his colleagues used FITC-labeled antibodies to localize Pneumococcal antigens in infected tissues. Since then improvements have been made in protein conjugation, tissue fixation methods, detection labels and microscopes, making immunohistochemistry a routine and essential tool in many laboratories.

In order to perform the standard staining procedure, first the tissue section was deparaffinized and then rehydrated before applying the primary antibody. Enzyme-conjugated secondary antibodies were then applied and the specific staining was visualized after adding the enzyme-specific substrate.

After deparaffinization and rehydration, the sections were incubated in 1 % hydrogen peroxide in phosphate-buffered saline (PBS) (pH 7.4) for 15 minutes to block endogenous peroxidase activity, followed by a 10 minutes washing in PBS. Tissue sections were then incubated with the first antibody with the appropriate dilution for 1 h. The antibody was diluted in PBS or milk and incubations were performed at room temperature in a humidity chamber. After this step, slides were washed 2 times for 5 min in PBS. Next the slides were incubated with the secondary antibody generally horseradish peroxidase conjugated anti-rabbit or anti-mouse for 1 h. After 10 minutes washing in PBS, the immunoreactivity was visualized using 3,3' diaminobenzidine tetrahydrochloride dihydrate (Fluka, Buchs, Switzerland) as a chromogen. Tissues sections were counterstained with Mayer's hemalaun solution, dehydrated in an ascending series percentage of alcohols, cleared in xylene and mounted under glass coverslips using Histofluid^R (Superior, Lauda-Königshofen, Germany).

3.9.4. <u>Immunofluorescence</u>

Immunofluorescence is a technique calling for a solubilisation of membranes in a buffer that preserves the nucleo- and cytoskeleton prior to fixation. Cells were grown on coverslips in a 6 well plate. At the indicated time points, the medium was removed from the dish, the grown cells on the coverslips were rinsed in 1x PBS. Cells were then fixed in a 2 % paraformaldehyde (PFA) for 5 minutes, at room temperature. The fixation buffer was removed and cells were permeabilized with 0.3% Triton in PBS for 10 minutes at room temperature. Next, the triton solution was removed, the coverslips were rinsed and washed 1x for 3 minutes with PBS. Fresh PBS will be added and the coverslips were stored at 4°C. The cells were blocked for 30 minutes in blocking buffer in humid chamber, which was lined with PBS soaked Whatmann paper. A piece of parafilm was placed on top of it. The coverslips were incubated with the primary antibody diluted in blocking buffer for 1 hour in the humid chamber. After incubation the coverslips were washed 3 times every 5 minutes with PBS. Again the coverslips were incubated with the secondary antibody diluted in blocking buffer for 1 hour. This was followed by 3 times washing steps per 5 minutes with PBS and then 2 times with distilled water. At the end the coverslips were mounted in Moviol, and stored at 4°C overnight to dry and kept covered to avoid photobleaching.

For nephrin and podocin staining, cryosections were fixed in cold acetone, rinsed, and incubated in a bovine serum albumin-PBS solution to block unspecific binding sites. Sections were then incubated with the primary rabbit polyclonal antibody against nephrin (provided by L.B. Holzmann, Univesity of Michigan) or with the primary polyclonal anti-podocin (provided by C. Antignac, Hopital Necker, Paris), both diluted 1:100. After washing, sections were incubated with the secondary antibody (Alexa-Fluor 488 goat anti-rabbit; Molecular Probes, Invitrogen, S. Giuliano Milanese, Milan, Italy), then mounted with an anti-fading aqueous medium (Fluorsave, Chemicon Iinternational, Prodotti Gianni, Milano) and observed under a microscope equipped for fluorescence.

GBM components were stained using a rat anti-mouse laminin alpha1 mAb 8B3 (St John and Abrahamson, 2001) a gift from D.Abrahamson, University of Kansas Medical Center. Rat anti-mouse laminin alpha2 mAb 4H8-2 (Schuler and Sorokin, 1995) was purchased from Alexis Biochemicals (San Diego, CA). Rabbit antiserum 8948 to mouse laminin alpha5 has been described (Miner *et al.*, 1997). Rabbit polyclonal antisera to mouse laminin beta1 and 2 (Sasaki *et al.*, 2002) were gifts from T.Sasaki (Max Planck Institute for Biochemistry, Martinsried,

Germany). Rabbit antisera specific for the mouse alpha3, 4, and 5 chains of type IV collagen were as described (Miner and Sanes, 1994) . Rat mAbs to the human alpha1 (mAb H11) and 2 (mAb H22) chains of type IV collagen (Ninomiya *et al.*, 1995), which cross-react with the orthologous mouse proteins, were gifts from Y.Sado and Y.Ninomiya (Okayama, Japan). Alexa 488- and Cy3- conjugated secondary antibodies were obtained from Molecular Probes (Eugene, OR) and Chemicon (Temecula, CA), respectively. For laminin staining, sections were fixed in 2% paraformaldehyde in PBS for 10 minutes and rinsed in PBS. For collagen IV staining, sections were fixed and denatured in urea and blocked in 5% nonfat dry milk in PBS. Antibodies were diluted in PBS with 1% BSA, applied to sections for 1 hour, and rinsed in PBS. Secondary antibodies were then applied in a similar fashion. After rinsing the sections were mounted in 90% glycerol containing 0.1x PBS and 1 mg/ml *p*-phenylenediamine and viewed under epifluorescence with a Nikon Eclipse 800 compound microscope. Images were captured with a Spot 2 cooled color digital camera (Diagnostic Instruments, Sterling Heights, MI). The streptavidin-biotin-method was used on formalin fixed, paraffin embedded tissue to localize ILK (Clone 65.9.1, Upstate Biotechnologies, USA).

Negative controls were performed concurrently by substituting buffer or isotype control immunoglobulins (Rabbit primary antibody isotype control, Zymed, Histoline, Milan, Italy) for the primary antibody.

PFA fixing buffer:

> 2 % PFA
>
> 4 % Sucrose
>
> in 1x PBS

Blocking buffer:

> 2 % FCS
>
> 2 % BSA
>
> 0.2 % Fish-gelatine in PBS

Moviol:

> 40 ml PBS + 10 g Moviol (Calbiochem), stir at RT for 24 h
>
> add 20 ml Glycerol, stir another 24 h at RT
>
> spin in 50 ml Facon at 4000 RPM for 15 min.
>
> take the supernatant, aliquot and store at -20°C

3.10. <u>Transmission electron microscopy</u>

Following perfusion fixation, the left kidney was postfixed by immersion in 3% glutaraldehyde for 24 hours for light microscopic investigations, scanning electron microscopy (SEM), and transmission electron microscopy (TEM), respectively. For transmission electron microscopy (TEM), two to four 1 mm^3 samples of the renal cortex per animal were post-fixed in 1% osmium tetroxide and routinely embedded in Epon. Semithin sections (0.5 μm) were stained with toluidine blue and safranin. Ultrathin sections (70-80 nm) were stained with uranyl citrate and lead citrate and examined with a transmission electron microscope (EM10, Zeiss, Oberkochen, Germany). 2-3 kidney tissue samples per mouse belonging to wt and podoILK -/- mice (n= 2-6) were examined.

3.11. <u>Scanning electron microscopy</u>

For scanning electron microscopy (SEM), 2 mm thick kidney slices were dried by the critical point technique (critical point dryer CPD 030, BAL-TEC, Germany) with liquid carbon dioxide as the transitional medium, mounted on metal stubs with conductive carbon cement (Neubauer Chemikalien, Germany), sputter coated with gold (Sputter Coater 050, BAL-TEC, Germany) and examined with a scanning electron microscope (DSM 940A, Zeiss, Germany) at 15 or 20 kV. Two podoILK -/- mice were examined by scanning electron microscopy each at 3, 4 and 12 weeks of age. At least one wild-type mouse per age-group served as control.

3.12. <u>Determination of the mean glomerular volume</u>

Morphometric evaluation was carried out on a Videoplan$^®$ image analysis system (Zeiss-Kontron, Germany) attached to a microscope by a colour video camera. The mean glomerular volume was determined from the mean glomerular profile area according to the method developed by Weibel and Gomez (Weibel and Gomez, 1962). Cross-sectional area of glomerular profiles in H&E stained plastic sections were systematically sampled according to the unbiased counting rule (Gundersen and Osterby, 1977) and measured planimetrically. The mean glomerular profile area ($\overline{A}_{Glom}$) was determined for an average of 115 glomerular profiles per animal (range: 104-133) and the mean glomerular volume ($\overline{v}_{(Glom)}$) was calculated as $\overline{v}_{Glom} = \dfrac{\beta}{k} * \overline{A}_{Glom}^{3/2}$, where the

shape coefficient β=1.38 pertained to spheres and k=1.04 is a size distribution coefficient assuming a 15% coefficient of variation (Weibel and Gomez, 1962).

3.13. Determination of the filtration slit frequency

In the identical glomerular TEM micrographs, the determination of the filtration slit frequency (FSF) was carried out. The FSF was determined by counting the number of epithelial filtration slits and dividing that number by the length of the peripheral capillary wall at the epithelial interface. On average 324 filtration slits (range 265-387) were counted per animal.

3.14. Microdissection and RNA isolation

3.14.1. Microdissection

Murine renal tissue was used for the microdisection. Mice were sacrificed and the kidneys were removed immediately. The microdissection was performed manually under a stereomicroscope using two dissection needle holders. The material was microdissected in an ice-cold solution. The microdissection was performed in phosphate-buffered saline (PBS) with vanadyl ribonucleoside complex (VRC), VRC (10 mmol/ L; Life Technologies, Karlsruhe, Germany). Only glomeruli without tubuli were transfered in a 1.5 centrifugation tube with 350 µ RLT-buffer, and stored at – 20 °C or directly for the RNA isolation.

3.14.2. RNA isolation

Total RNA was isolated from the glomerulus and from the kidney cortex using the RNeasy kit (Qiagen, Hilden, Germany) according to the manufacturer's instructions. cDNA synthesis was carried out with the SuperScript Choise System kit (Invitrogen, Life Technologies, Breda, The Netherlands). Real-time reverse transcription-PCR (RT-PCR) analysis was performed as previously described 3.16.4

Tissue were minced with a razor blade and 350 µl RLT buffer was added, the same was added for the glomerulus, and homogenised at RT for 30 min. on a shaker. In RLT buffer β-ME (2-Mercaptoethanol) was added before use (β-ME must be added to buffer RLT and RLC before use, Rneasy Mini handbook, Qiagen). The samples were centrifuged for 3 min at 13 000 rpm.

The supernatant was transferred to a new tube and 350 μl of 70 % ethanol was added. The lysate were mixed by pipetting. The contents of the samples were applied to a mini spin column sitting in a 2 ml collection tube and than centrifuged for 15 sec. The flow-through was discarded and 350 μl of RW 1 solution was added then centrifuged for 15 sec at 13 000 rpm. DNAse I mix (10 μl DNAse I + 70 μl RDD buffer) was added to each sample and incubated at RT for 15 min. After the incubation, 350 μl RW 1 was added and centrifuged for 15 sec at 13 000 rpm. The column was placed in the new 2 ml collection tube, and washed 2 times with 500 μl RPE buffer for 2 min at 13 000 rpm. The column was again centrifuged for 1 min. The column was then transferred into a new 1.5 ml collection tube and eluted with 30 μl RNase-free water for 5 min at room temperature incubation, after that the collection tube was centrifuged for 2 min at 13 000 rpm. The RNA was stored at −80 °C or directly transcribed to cDNA. The concentration and purity of RNA was determined by measuring the absorbance (optical density) at 260 nm (A_{260}) and 280 nm (A_{280}). The purity was given trough the ratio between the absorbance values at 260 and 280 nm and had to be in the range from 1.5-1.9.

3.14.3. Reverse transcription

Reverse transcription was performed in a 45 μl volume, containing 9 μl buffer, 2 μl dithiothreitol (DTT; both from Life Technologies), 0.9 μl 25 mmol/L dNTP (Amersham Pharmacia, Freiburg, Germany), 1μl RNase inhibitor (Rnasin; Promega, Mannheim, Germany) and 0.5 μl Microcarrier (Molecular Research Center, Cincinnati, OH, USA), 1μg random hexamers (2 mg/mL stock; Roche, Mannheim, Germany) and 200 U reverse transcriptase (Superscript, Life Technologies) for one hour at 42°C. No DNase treatment was performed, as cDNA-specific primers are available for most targets, the contamination by genomic DNA was low, and a contamination of the cDNA solution by DNase may lead to the loss of the template during prolonged storage.

3.14.4. Real-time quantitative RT-PCR

Real-time RT-PCR was performed on a TaqMan ABI 7700 Sequence Detection System (Applied Biosystems, Weiterstadt, Germany) using heat-activated TaqDNA polymerase (Amplitaq Gold; Applied Biosystems). After an initial hold of 2 min at 50°C and 10 min at 95°C, the samples were cycled 40 times at 95°C for 15 s and 60°C for 60 s. Target gene forward and reverse primers and probes were designed using Primer Express 1.5 software (Applied Biosystems, Foster City, CA). Commercially available predeveloped TaqMan assay reagents were used for the internal

standards human glyceraldehyde-3-phosphate-dehydrogenase (GAPDH) and 18S ribosomal RNA (18 S rRNA). All primers and probes were obtained from Applied Biosystems. The primers for GAPDH, ACTN4, WT-1, synaptopodin, nephrin (NPHS1), and podocin (NPHS2) were cDNA-specific, not amplifying genomic DNA. The following sequences of oligonucleotide primers (300 nM) and probes (100 nM) were used (see Primer list 3.17).

3.15. <u>Statistics</u>

Statistical analysis was performed using the SPSS software (version 11.0; SPSS, Inc., Chigago, IL, USA). Data are generally given as mean ± standard deviation, if not otherwise stated. Student t test was used for paired data. Mean differences of non-parametric data were analysed by the Mann-Whitney U test. Significance was assessed using a Monte Carlo approach with a post-hoc Bonferroni correction. A difference was considered to be statistically significant at $p < 0.05$.

3.16. <u>Antibody list</u>

A detailed list of primary and secondary antibodies used in the study, containing the respective hosts and fixation, is given in Table below:

	Species	Source	Fixation
Nephrin	Rabitt polyclonal	L. B. Holzman	Cryosection
Podocin	Rabitt polyclonal	C. Antignac	
Laminin alpha1	Rat mAb 8B3	D. Abrahamson (St John and Abrahamson, 2001)	2%Paraformaldehyde
Laminin alpha2	Rat mAb 4H8-2	Alexis Biochem.(Schuler and Sorokin, 1995)	
Laminin alpha5	Rabbit polyclonal 8948	J. Miner (Miner *et al.*, 1997)	
Laminin beta1+2	Rabitt polyclonal	T.Sasaki (Sasaki *et al.*, 2002)	
Coll IV alpha 3,4,5	Rabitt polyclonal	J.Miner (Miner and Sanes, 1994)	Urea (Miner and Sanes, 1994)
Coll IV alpha 1,2	Rat mAbs H11 and H12	Y.Sado,Y.Ninomiya (Ninomiya *et al.*, 1995)	

3.17. <u>Primer list for RT-PCR:</u>

Gene		Primer	Accession No.
Alpha-Actinin 4	FP	5'-AGTGCATGGTCCCTCTTTGG-3'	AJ289242
	RP	5'-CGCTGAGAGCAATCACATCAA-3'	
	Probe FAM	5'-ACCAGCTGCTGCACCTTCTCCCA-3'	
Agrin	AoD, Context Seq	5´-GACTGAGAGTGAGAAAGCGCTGCAG-3´	NM_021604
Coll1alpha1	FP	5'-TGCTTTCTGCCCGGAAG A-3'	X54876
	RP	5'-GGGATGCCATCTCGTCCA-3'	
	Probe FAM	5'-CCAGGGTCTCCCTTGGGTCCTACATCT-3'	
Coll4 alpha 1	AoD, Context Seq	5´-GGCTATTCCTTCGTGATGCACACCA-3´	NM_009931
Coll4 alpha 2	AoD, Context Seq	5´-TTGGCCAGGAAGGGGAGCCAGGCCG-3´	NM_009932
Coll4 alpha 3	AoD, Context Seq	5´-TCACCCAGGAAAACCAGGTCCTGCT-3´	NM_007734
Coll4 alpha 4	AoD, Context Seq	5´-ATCAAGATCTTGGTTTGGCAGGCTC-3´	NM_007735
Coll4 alpha 5	AoD, Context Seq	5´-TGTCAGACATGTTCAACAAACCTCA-3´	NM_007736
Coll4 alpha 6	AoD, Context Seq	5´-CCAGGATCTGGGATTTGCTGGCTCC-3´	NM_053185
Dystroglycan	AoD, Context Seq	5´-GGGAGATCATCAAGGTGTCTGCAGC-3´	NM_010017
Fibronectin 1	AoD, Context Seq	5´-GTTTCGGAGGCCAGCGGGGCTGGCG-3´	NM_010233
ILK	FP	5'-ATGAGAATCATTCTGGAGAGCTTTG-3'	U94479
	RP	5'-TGTACTCCAGTCTCGAACCTTCAG-3'	
Integrin alpha3	AoD, Context Seq	5´-GCCTCGCTCAGCTTAATGAATCATC-3´	NM_013565
Integrin beta 1	AoD, Context Seq	5´- GTGGAGCCTGCAGGTGCAATGAGGG-3´	NM_010578
Laminin beta2	AoD, Context Seq	5´-GAGGCTGAGAAACAACTACGGGAAC-3´	NM_008483
Nephrin	AbD, FP	5'-ACCCTCCAGTTAACTTGTCTTTGG-3'	AF168466
	AbD, RP	5'-ATGCAGCGGAGCCTTTGAA-3'	
	AbD, Probe FAM	5'-TCCAGCCTCTCTCC-3'	
Nidogen-1	AoD, Context Seq	5´-TGGGTGGATGCAGGCACCCATAGGG-3´	NM_010917
P-Cadherin	FP	5'-GCTCTACCACGACGGCAGAG-3'	X06340
	RP	5'-GCCTCATACTTCTGCGGCTC-3'	
	Probe FAM	5'-CCTTGATGCCAACGATAACGCTCCG-3'	
Perlecan	AoD, Context Seq	5´-GTACGGCCAAGAGCAAATCCCCAGC-3´	M77174
Podocin	AbD, FP	5'-GGGACATCTGCTTCCTGGAA-3'	AY050309
	AbD, RP	5'-TGATAGGTGTCCAGACAGGGTAAAA-3'	
	AbD, Probe FAM	5'-AACAGGCCAGGACCT-3'	
18S rRNA	PDAR		
Synaptopodin	AbD, FP	5'-TTCCTTGCCCTCACTGTTCTG-3'	AF077003
	AbD, RP	5'-TCCTAGCAGCAATCCACATCTG-3'	
	AbD, Probe FAM	5'-CCTAGCTTTCTAAAGGAC-3'	
WT-1	AbD, FP	5'-CAGCTCAAAAGACACCAAAGGA-3'	M55512
	AbD, RP	5'-CGCTGACAAGTTTTACACTGGAAT-3'	
	AbD, Probe FAM	5'-ACACAGGTGTGAAACC-3'	
ZO-1	AoD, Context Seq	5´-TCTGAGGGGAAGGCGGATGGTGCTA-3´	NM_009366

Forward-Cre	5' GCA TAA CCA GTG AAA CAG CAT TGC TG 3'
Reverse-Cre	5' GGA CAT GTT CAG GGA TCG CCA GGC G 3'
Forward-ILK	5' CCA GGT GGC AGA GGT AAG TA 3'
New-For-ILK	5' AAG GTG CTG AAG GTT CGA GA 3'
Reverse-ILK	5' CAA GGA ATA AGG TGA GCT TCA GAA 3'

3.18. Equipment and reagents

Cell culture incubator	Cytoperm 8080, Heraeus GmbH, Hanau, Germany
Electrophoresis equipment	Biorad laboratories, München Hercules, CA, USA
Confocal microscope	Leica, Bensheim
E. coli Pulser	Biorad, München
Zentrifuge 5417	Eppendorf, Hamburg
Spectrophotometer	Pharmacia, Hamburg
Water bath	Köttermann labortechnik, Uetze-Hänigsen

3.18.1. Product list

Name	Supplier
Acrylamid	Bio Rad, München
Agarose (electrophorese)	Biozym
Agarose high EEO	Biomol
Ammoniumpersulfate (APS)	Sigma, Deisenhofen
Ampicillin	Sigma, Deisenhofen
Anti-DIG-FAB-fragments alkaline phosphatase	Roche, Karlsruhe
Bacto-Agar	DIFCO laboratories
Beta-mercaptoethanol	Merck, Darmstadt
Blocking reagent	Roche, Karlsrhe
Boric acid	Merck, Darmstadt
Bromphenol blue	Merck, Darmstadt
BSA	Sigma, Deisenhofen

CaCl$_2$	Sigma, Deisenhofen
CO$_2$-Gas	Air Liquide
Coomassie brilliant blue R 250	Serva, Heidelberg
DAPI	Pierce
Denhardt's solution	Sigma, Deisenhofen
Dextran sulfate	Sigma, Deisenhofen
Diethylether	Hoechst
DIG-RNA labelling mix (10x; GIG-UTP)	Roche, Karlsruhe
Di-Sodiumhydrogenphosphate Na$_2$HPO$_4$	Merck, Darmstadt
DMEM/Nut. Mix.F12	Gibco BRL, Karlsruhe
DNTP	Pharmacia Biotech
Dulbecco's modified Eagle Medium (DMEM)	Gibco BRL, Karlsruhe
ECL	Amersham Biosciences
EDTA	Merck, Darmstadt
EGF	Sigma, Deisenhofen
Ethanol absolute (EtOH)	Merck, Darmstadt
Foetal Calf Serum (FCS)	Life technologies, Karlsruhe,
Formamide	Merck, Darmstadt
Gentamycin	Gibco BRL, Karlsruhe
Glycerol	Merck, Darmstadt
Glycin	Sigma, Deisenhofen
Hank's buffered salt solution (HBSS)	Gibco BRL, Karlsruhe
Heparin sodium salt, grade II	Sigma, Deisenhofen
HEPES-Buffersolution	Gibco BRL, Karlsruhe
HotStar Taq-Polymerase	Qiagen, Hilden
HRP-conjugated secondary anti-mouse antibody	Amersham LifeScience

Immersion oil	Zeiss, Oberkochen
Insulin	Sigma, Deisenhofen
Isopropanol	Merck, Darmstadt
Kaliumchloride KCl	Merck, Darmstadt
Kaliumdihydrogenphosphate KH_2PO_4	Merck, Darmstadt
LB broth base	Gibco BRL, Karlsruhe
l-glutamine	Gibco BRL, Karlsruhe
Maleic acid	Fluka, Buchs, Switzerland
Methanol absolute (MeOH)	Merck, Darmstadt
$MgCl_2$	Merck, Darmstadt
$MgSO_4-7H_2O$	Merck, Darmstadt
MidiPrep-Kit	Qiagen, Hilden
MidiTip 100 column	Qiagen, Hilden
Molecular weight marker (1kb-ladder)	Gibco BRL, Karlsruhe
Molecular weight marker (500bp-ladder)	Peqlab, Erlangen
NaCl	Merck, Darmstadt
NaH_2PO_4	Merck, Darmstadt
$NaHCO_3$	Merck, Darmstadt
Natriumtetraborate (Borax) $Na_2B_4O7-H_2O$	Sigma, Deisenhofen
Paraformaldehyde (PFA)	Merck, Darmstadt
PCR-buffer (10x)	Invitrogen
Penicillin/Streptomycin-solution	Gibco BRL, Karlsruhe
Polyoxyethylenesorbitanmonolaurate (Tween-20)	Biorad, München
Ponceau	Roth, Karlsruhe
Propidium-iodide (PI)	Sigma, Deisenhofen
Proteinase K	Roche, Karlsruhe

PVDF-membrane HybondECL	Amersham LifeScience
Restriction enzymes	New England Biolabs
RNA polymerase	Stratagene
RNAse A	Qiagen, Hilden
RNAse inhibitor	Boehringer Mannheim
RNeasy Kit	Qiagen, Hilden
RT-PCR Enzyme Mix	Roche, Karlsruhe
RT-PCR Reaction Mix SYBR green	Roche, Karlsruhe
SDS/Natriumlaurylsulfat	Roth, Karlsruhe
Selenite	Sigma, Deisenhofen
Skimmed dry milk	Glücksklee
Sodium citrate	Merck, Darmstadt
Sodiumacetate	Merck, Darmstadt
Sucrose	Merck, Darmstadt
Superscript Reverse Traskriptase	Gibco BRL, Karlsruhe
Taq-DNA-Polymerase	Qiagen, Hilden
TaqMan Master Mix	PE Applied Biosystems
TEMED	Sigma, Deisenhofen
Thyraxine	Sigma, Deisenhofen
Transcription buffer (5x)	Stratagene
Transferrin	Sigma, Deisenhofen
Tris-base	Merck, Darmstadt
Tris-HCl	Merck, Darmstadt
Triton X-100	Roth, Karlsruhe
Trypsin-EDTA	Gibco BRL, Karlsruhe
Tween 20	Sigma-Aldrich, St.Louis, Mo, USA

Xylol   Roth, Karlsruhe,

Yeat extract   ICN pharmaceuticals,

                                         Aurora, OH, USA

3.18.2. <u>Consumables</u>

Name	**Supplier**
Cell culture dishes	Falcon
Cell culture flasks	Falcon
Cell culture tubes	Falcon
Color slide film Elite Chrome	Kodak
Coverslips	Peske
Eppendorf tubes	Eppendorf, Hamburg
Glass slides	Menzel Gläser
Multi-well cell culture-plates	Nunc
Parafilm	American National can
Pasteur pipettes	Volac
PCR-tubes (0.2 ml)	Roth, Karlsruhe
Permeable filtermembrane inserts Millicell-CM	Millipore
Pipettes, sterile (5, 10, 25 ml)	Falcon
Razor blades	Gilette
Syringe filters	Renner
Syringe needles	Terumo
Syringe fine dosage 1 ml	Braun
Syringes (10-50 ml)	Becton Dickinson
Whatman chromatography paper	Whatman
X-ray films	Kodak

3.18.3. <u>Instruments</u>

Name	Supplier
Agarose gel chambers	MPI-workshop
Bacterial incubater	Heraeus, Hanau
Bacterial shaker	New Brunswick Science
Bench centrifuge	Eppendorf, Hamburg
Cell culture incubator	Heraeus, Hanau
Cooling centrifuge Sepatech Omnifuge	Heraeus, Hanau
Cryostate	Leica, Bensheim
Lightcyler	Roche, Karlsruhe
Neubauer-counting chamber	Superior
Phase contrast microscope Diavert	Leitz, Wetzlar
Semibry blotting chamber	MPI-workshop
Sorvall RC-5B refrigerated superspeed centrifuge	DuPont Instruments
Spectrophotometer, Ultrospec 3000	Pharmacia Biotech
Stereomicroscope	Leica, Bensheim
Steril hood Edge Gard Hood	The Baker Combany
Tissue chopper	Mickle Laboratorye
Vibratome Vibraslice 752M	Campden Instruments
Waterbath	GFL
Western-blotting chamber	Biorad, München

Results

4. Results

4.1. Cre transgenic mouse

The podocin-specific Cre recombinase transgenic male mice were backcrossed with wild-type C57BL/6 female mice to maintain the transgenic background. The resulting offspring were heterozygous for Cre and wild type littermates.

To determine the presence of Cre transgene in a diverse offspring population consisting of heterozygous and wild-type littermates, genomic DNA isolated from the tails of 3 week old littermates was subjected to PCR (Moeller *et al.*, 2002) as described in detail in materials and methods. This resulted in the amplification of a 364 bp DNA fragment (Fig.11) indicating the presence of the Cre transgene. Mice lacking the presence of this DNA fragment were considered to be wild type. As expected, the Cre-transgenic mice were born according to the Mendelian frequency.
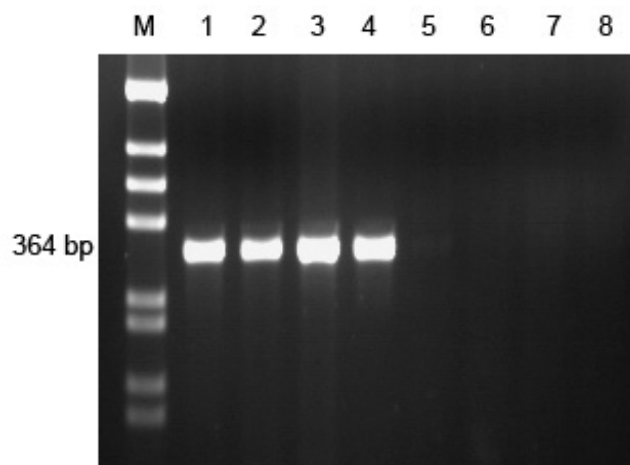

Figure 11 : Genotypic analysis for Cre mice.

DNA from 3 week old Cre/ C57BL-6 backcrossed offspring was subjected to PCR as described in materials and methods. The amplified product was subjected to 2% agarose gel electrophoresis. Ethidium bromide staining of the gel confirmed the presence of a 364 bp band corresponding to the transgenic and no band for the wild type litter mates.

4.2. <u>ILK-Lox transgenic mice</u>

The flox-ILK transgenic mice having LoxP sites inserted downstream from exons 4 and 12 at the ILK locus had been created through homologous recombination in embryonic stem cells as described (Terpstra 2003). Male and female flox-ILK mice were bred to maintain the same background genotype. Genomic DNA isolated from the tails of 3 week old littermates was subjected to normal PCR with the conditions described in materials and methods. Offspring which were homozygous for flox-ILK gave a band of 2.1 Kb indicating homozygosity for the floxed allele (ILK$^{flox+/+}$). Backcrossing flox-ILK with another mouse line showed an additional band of 1.9 Kb for wild type and 2 bands of 2.1 Kb and 1.9 kb indicating the heterozygosity of the mice.
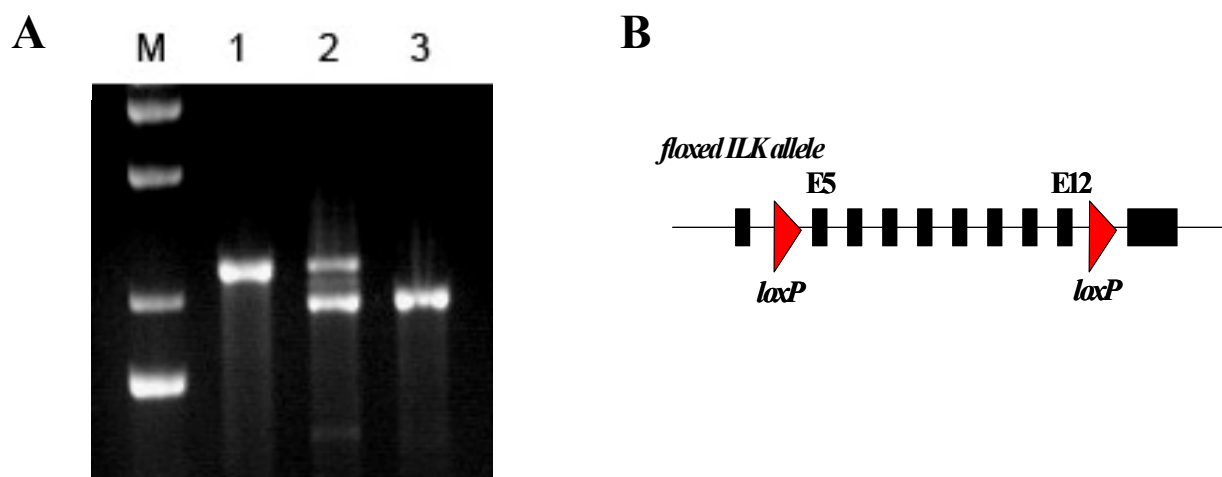
A

B

Figure 12 : Generation of ILK lox mice

A. DNA from 3 week old Flox-Ilk mice was subjected to PCR as described in materials and methods. The amplified product was subjected to 0.7% agarose gel electrophoresis. Ethidium bromide staining of the gel confirmed the presence of a 2.1 kb band corresponding to the homozygous flox-ILK +/+ transgenic, 2 bands for the heterozygote flox ILK+/- and a band of 1.9 kb for wild type littermates.

B. Schematic representation of the floxed ILK allele. Red triangles are the loxP sites, E: exon.

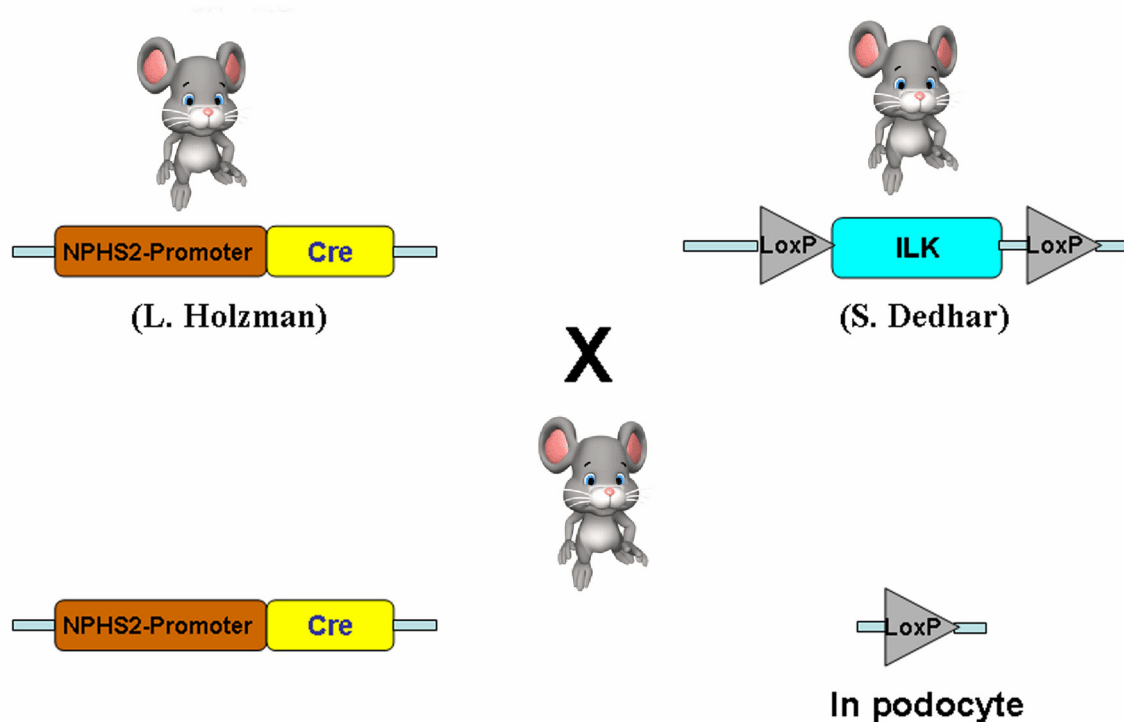## 4.3. <u>Breeding scheme for the inactivation of ILK</u>

Figure 13: Strategy of podocyte specific ILK deletion.

Two mouse lines are needed to delete the ILK gene. The first line expressing, the Cre-recombinase under the control of the podocin promoter and the second mouse line is containing the flox sequences flanking the ILK gene. The two mouse lines were crossed to get a line with deleted ILK.

This strategy was designed to delete the kinase domain of the ILK. By mating floxed ILK mice with Podocin-Cre transgenic mice lines, mice heterozygous from the F1 generation were obtained having the genotype ILK$^{flox+/-}$, Cre$^{+/-}$. These mice were crossed with the homozygous floxed ILK mice to inactive both ILK alleles by Cre-mediated excision having the genotype ILK$^{flox+/+}$ and Cre$^{+/-}$. The ability of Cre to recombine the floxed ILK allele was examined by PCR analysis of tail genomic DNA. DNA from other tissues like lung, spleen, muscles and thymus was also used for the PCR analysis. The 396bp amplicon corresponding to the excised floxed ILK allele was detected only in kidney cortex in both ILK$^{flox+/-}$, Cre$^{+/-}$ (heterozygous for Lox-ILK) and ILK$^{flox+/+}$, Cre$^{+/-}$ (homozygous for Lox-ILK) mice, indicating that Cre was expressed only in podocytes and that the Cre was capable of recombining the loxP sites within the ILK gene. Mice of all genotypes were born at the expected Mendelian frequency.

4.4. Targeted inactivation of ILK in podocytes of podoILK-/- mice

To prevent embryonic mouse lethality in ILK null embryos (Sakai *et al.,* 2003), the mice with flanking LoxP sites (floxed) of the ILK exons 5 to 12 (ILK$^{flox+/+}$) were crossed with mice expressing the Cre recombinase under the control of a podocyte specific promoter podocin$^{Cre+/-}$ as shown in the Fig. 13. Resulting bitransgenic mice were crossed to homozygous ILK$^{flox+/+}$ mice to obtain the ILK$^{flox+/+}$/podocin$^{Cre+/-}$ (podoILK -/-).

To determine whether the ILK gene was specifically depleted or inactivated in podocytes of ILK$^{flox+/+}$ mice, and to evaluate the ability of the podocin-Cre recombinase to excise the floxed ILK alleles, DNA from kidney cortex was subjected to PCR amplification by using appropriate primers . The PCR amplification resulted into a 369 bp amplicon corresponding to the excised floxed ILK allele. This amplicon product was neither detected in tail or in lungs (Fig. 14) nor in other organs like thymus, heart, muscles etc. (data not shown) of ILK$^{flox+/+}$/podocin$^{Cre+/-}$ mice (podoILK -/-). This data confirms a tissue specific recombination of the loxP sites within the ILK locus.
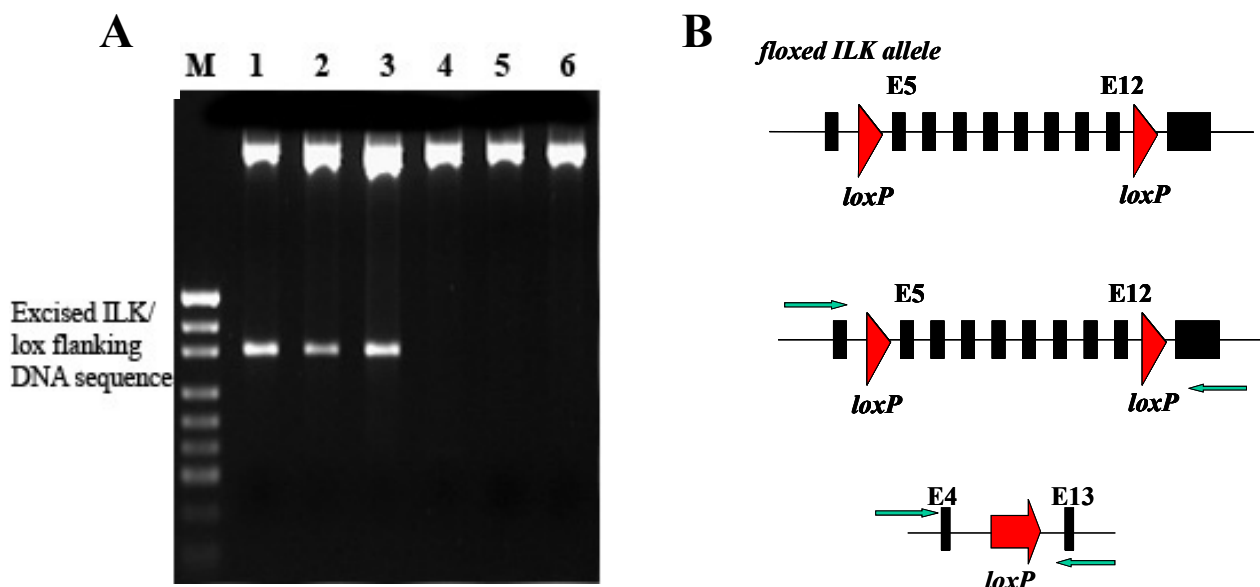

Figure 14: Genotypic analysis of Cre-mediated excision of the floxed ILK allele in podocytes.

A. DNA was prepared from kidney cortex and analyzed by PCR, resulting in a 1.9kb product in wild type, a 2.1kb product in floxed and a 230bp product after Cre mediated-excision in podocytes. Lanes 4, 5 and 6 are floxed not expressing Cre – tail DNA.

B. Schematic representation of the deletion strategy.

To investigate changes in the basal expression of the ILK gene, mRNA from microdissected glomeruli of podoILK -/- mice was analyzed by a Real Time quantitative RT-PCR. The results showed that the steady state ILK mRNA was reduced by 74% (Fig. 15) in Cre-positive littermates i.e. podoILK -/- vs. 18S rRNA ($0.59 \pm 0.53 \times 10^{-3}$; n=4) as compared with Cre-negative i.e. podoILK +/+ vs. 18S rRNA ($2.29 \pm 1 \times 10^{-3}$; n=7).
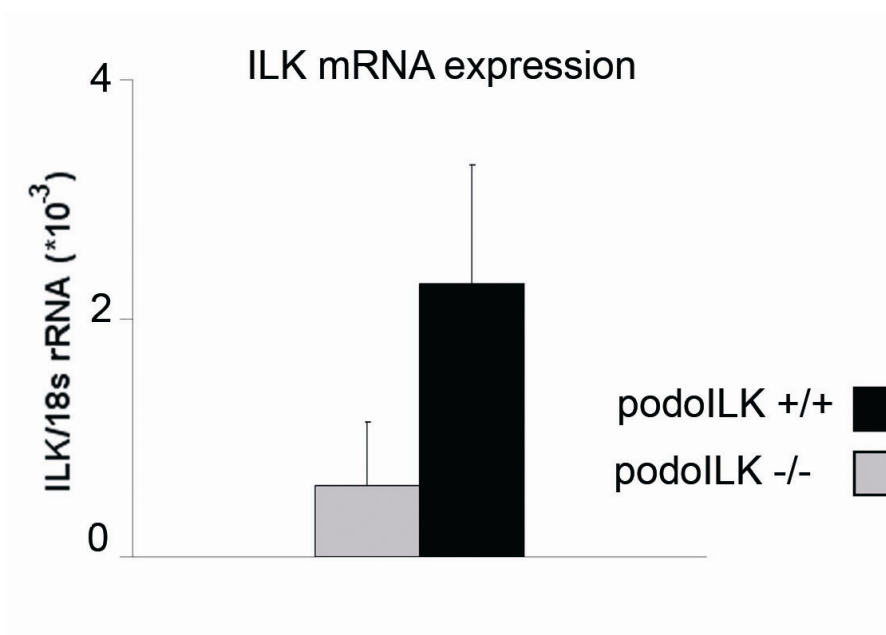

Figure 15: ILK mRNA levels in microdissected glomeruli.

25 microdissected glomeruli per mouse of 2 week old mice were examined. The diagram showed a reduction of ILK mRNA by 74% in real-time RT-PCR, expressed as ratio to 18s rRNA as the reference gene.

ILK has been shown to be expressed in glomerular mesangial cells and glomerular podocytes (Hammes *et al.*, 2001; Kretzler *et al.*, 2001). To demonstrate ILK deletion and the localization of ILK protein expression in podocytes by immunohistochemical (IHC) analysis, a monoclonal mouse anti-ILK antibody was used to detect the expression of ILK in various segments of the kidney of podoILK +/+ and podoILK -/- mice. Intra-glomerular ILK protein expression was detected in the mesangium and at the periphery of the GBM to which the podocyte foot processes are firmly attached. In podoILK -/- mice the mesangial staining remained unchanged, but the GBM-associated signal was lost, confirming loss of podocyte ILK expression (Fig. 16).
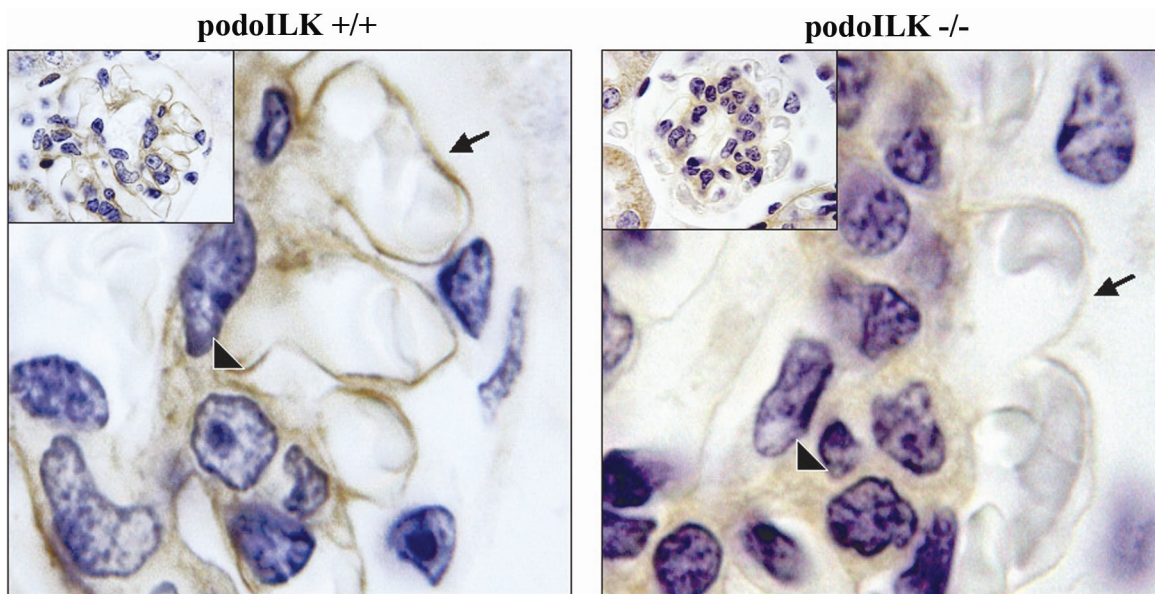
Figure 16: Glomerular ILK protein expression.

In wild type animals (podoILK +/+), ILK is detected by immunohistochemistry in the mesangium and in podocyte foot processes along the filtration barrier (perimesangial and pericapillary GBM). In homozygous floxed ILK / heterozygous podocin Cre mice (podoILK -/-) the ILK signal is lost at the filtration barrier (arrow). The ILK staining in the mesangium (arrow head) remained unaltered.

4.5. PodoILK -/- mice exhibit changes in bio-physical parameters

4.5.1. Body weight

Female and male wild type podoILK +/+ and podoILK -/- mice were weighed at 4 weeks and 12 weeks of age. There was no difference in body weight of podoILK -/- and wildtype mice at 4 weeks in either sex (Fig. 17).

At 12 weeks of age the body weight decreased significantly in female and male podoILK -/- mice compared to the wild type mice (Figure 17).

There was no difference in the body weight of Flox-ILK transgenic (alone) and Cre transgenic mice (alone) compared to the wild type control mice irrespective of the sexes (data not shown).
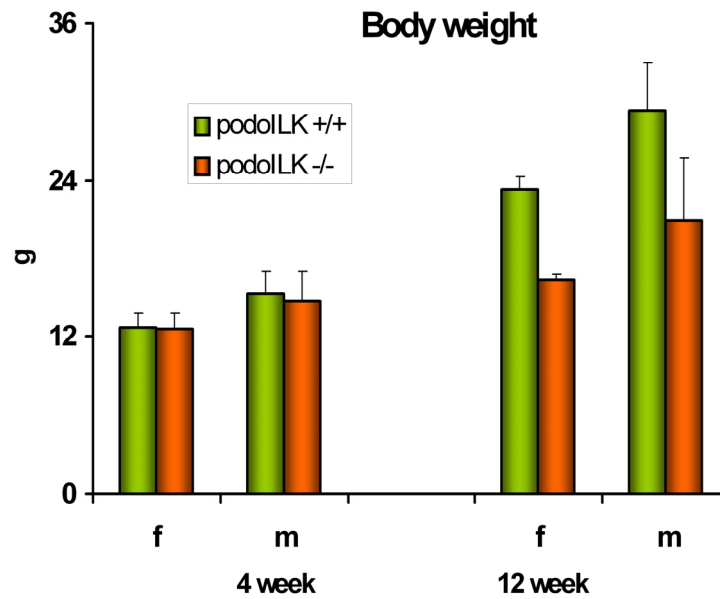
Figure 17: Body weight at 4 and 12 weeks.

Male and female wild type and podoILK -/- mice were weighted at 4 and 12 week. Only at 12 weeks of age a significant decrease of body weight of podoILK -/- mice was observed. Number of animals was at least 6 in each group.

4.5.2. Kidney weight

Kidney weight was determined at 4 and 12 weeks of age when mice were sacrificed. No differences was seen in kidney weight and kidney-to-body weight ratio at 4 weeks of age in male and female podoILK -/- compared to the control mice.
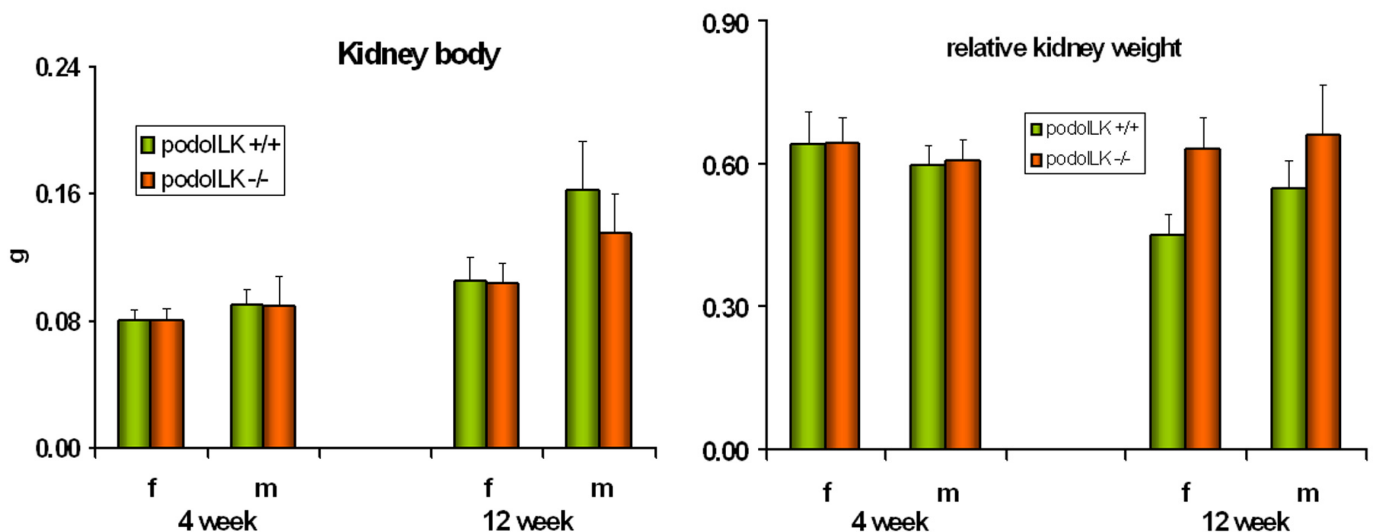

Figure 18: Absolute (A) and relative (B) kidney weight.

Kidneys from control and knockout mice were weighed at 4 and 12 week of age. Number of animals examined was 6 in each group.

At 12 weeks of age, no significant differences of kidney weight in female podoILK -/- was observed as compared to sex matched wild type mice. Both absolute and relative kidney weights of male podoILK -/- mice were decreased and increased respectively.

4.5.3. <u>Urine protein analysis</u>

To determine the level of proteinuria, urine from 2, 4 and 12 week old podoILK -/- and podoILK +/+ mice was examined using SDS-PAGE. A mouse albumin standard was used as a positive control. A 66 kDa band corresponding to the albumin standard was detected in some 2 and consistently in 4 and 12 week old podoILK -/- mice (Fig. 19 A, lanes 1-6). However, wild type podoILK +/+ mice did not show any presence of albumin in the urine.

Heterozygous mice for the floxed ILK allele (ILK$^{flox+/-}$/podocin$^{Cre+/-}$) had no overt phenotype and urine analysis showed the absence of albuminuria up to 15 month of age (data not shown). Moreover, podoILK -/- mice show rapid progression of proteinuria to terminal renal failure.

Additionally, the total protein level was measured using the Bradford method as described in the material and methods. 12 week old podoILK -/- mice showed a massive increase in total urine protein content as compared to 4 and 2 week old podoILK -/- mice. PodoILK +/+ mice did not show an increase in the total urine protein content (Fig. 19 B).
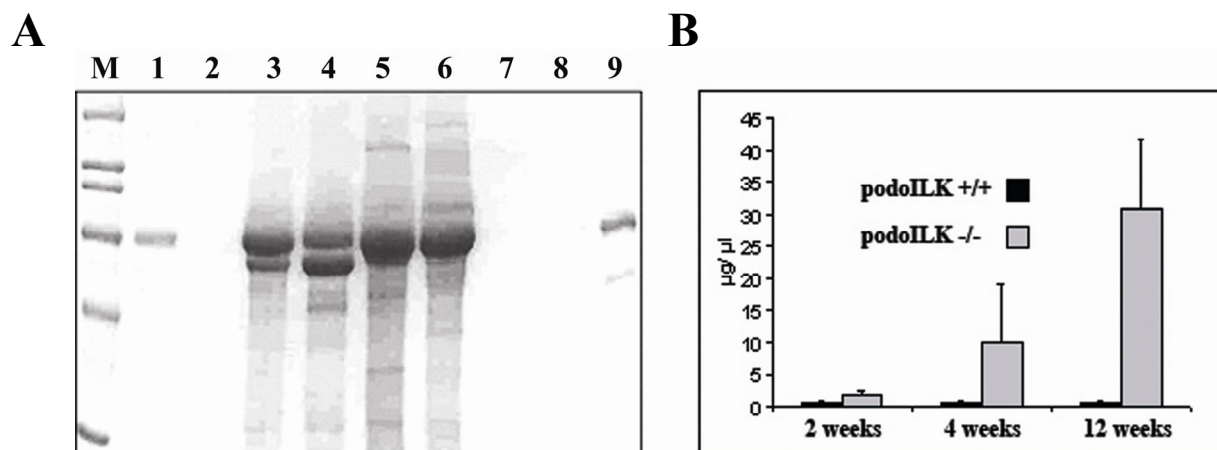

Figure 19: SDS-PAGE.

A) 3 µl of mouse urine is analysed on SDS-PAGE stained with comassie blue. PodoILK -/- mice show a selective albuminuria as early as 2 weeks of age (lane 1- 2; 2 week old animals) and progresses rapidly to unselective proteinuria (lane 3-4; 4 week old animals and lane 5-6; 12 week old animals). Wild type control shows no proteinuria (lane 7-8; 12 week old animals). Lane 1 contains molecular weight markers. Lane 9 shows albumin standard.
B) Protein to creatinine ratio detects progressive proteinuria in podoILK -/- mice. The bar graphs show elevated protein/ creatinine ratio at 4 and 12 weeks.

4.5.4. <u>Biochemical analysis of blood</u>

To determine the biochemical alteration in the disease, blood was collected from wild type und podoILK -/- mice at 12 weeks of age to determine serum parameters. The biochemical analysis was consistent with massive proteinuria and impaired renal function. Creatinine, cholesterol and triglyceride levels were significantly increased compared to wild type mice. In contrast, blood urea nitrogen, albumin and total protein levels were not changed comparing both groups (table 1.)

Group (n)	Crea-tinine mg/dl	Urea mg/dl	Choles-terol mg/dl	Albumin g/dl	Total protein g/dl	Triglyc-eride mg/dl
Podo ILK +/+	0,36 ± 0,03	27,15 ± 4,57	78,25 ± 7,59	3,44 ± 0,28	5,55 ± 0,24	86,00 ± 24,86
Podo ILK -/-	0,66* ± 0,24	79,42 ± 61,65	400,25* ± 189,65	2,54 ± 0,43	5,72 ± 0,54	124,0* ± 30,08

Table 1: Serum analysis.

Wild type; n = 4 (podoILK +/+) and podoILK -/-; n = 4 at 12 weeks of age were analysed. An increase of creatinine, cholesterol and triglyceride were observed in podoILK -/- mice. Data presented are the means ± SD. The statistical analysis was carried out using the students t test. * p< 0.05.

4.5.5. <u>Survival curve</u>

Transgenic mice were observed up to 1 year of age. PodoILK -/- mice appeared normal at birth, but showed a drastically reduced life span with a median age of death at 19 weeks (Range: 8-32 w) (Fig. 20). Sequential urine analysis revealed the first appearance of selective albuminuria at 2-4 weeks of age, progressing to unselective proteinuria between 4 -12 weeks (Fig. 19A). In contrast, all ILK$^{flox+/-}$/podocin$^{Cre+/-}$ survived the 12 months observation period as well as the the control mice ILK$^{flox+/+}$/podocin$^{Cre-/-}$ (data not shown).

Survival curve

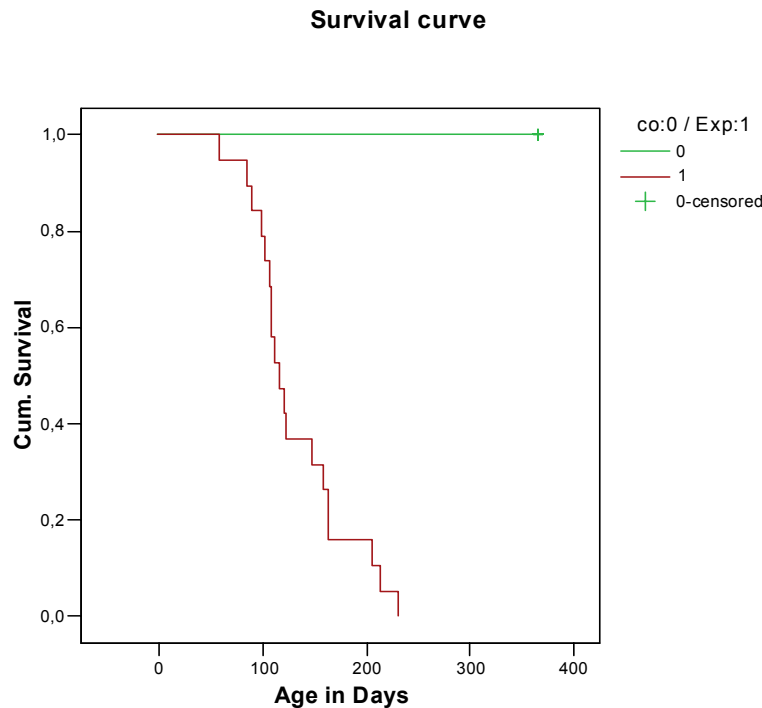**Figure 20: Caplan Meyer survival curve.**

PodoILK +/+ and podoILK -/- mice were observed for 12 months, demonstrating 100% lethality of podoILK -/- with an average of 19 weeks (range 8-32 weeks). All transgenic animals died within the period investigated. Green line is the wild type mice and the rust line is the ILK$^{flox+/+}$/podocin$^{Cre+/-}$. Green line represents the wild type mice and the brown represents podoILK -/- mice.

4.5.6. <u>Histological analysis</u>

Macroscopically, kidneys from podoILK -/- mice showed the classical features of nephrotic, endstage kidneys with rough surface and yellow appearance, but were comparable in size to podoILK +/+ mice (Fig. 21 A). From 12 weeks of age on wards, all podoILK -/- mice show this classical end stage phenotype of the kidney. Histological staining of the sections of the kidney showed normal glomerular and tubular staining in the wild type in contrast to the podoILK -/-mice. Tubules were loaded with proteinacouse casts and the glomeruli showed a total loss of texture (Fig. 21 B).
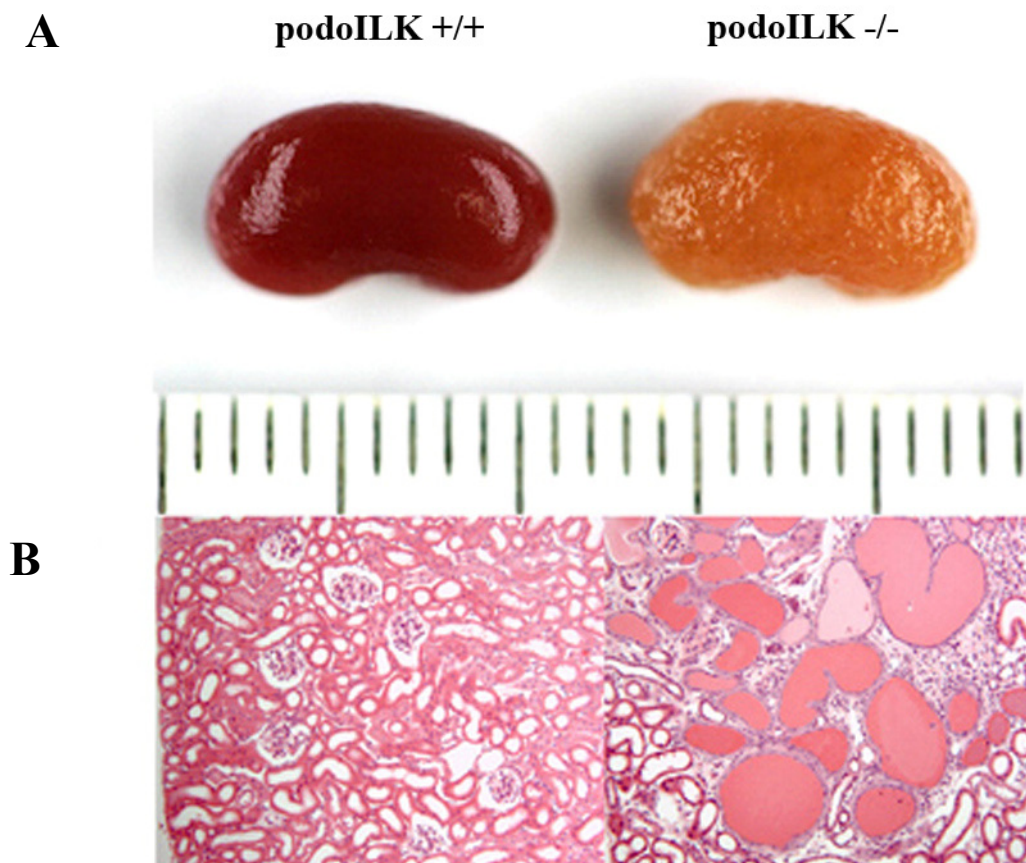
Figure 21: Structural alteration in podoILK -/- mice.

A) Kidneys from podoILK +/+ and podoILK -/- mice at 16 weeks of age. Endstage, fibrotic kidneys with   loss   of renal architecture are observed in podoILK -/- mice.

B) Section of the kidney stained with H&E from wild type and podoILK -/- at 12 weeks. Glomeruli from wild type mice are with a normal tubular interstitium.

4.6. PodoILK -/- mice develop progressive focal segmental glomerulosclerosis

Histological examination of kidneys from wild-type mice, podoILK +/- and podoILK -/- mice from 1 to 16 weeks of age revealed the development of progressive filtration barrier failure in podoILK -/- mice (Fig. 22 and 23). Light microscopic examination was carried out on the kidneys from six wildtype mice, seven podoILK +/- and seven podoILK -/- mice at 1 and 12 days of age, five wildtype and five podoILK -/- mice at 19 days of age, five wildtype, four podoILK +/- and six podoILK -/- mice at 25-28 days of age as well as four wildtype and 12 podoILK -/- mice

ranging from 53 to 119 days of age.

Kidneys from 1 and 12-day-old podoILK -/- mice showed the typical gradient of postnatal renal development and were indistinguishable from those of wild-type mice, thereby indicating normal nephrogenesis in podoILK -/- mice.

At the onset of microalbuminuria at 3 weeks of age, podoILK -/- mice showed hypertrophy of single podocytes and their nuclei, predominantly in juxtamedullary glomeruli, as compared to wildtype mice. At 4 weeks, juxtamedullary glomeruli of podoILK -/- mice frequently demonstrated enlarged podocytes, which occasionally exhibited vacuolization and pseudocyst formation as well protrusions and microvillous transformation of the epithelial surface, which became particularly evident in semithin sections (Fig. 23). Further findings in juxtamedullary glomeruli included segmental mesangial expansion with increased matrix deposition and large distorted capillaries.

More advanced glomerular lesions, associated with tubulointerstitial changes, were consistently found in podoILK -/- animals ranging from 8-16 weeks of age. Numerous podocytes were severely enlarged, showed multiple vacuoles, protrusions and microvillous transformation. Glomerular changes included focal and segmental sclerotic lesions, characterized by tuft adhesions to Bowman's capsule with collapse and occasional occlusion of capillaries by hyaline material, detachment of podocytes and loss into the urinary space, crescent formation, mesangial expansion with increased matrix deposition, dilated and distorted capillaries and focal glomerular obsolescence. Protein reabsorption droplets were observed in proximal tubular epithelia as well as proteinaceous casts in some distal tubules, and small fibrotic foci were evident in the interstitium. End-stage kidney lesions were characterized by diffuse glomerulosclerotic changes, with severe vacuolization of podocytes and epithelia of Bowman's capsule, segmental to circumferential synechiae, fibrocellular or epithelial crescents with pseudotubular structures, and mesangial expansion with accumulation of mesangial matrix. Less severely damaged glomeruli showed distortion of the tuft structure including derangements of the capillary folding pattern as well as dilatation of capillaries. Further, glomerular obsolescence due to hyalinosis was a common finding. Tubulo-interstitial lesions included cystic dilation of tubules with proteinaceous casts in distal tubules, tubular atrophy, severe interstitial fibrosis and focal edema as well as predominantly perivascular, mononuclear infiltration and accumulation of hemosiderin containing macrophages. PodoILK +/- and wild-type mice of the different age-groups showed no pathological kidney changes.
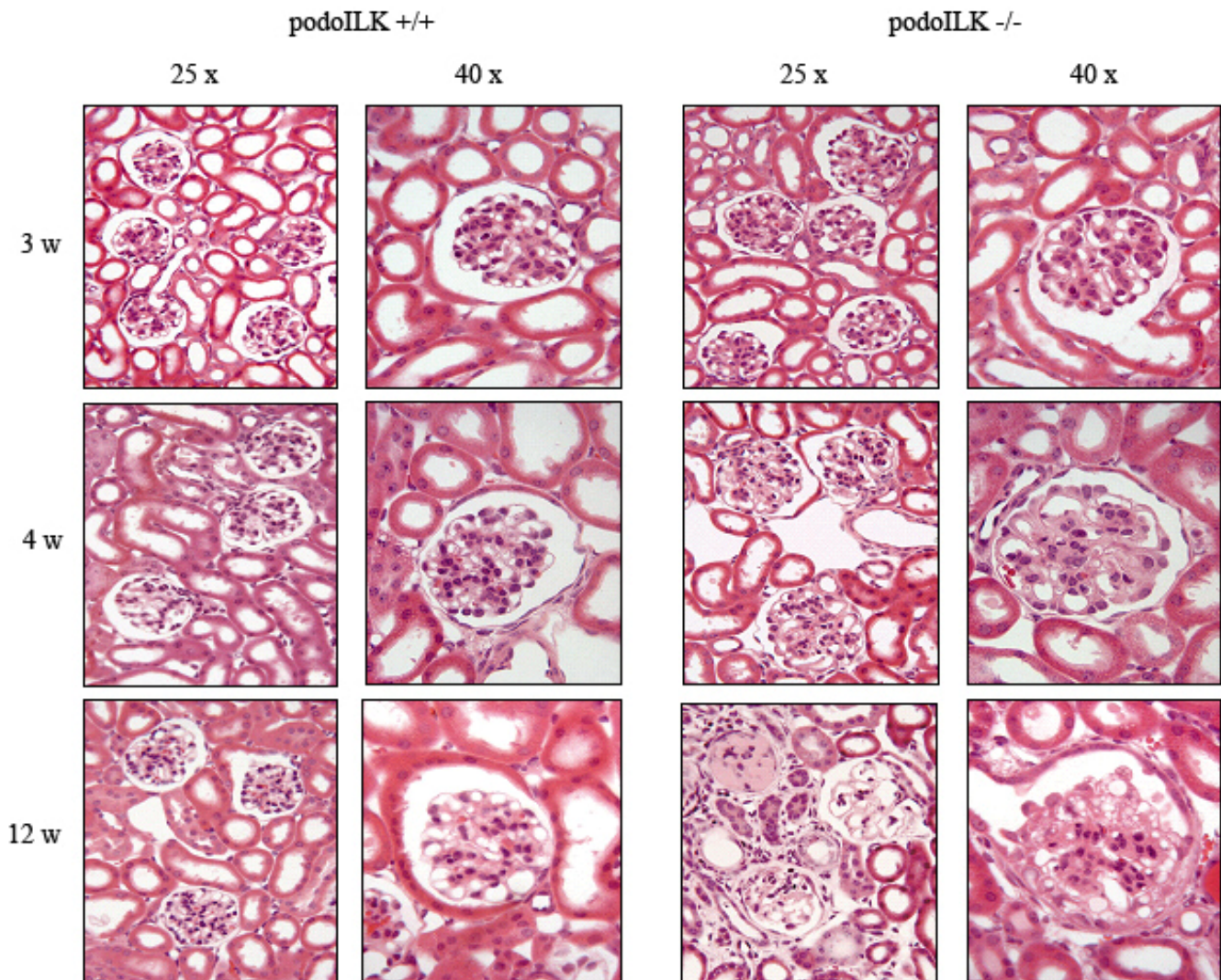
Figure 22: Progressive glomerulosclerosis and tubulointerstitial fibrosis in podoILK -/- mice.

At 3 weeks of age, no differences in podoILK -/- mice are seen compared to wild type animals. At 4 weeks of age, juxtamedullary glomeruli of podoILK -/- mice frequently demonstrate hypertrophy of podocytes and segmental mesangial expansion with increased matrix deposition and large distorted capillaries.

At 12 weeks of age, more advanced glomerular lesions, associated with tubulo-interstitial changes, are seen in podoILK -/- mice. Glomeruli showed focal and segmental sclerotic lesions, characterized by tuft adhesions to Bowman's capsule with collapse and occasional occlusion of capillaries by hyaline material, detachment of podocytes and loss into the urinary space, crescent formation, mesangial expansion with increased matrix deposition, large distorted capillaries and focal glomerular obsolescence. Tubulointerstitial lesions show tubular atrophy, severe interstitial fibrosis and a mononuclear infiltration.
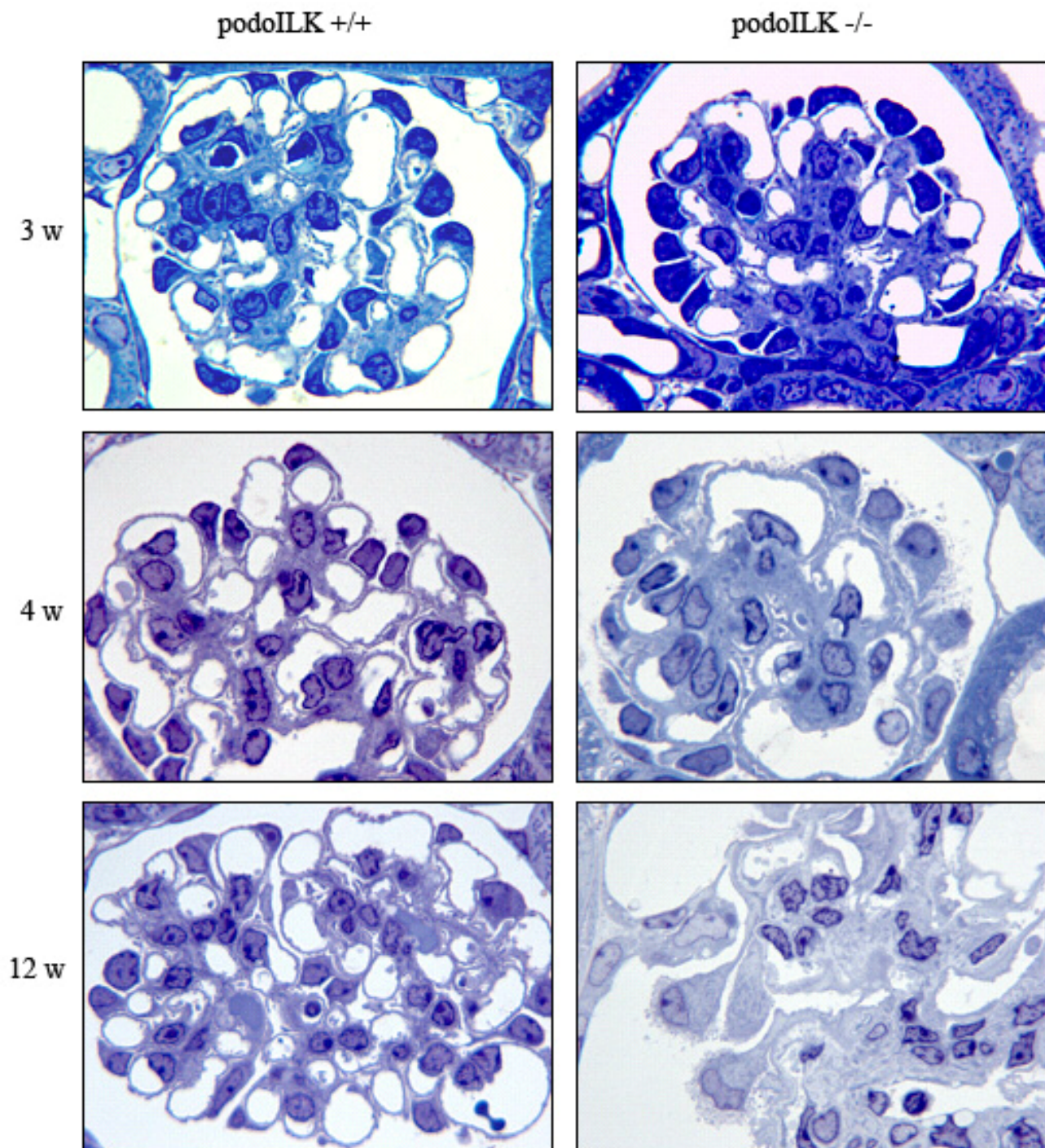
Figure 23: Glomerular architecture in semi-thin sections of podoILK -/-.

At 3 weeks of age, in the juxtamedullary glomerulus shown, podoILK -/- mice show single hypertrophic podocytes compared to wild type mice.

At 4 weeks, juxtamedullary glomeruli of podoILK -/- mice demonstrate hypertrophy of podocytes with protrusions and microvillous transformation of the epithelial surface.

4.7. PodoILK -/- mice show GBM and podocyte alteration at onset of albuminuria

As albuminuria preceded the development of the FSGS lesions, the ultrastructure of the filtration barrier was evaluated at the first sign of filtration barrier damage in podoILK -/- and thereafter. Two to three samples per mouse of two to three wild type and two to six podoILK -/- mice of each age group were examined by transmission electron microscopy.

At 1 and 12 days of age, no differences between podoILK -/- and wildtype mice were observed. At 3 weeks with onset of albuminuria, prominent podocytes in the juxtamedullary glomeruli of podoILK -/- mice were frequently enlarged and demonstrated few pseudocysts and occasional vacuoles, focal microvillous transformation and protrusions. Foot processes showed a normal architecture and slit diaphragm remained morphologically intact. The glomerular basement membrane was homogenously thickened (Fig. 24, see below).

At 4 weeks of age, podocytes of podoILK -/- mice were enlarged, showed pseudocysts and vacuolization, focal microvillous transformation and protrusions as well as multifocal foot process effacement. The glomerular basement membrane was clearly thickened, both homogenously and in a nodular manner and showed electron-lucent areas in the lamina densa (Fig. 24).

At 8-12 weeks of age, glomeruli of podoILK -/- mice displayed severely enlarged podocytes, exhibiting massive vacuolization and occasional accumulation of absorption droplets, multiple pseudocysts, as well as microvillous transformation and protrusions of the epithelial surface. Further, widespread foot process effacement and focal detachment from the basement membrane was observed. The glomerular basement membrane exhibited diffuse and irregular thickening and showed electron-lucent areas, and was sometimes collapsed and tortuous. Severe vacuolization was also found in the epithelia of Bowman`s capsule (Fig. 24).
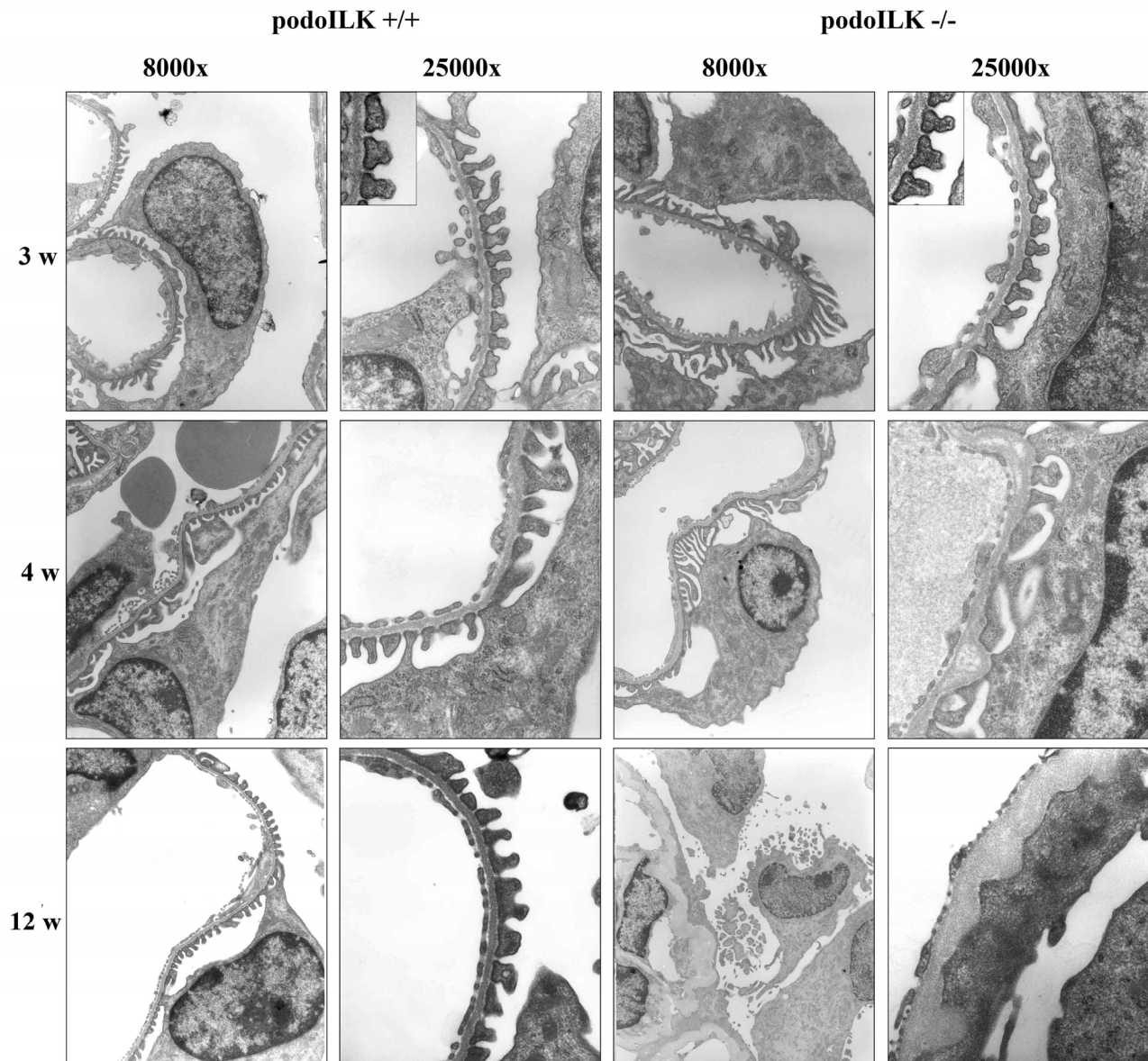
Figure 24: Transmission Electron Micrographs of 3, 4, and 12 week old glomeruli.

At 3 weeks, no obvious differences between podoILK -/- podocytes and podoILK +/+ controls can be seen. Foot processes and slit diaphragm appear intact. The glomerular basement membrane seemed homogenously thickened.

At 4 weeks of age, podoILK -/- podocytes show focal effacement of foot processes, the glomerular basement membrane is clearly thickened, both homogenously and in a nodular manner and showed electron-lucent areas in the lamina densa.

At 12 weeks of age, glomeruli of podoILK -/- mice displayed prominent podocytes, exhibiting microvillous transformation and protrusions of the epithelial surface. Widespread foot process effacement and elongated, flattened primary processes are seen. The glomerular basement membrane exhibited diffuse and irregular thickening and shows electron-lucent areas.

4.7.1. <u>Morphometric analysis of GBM composition in podoILK -/- mice</u>

As the GBM alterations were the first ultrastructural lesions seen, morphometric analysis of the GBM width was performed at 3 weeks of age in animals with selective albuminuria. Using orthogonal intercepts, the true harmonic mean GBM thickness was found to be significantly increased by 22.6% in podoILK -/- compared to wild-type litter mates (n=4, p<0.05, Fig. 25). The mean glomerular volume, as a parameter for overall glomerular architecture, was not different comparing wild-type and podoILK-/- mice (wt: $91,300 \pm 15,600$ vs. podoILK-/-: $78,500 \pm 8,600$ μm^3).
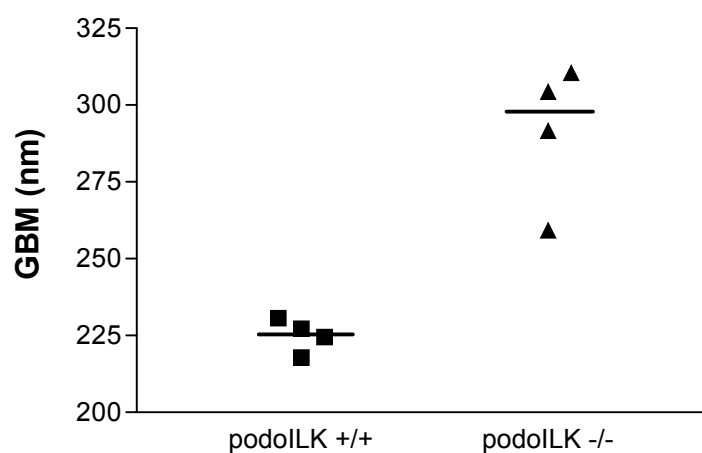

Figure 25: True harmonic GBM thickness is increased in podoILK -/- mice.

Morphometric analysis of the GBM width of 3 week old animals with selective albuminuria. Using orthogonal intercepts, the true harmonic mean GBM thickness was found to be significantly increased by 22.6 % in podoILK -/- compared to wild type litter mates, n=4 in each group, p<0.05.

4.7.2. <u>Analysis of GBM composition in podoILK -/- mice</u>

To define the molecular composition of the GBM alterations, the expression levels and distribution of the major GBM components were evaluated by real-time RT-PCR and immunofluorescence. Analysis of laminin-β 1-2, laminin-α 1, 2, 4 and 5, collagen type IV α 1-6, agrin, perlecan, nidogen-1 and fibronectin did not reveal an increase on mRNA and / or protein level in any of these molecules (Figure 26 and table 2 for more details). However, in animals with progressive filtration barrier failure and glomerular scarring (> 8 weeks of age), increased mRNA and immunostaining for fibronectin and collagen type I α1 in glomeruli with mesangial expansion or sclerotic changes was evident. In contrast collagen type IV α 3, 4 and 5, a significant decrease was observed only by 12 weeks of age compared to wild type mice.
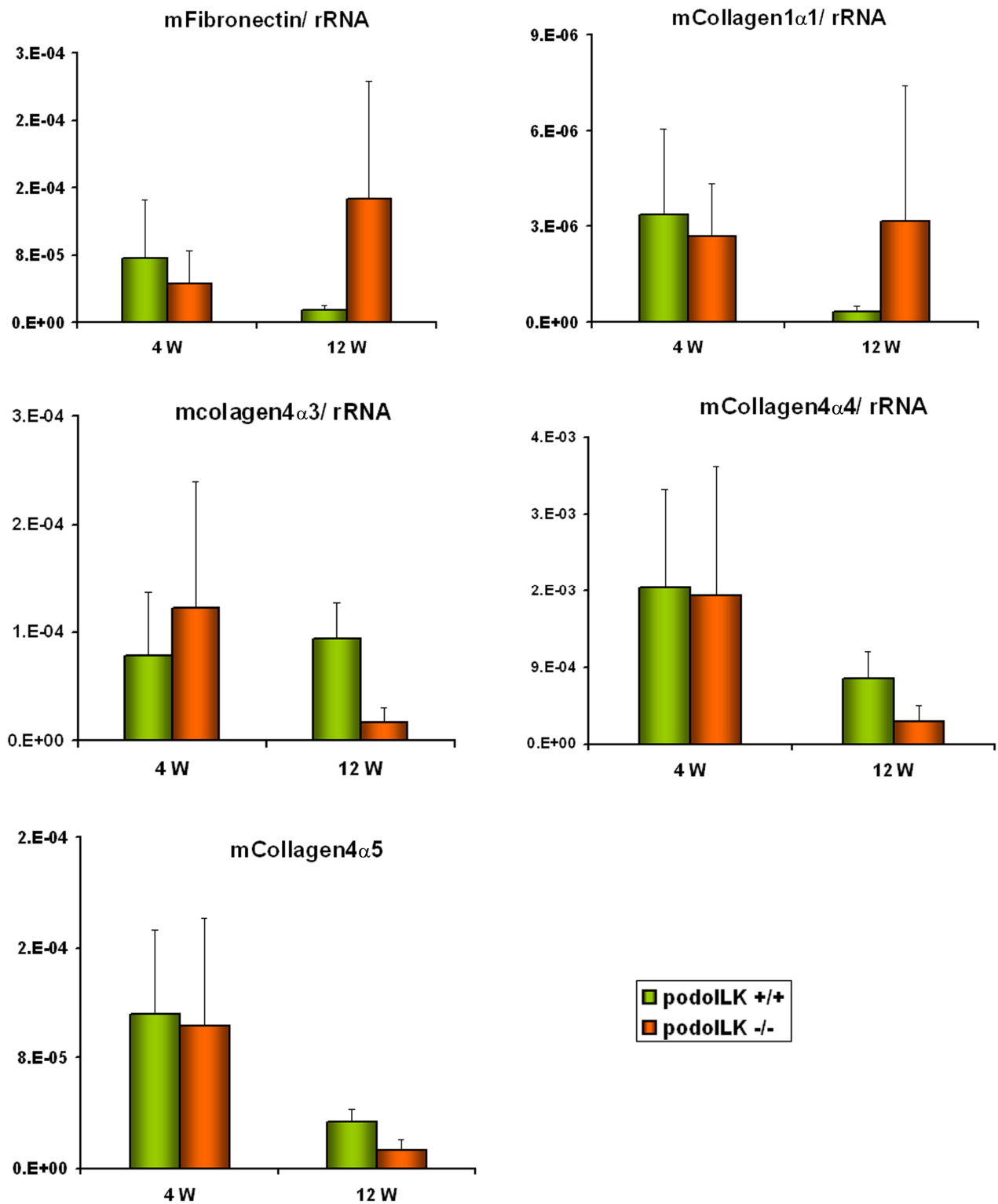
Figure 26: Quantification of GBM candidate gene expression by real-time RT-PCR in wild type and podoILK -/- mice.

Microdissected glomeruli were isolated and cDNA was used for the RT-PCR as described in materials and methods. All expression levels are given as ratio to 18S rRNA. No significant difference was seen at 4 weeks of age between wild type and podoILK -/- mice. But at 12 weeks this was significantly increased or decreased (**$P< 0.05$).

Target	4 week					12 week				
	PodoILK +/+		PodoILK -/-			PodoILK +/+		PodoILK -/-		
	mean N=6	SD	mean N= 5	SD	p	mean N= 4	SD	mean N= 6	SD	p
Collagen I, α 1	$3.06^{10\text{-}6}$	$2.72^{10\text{-}6}$	$2.69^{10\text{-}6}$	$1.66^{10\text{-}6}$	n.s.	**$0.33^{10\text{-}6}$**	**$0.18^{10\text{-}6}$**	**$3.17^{10\text{-}6}$**	**$4.22^{10\text{-}6}$**	**< 0.05**
Collagen IV, α 1	$2.18^{10\text{-}3}$	$2.10^{10\text{-}3}$	$1.47^{10\text{-}3}$	$1.21^{10\text{-}3}$	n.s.	$5.18^{10\text{-}4}$	$2.29^{10\text{-}4}$	$7.22^{10\text{-}4}$	$5.09^{10\text{-}4}$	n.s.
Collagen IV, α 2	$4.73^{10\text{-}5}$	$3.14^{10\text{-}5}$	$4.13^{10\text{-}5}$	$3.30^{10\text{-}5}$	n.s.	$0.62^{10\text{-}5}$	$0.30^{10\text{-}5}$	$1.35^{10\text{-}5}$	$0.88^{10\text{-}5}$	n.s.
Collagen IV, α 3	$7.84^{10\text{-}5}$	$5.91^{10\text{-}5}$	$12.2^{10\text{-}5}$	$11.7^{10\text{-}5}$	n.s.	***$9.36^{10\text{-}5}$***	***$3.36^{10\text{-}5}$***	***$1.69^{10\text{-}5}$***	***$1.34^{10\text{-}5}$***	***< 0.05***
Collagen IV, α 4	$1.83^{10\text{-}3}$	$1.16^{10\text{-}3}$	$1.75^{10\text{-}3}$	$1.52^{10\text{-}3}$	n.s.	***$7.65^{10\text{-}4}$***	***$3.16^{10\text{-}4}$***	***$2.63^{10\text{-}4}$***	***$1.89^{10\text{-}4}$***	***< 0.05***
Collagen IV, α 5	$1.12^{10\text{-}4}$	$6.12^{10\text{-}4}$	$1.03^{10\text{-}4}$	$0.78^{10\text{-}4}$	n.s.	***$3.34^{10\text{-}5}$***	***$0.94^{10\text{-}5}$***	***$1.34^{10\text{-}5}$***	***$0.78^{10\text{-}5}$***	***< 0.05***
Fibronectin 1	$7.60^{10\text{-}5}$	$6.99^{10\text{-}5}$	$4.63^{10\text{-}5}$	$3.81^{10\text{-}5}$	n.s.	**$0.15^{10\text{-}4}$**	**$0.05^{10\text{-}4}$**	**$1.46^{10\text{-}4}$**	**$1.40^{10\text{-}4}$**	**< 0.05**
Laminin, beta 2	$3.97^{10\text{-}5}$	$2.78^{10\text{-}5}$	$3.08^{10\text{-}5}$	$2.28^{10\text{-}5}$	n.s.	$1.79^{10\text{-}5}$	$0.56^{10\text{-}5}$	$1.17^{10\text{-}5}$	$0.26^{10\text{-}5}$	n.s.
Agrin	$5.28^{10\text{-}1}$	$2.99^{10\text{-}1}$	$3.54^{10\text{-}1}$	$1.70^{10\text{-}1}$	n.s.	$2.52^{10\text{-}1}$	$1.49^{10\text{-}1}$	$3.02^{10\text{-}1}$	$1.71^{10\text{-}1}$	n.s.
Perlecan	$2.72^{10\text{-}4}$	$1.99^{10\text{-}4}$	$1.31^{10\text{-}4}$	$0.89^{10\text{-}4}$	n.s.	$8.37^{10\text{-}5}$	$3.36^{10\text{-}5}$	$9.68^{10\text{-}5}$	$5.73^{10\text{-}5}$	n.s.
Nidogene 1	$4.89^{10\text{-}4}$	$7.22^{10\text{-}4}$	$2.50^{10\text{-}4}$	$1.77^{10\text{-}4}$	n.s.	$9.72^{10\text{-}5}$	$4.37^{10\text{-}5}$	$7.28^{10\text{-}5}$	$4.53^{10\text{-}5}$	n.s.
Integrin alpha 3	$2.71^{10\text{-}4}$	$2.08^{10\text{-}4}$	$3.30^{10\text{-}4}$	$2.42^{10\text{-}4}$	n.s.	$1.93^{10\text{-}4}$	$0.30^{10\text{-}4}$	$1.47^{10\text{-}4}$	$1.00^{10\text{-}4}$	n.s.
Integrin beta 1	$6.60^{10\text{-}4}$	$5.60^{10\text{-}4}$	$5.20^{10\text{-}4}$	$3.00^{10\text{-}4}$	n.s.	$4.19^{10\text{-}4}$	$2.10^{10\text{-}4}$	$4.16^{10\text{-}4}$	$2.50^{10\text{-}4}$	n.s.
Dystroglycan	$9.98^{10\text{-}4}$	$9.31^{10\text{-}4}$	$9.86^{10\text{-}4}$	$5.66^{10\text{-}4}$	n.s.	$3.77^{10\text{-}4}$	$1.58^{10\text{-}4}$	$3.41^{10\text{-}4}$	$2.35^{10\text{-}4}$	n.s.
Nephrin	$5.38^{10\text{-}4}$	$4.90^{10\text{-}4}$	$21.7^{10\text{-}4}$	$14.3^{10\text{-}4}$	n.s.	***$1.01^{10\text{-}3}$***	***$0.66^{10\text{-}3}$***	***$0.18^{10\text{-}3}$***	***$0.10^{10\text{-}3}$***	***< 0.05***
Podocin	$1.82^{10\text{-}4}$	$1.09^{10\text{-}4}$	$1.36^{10\text{-}4}$	$0.78^{10\text{-}4}$	n.s.	$1.33^{10\text{-}4}$	$0.79^{10\text{-}4}$	$0.60^{10\text{-}4}$	$0.29^{10\text{-}4}$	n.s.
P-Cadherin	$4.13^{10\text{-}6}$	$2.43^{10\text{-}6}$	$3.19^{10\text{-}6}$	$2.70^{10\text{-}6}$	n.s.	$2.97^{10\text{-}6}$	$1.77^{10\text{-}6}$	$9.18^{10\text{-}6}$	$8.64^{10\text{-}6}$	n.s.
ZO-1/Tjp1	$7.26^{10\text{-}4}$	$5.92^{10\text{-}4}$	$7.22^{10\text{-}4}$	$5.39^{10\text{-}4}$	n.s.	$3.53^{10\text{-}4}$	$1.13^{10\text{-}4}$	$2.01^{10\text{-}4}$	$0.76^{10\text{-}5}$	n.s.
WT-1	$2.16^{10\text{-}4}$	$1.38^{10\text{-}4}$	$1.86^{10\text{-}4}$	$1.57^{10\text{-}4}$	n.s.	***$1.36^{10\text{-}4}$***	***$0.47^{10\text{-}5}$***	***$0.76^{10\text{-}5}$***	***$0.27^{10\text{-}5}$***	***< 0.05***
Alpha-Actinin 4	$5.15^{10\text{-}4}$	$4.03^{10\text{-}4}$	$7.64^{10\text{-}4}$	$3.36^{10\text{-}4}$	n.s.	***$3.85^{10\text{-}4}$***	***$2.27^{10\text{-}4}$***	***$1.42^{10\text{-}4}$***	***$0.69^{10\text{-}5}$***	***< 0.05***
Synaptopodin	$2.70^{10\text{-}4}$	$3.54^{10\text{-}4}$	$1.26^{10\text{-}4}$	$0.76^{10\text{-}5}$	n.s.	***$6.33^{10\text{-}5}$***	***$1.99^{10\text{-}5}$***	***$1.69^{10\text{-}5}$***	***$0.64^{10\text{-}6}$***	***< 0.05***

Table 2: Glomerular gene expression of GBM, podocyte slit membrane molecules and cell-matrix receptors.

mRNA levels were determined by real-time mRNA quantification from 4 and 12 week old mice. Significant expression induction is displayed in bold, significant expression repression in bold italics. At 4 weeks in proteinuric animals no significant differences are seen, at 12 weeks in mice showing progressive glomerulosclerosis repression of podocyte specific molecules and induction of the matrix molecules Col I α 1 and fibronectin is detected.
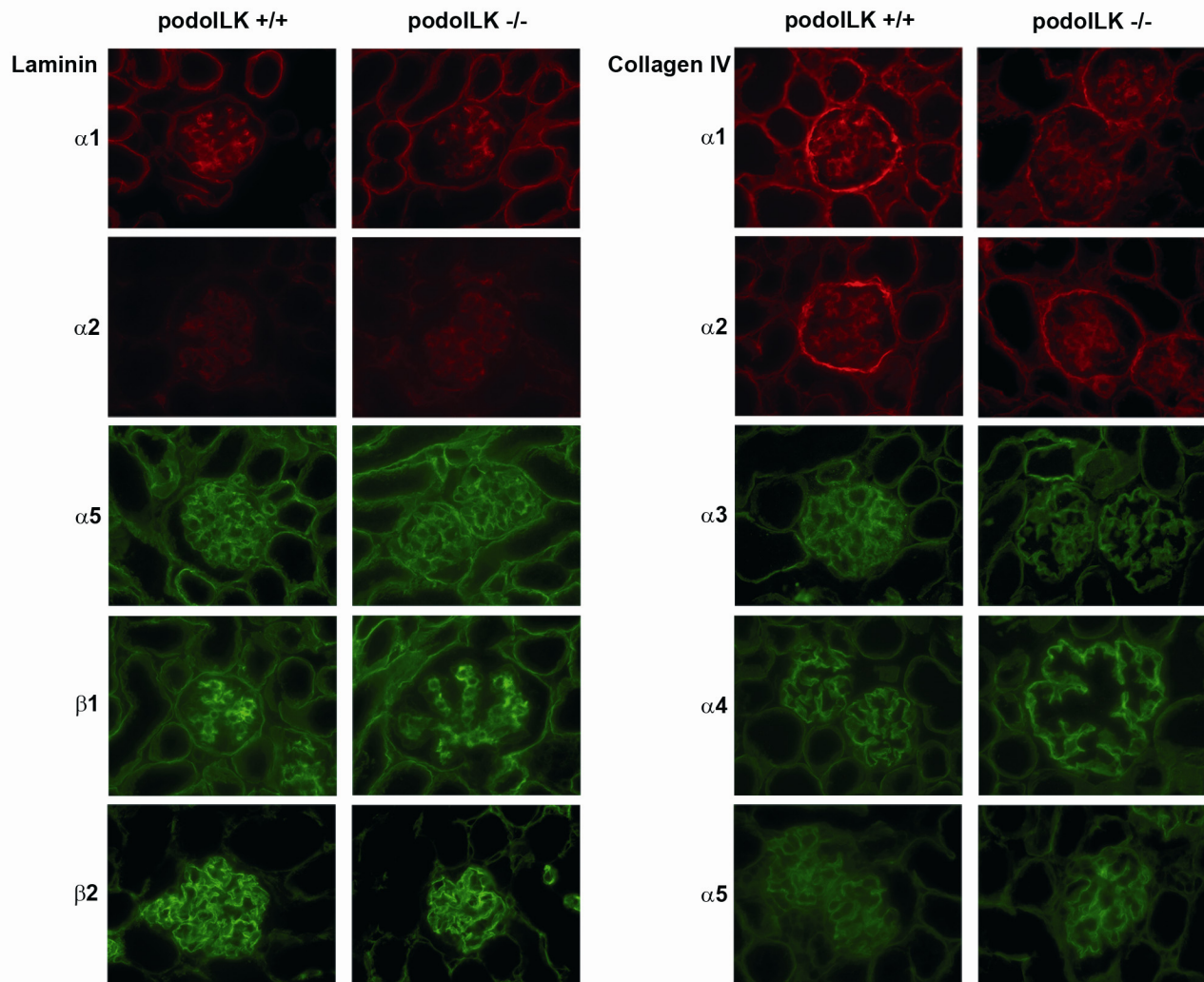
Figure 27: Immunofluorescence of GBM molecules.

The distribution and signal intensity of the major components of the murine GBM was evaluated and did not show any consistent difference between wild type and podoILK -/- mice at onset of albuminuria at 4 weeks of age. Staining for developmental and mature laminins and collagen type IV minor chains are shown. For corresponding mRNA expression analysis see table 2.

As ILK has been reported to be involved in matrix assembly via transmembrane matrix receptor (Wu *et al.*, 1998b), concentration and distribution of integrin-α3 and -β1 were evaluated. In immunofluorescence studies, no difference in the distribution of integrin- β 1, found in mesangial, endothelial and podocytes, could be observed. For integrin-α3, concentrated in podocyte foot processes facing the GBM, the staining in podoILK -/- mice showed a more granular pattern, consistent with an ILK dependent redistribution of this integrin at the onset of albuminuria (Fig. 27- 28).
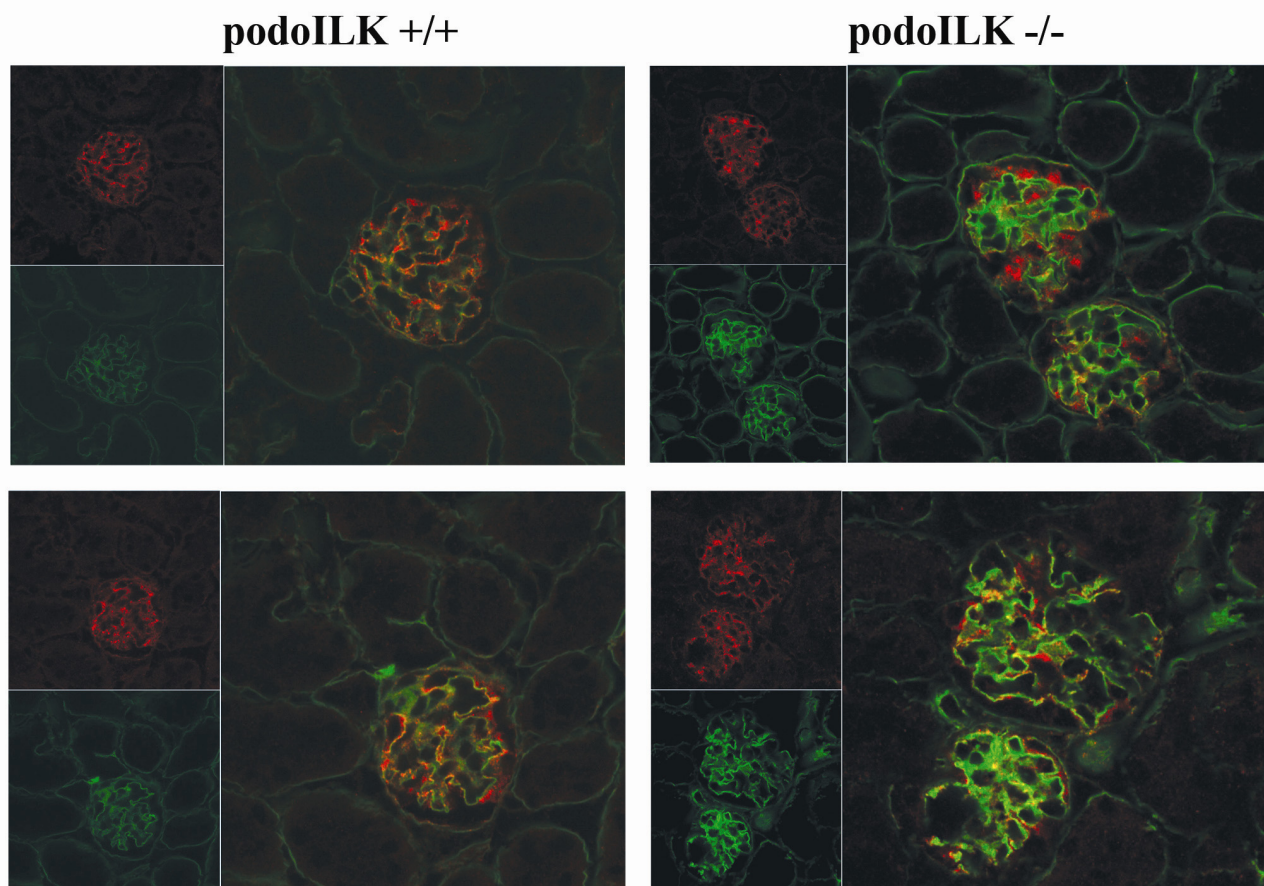
Figure 28: Immunofluorescence of α3-integrins.

The main transmembrane matrix receptors in podocytes, α3-/β1 integrins were evaluated and a granular signal of α3-integrins in 2 weeks old podoILK -/- compared to wild type littermates found. α3 integrin expressed as red and entactin expressed as green after staining. β1-integrins, expressed on endothelium, mesangium and podocytes did not show a significant different staining pattern (data not shown).

4.7.2.1. Immunohistochemistry staining for GBM components

Two podoILK -/- and two wild type mice were analyzed immunohistochemically each at 3 week, 4 week and over 12 weeks of age, respectively. At 19 and 25 days of age, staining for collagen type IV, laminin and fibronectin was indistinguishable between podoILK -/- and wild type kidneys (Fig. 29- 30).

Over 12 week of age, increased immunostaining for collagen type IV, laminin and fibronectin in glomeruli with mesangial expansion or sclerotic changes were evident (Fig. 30).

VEGF-immunohistochemistry revealed staining of a small portion of podocytes of glomeruli from wildtype mice, whereas in podoILK -/- animals, the majority of podocytes was VEGF-positive. The GBM staining for murine IgA, IgG or IgM showed no difference (data not shown).
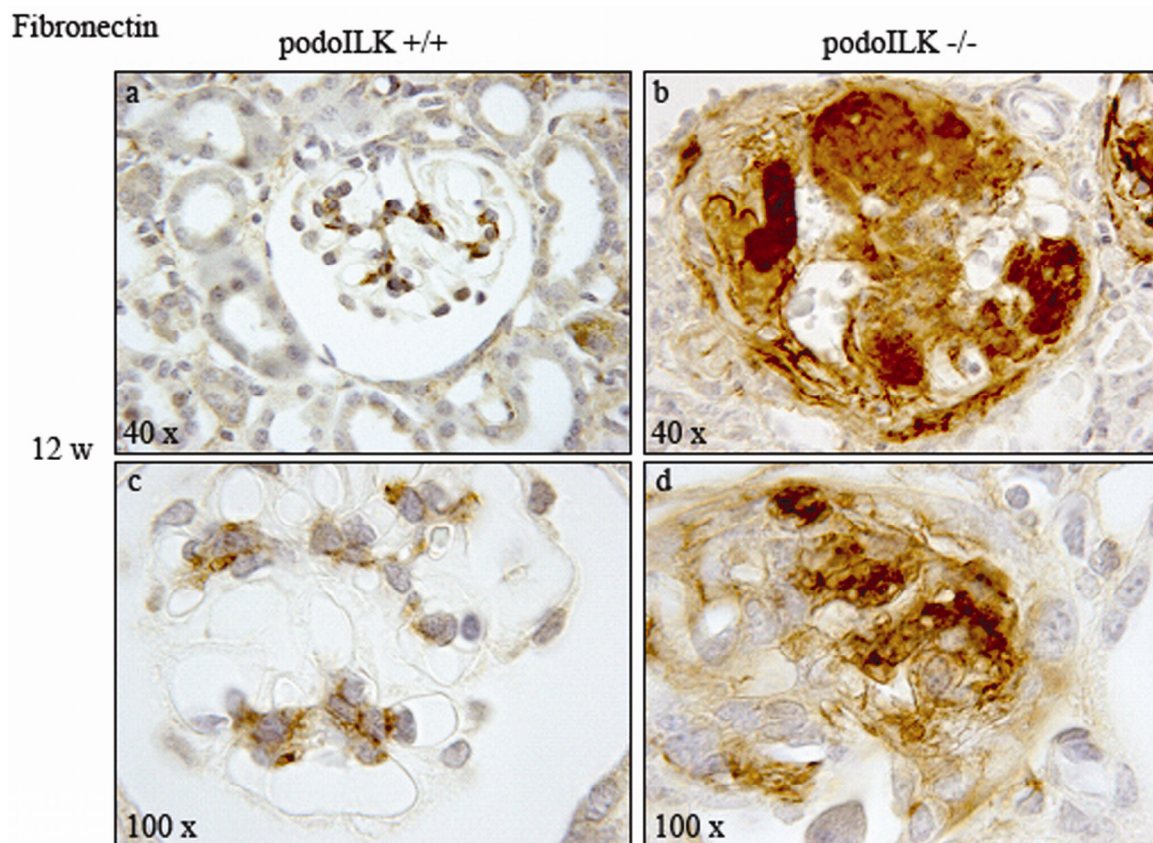

Figure 29: Immunohistochemistry for Fibronectin.

There is a marked increase in fibronectin deposition in the glomerulus of podoILK -/- mice (b,d) as compared to conrols (a,c)**.**
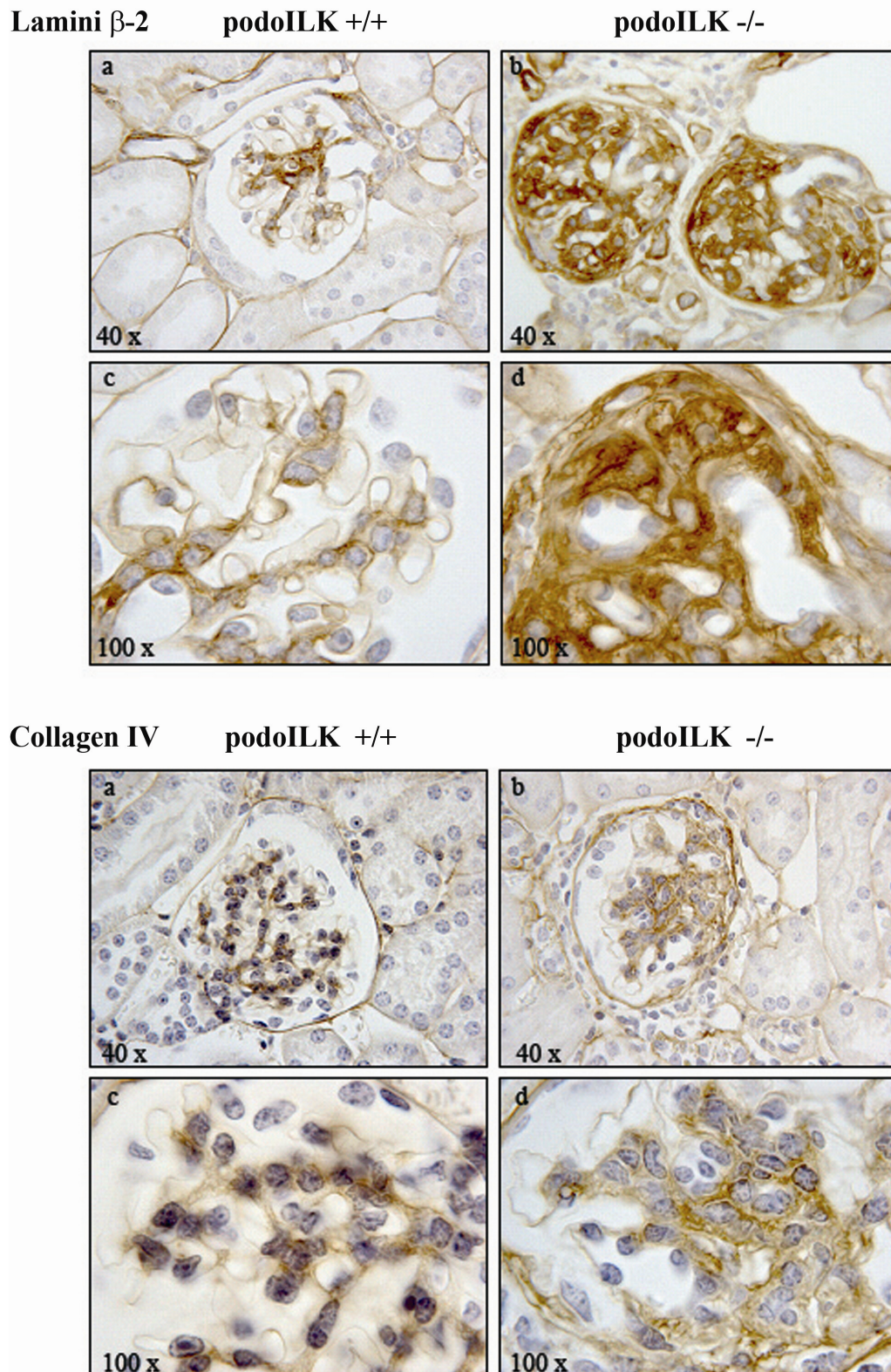
Lamini β-2   **podoILK +/+**   **podoILK -/-**

Collagen IV   **podoILK +/+**   **podoILK -/-**

Figure 30: Immunohistochemistry for laminin and collagen IV.

PodoILK -/- shows a massive deposition of laminin (b,d) as compared to conrols (a,c). Note the accumulation of collagen IV in the glomerulus of podoILK -/- mice (b,d) as compared to conrols (a,c).

4.8. <u>Effects of ILK deletion on podocyte gene expression</u>

Several podocyte specific molecules (podocin, synaptopodin, and α-actinin-4) were analyzed to determine the first affected genes after ILK deletion. Only WT-1 showed significantly reduced mRNA levels in microdissected glomeruli at 12 weeks of age, consistent with loss of podocytes from the glomeruli or repression of podocyte specific molecules. In contrast no significance was seen at 4 weeks of age compared to wild type mice.
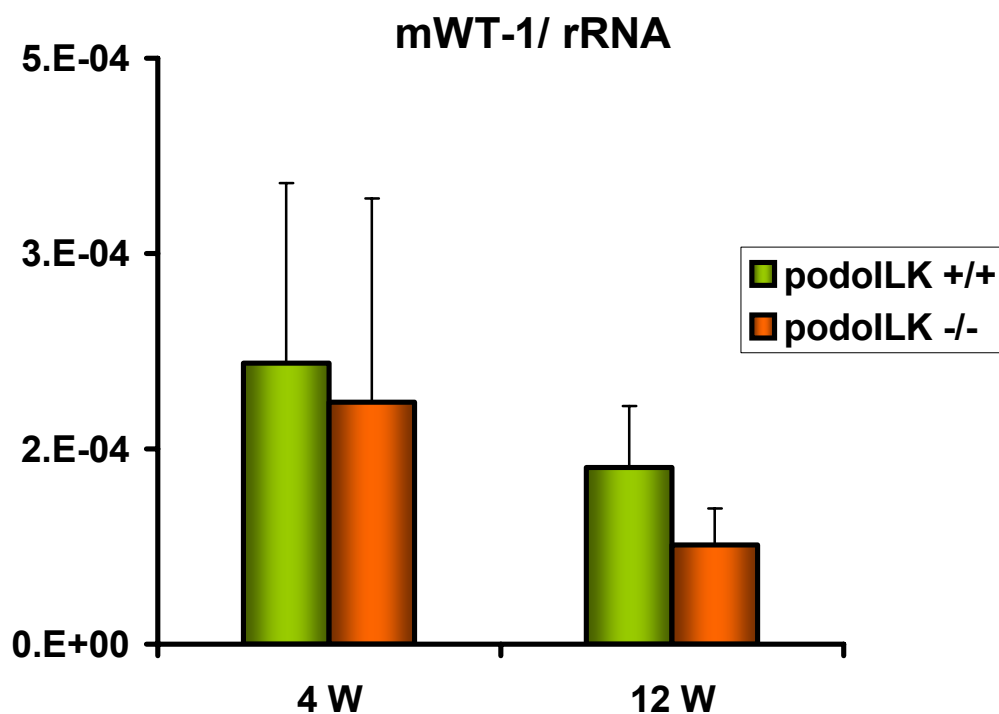

Figure 31: Real time RT-PCR quantification of mRNA expression of the WT-1 gene.

The graph shows expression ratios to 18S rRNA. A significant decrease of WT-1 was seen at 12 weeks of age in podoILK -/- mice (n = 5).

Further candidate genes such as dystroglycan, nidogen, agrin and perlecan, showed no difference in expression levels (data not shown).

4.8.1. <u>Raster Electron Microscopy</u>

To evaluate the consequences of ILK deletion on podocyte foot process architecture, raster electron microscopic analysis was performed. Two podoILK -/- mice were examined by scanning electron microscopy each at 19, 25 and over 53 days of age. At least one wildtype mouse per age-

group served as control.

Podocytes of glomeruli from 3 week old podoILK -/- mice demonstrated focal cell body attenuation and occasional pseudocyst formation, and major processes as well as pedicles appeared flattened and showed knobby protuberances. Further, ruptures of pseudocysts and occasional microvillous transformation were observed. Analysis of the older animals revealed progressive podocyte changes with age, including widespread flattening of the cell bodies and major processes, thus covering major parts of the filtration area without any visible interdigitating foot processes and massive microvillous transformation and numerous bulbous protrusions of the epithelial surface (Fig. 32).
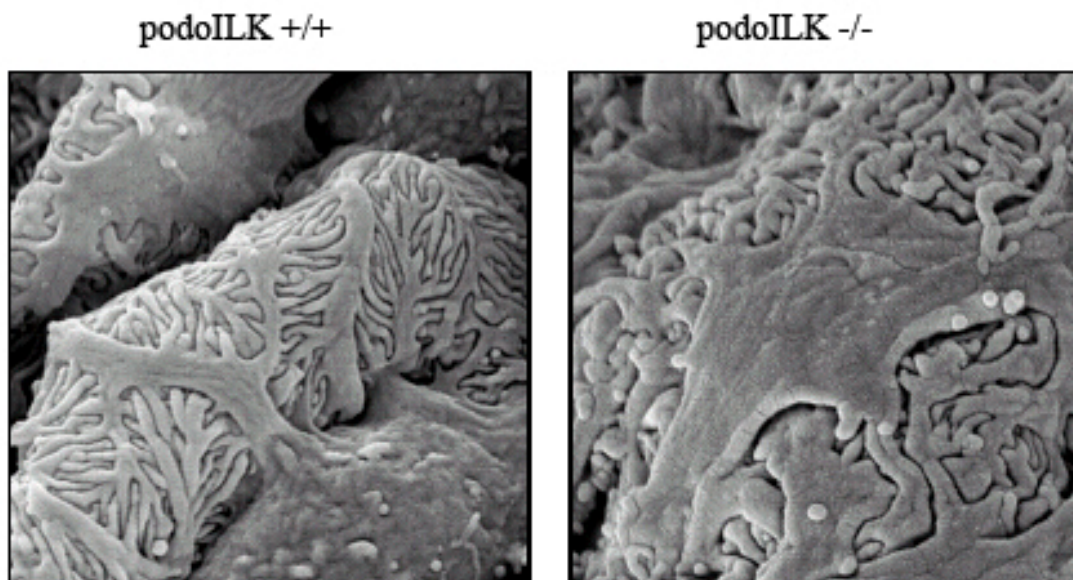

Figure 32: Scanning Electron Micrographs at 12 glomeruli.

View of capillar loop from Bowman's space, 10 000x magnification. For scanning electron microscopy, 2 mm thick kidney slices were used. Podocytes in podoILK -/- mice demonstrated focal cell body attenuation, flattening of major processes as well as foot process effacement. Note the irregular interdigitation in podoILK -/- compared to the highly regular pattern in wild type controls (podoILK +/+).
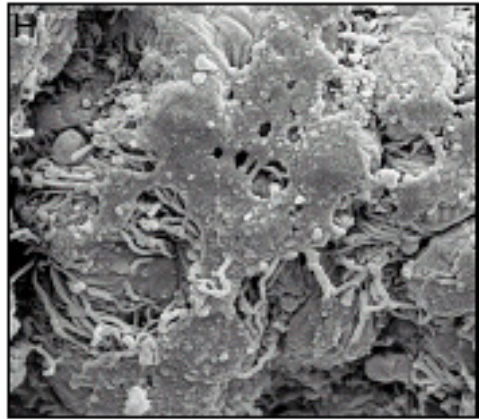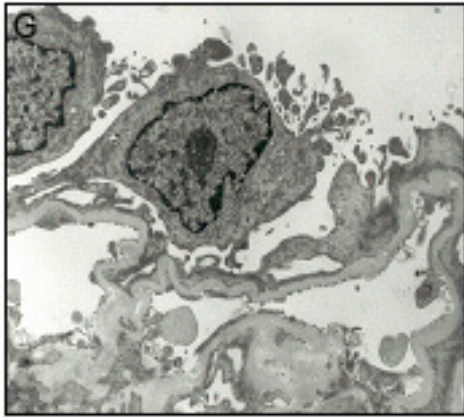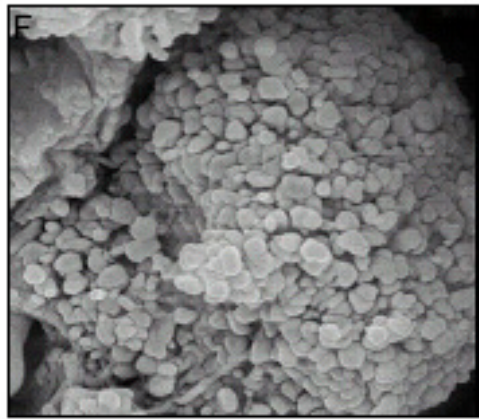
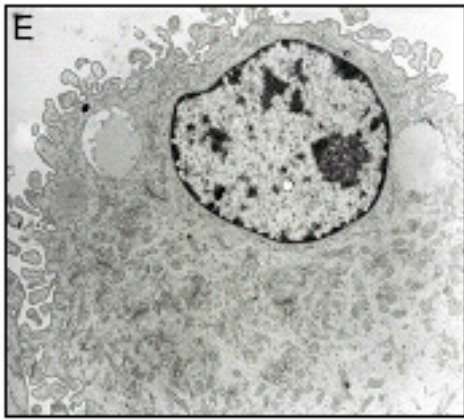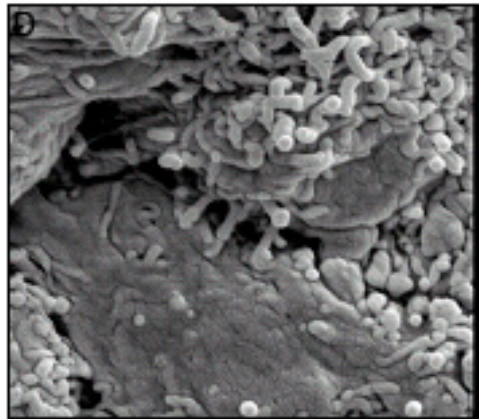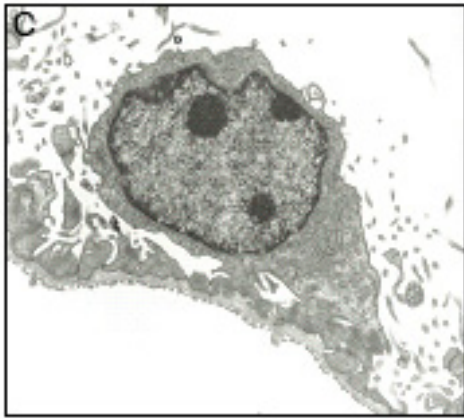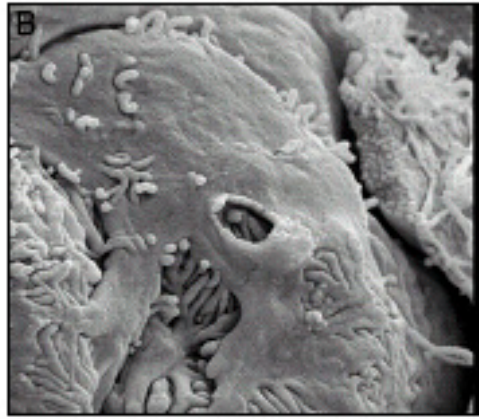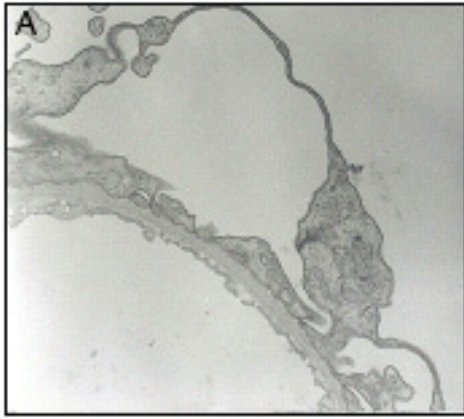**Figure 33: Comparison of TEM (left panel) and REM (lright panal).**

A/B: Pseudocyst (top left) and ruptured pseudocyst (top right). Thickening of the GBM and foot process effacement may be seen in the TEM picture. Flattening of the foot processes and the cell bodies as well as irregular interdigitating foot processes are shown in the REM picture.

C/D: microvillous transformation of the epithelial surface (2nd row).

E/F: invasive protrusions of the epithelial surface (3nd row). The TEM picture also shows vacuoles in the podocyte cytoplasm.

G/H: Irregular thickening of the GBM and microvillous transformation of the epithelial surface may be seen in the TEM picture (bottom left). The REM shows multiple ruptured pseudocysts, and protrusions of the epithelial surface of a severely flattened podocyte.

4.9. <u>The slit diaphragm and associated molecules are intact in proteinuric podoILK -/- mice</u>

As the podocyte slit diaphragm (SD) is considered to be a key element of the filtration barrier, transmission electron microscopic analysis focused on SD alterations at onset of albuminuria (3 weeks), did not identify alterations visible on the ultrastructural level (Fig. 24). In addition, overall foot process architecture appeared intact (Fig. 34). At later stages of progressive glomerulosclerosis, SD was lost and severe foot processes effacement was observed.
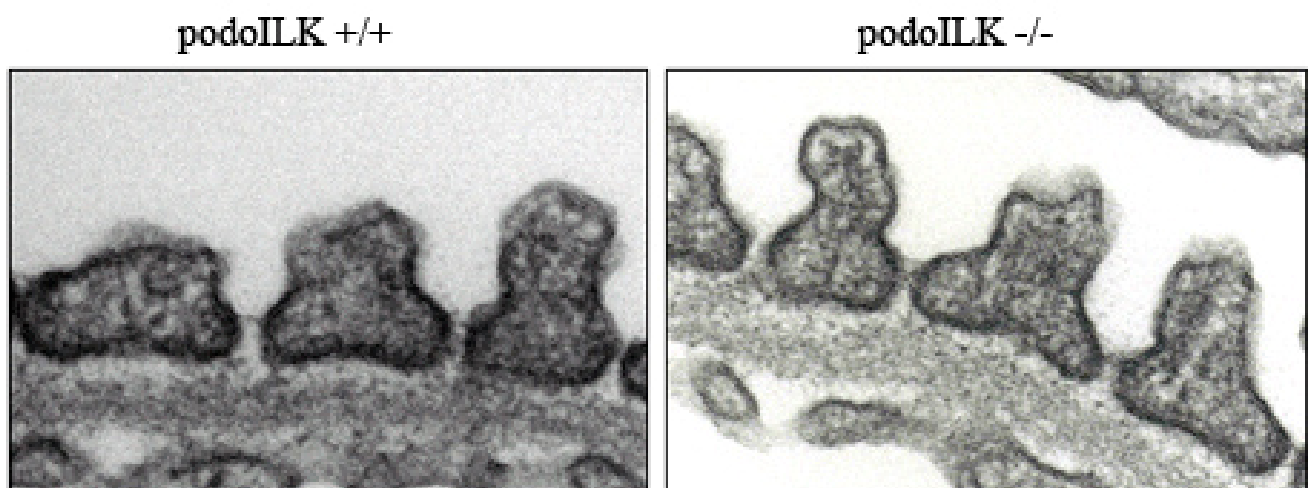
Figure 34: Transmission elctron microscopy of slit diaphragm.

Electron micrograph of an ultra thin section of slit diaphragm at 3 weeks of age showing no difference between the podoILK +/+ and podoILK -/- mice.

4.9.1. <u>Determination of the filtration slit frequency</u>

The determination of the filtration slit frequency (FSF) was carried out on the same TEM photographs, used for evaluation of the GBM thickness of 3-week-old animals. The filtration slit frequency was determined by counting the number of epithelial filtration slits and dividing that number by the length of the peripheral capillary wall at the epithelial interface. On average 324 filtration slits (range 265-387) were counted per animal. The filtration slit frequency (FSF) was equal in podoILK -/- mice (n=4) and wild type controls (n=4) (1,655.47 +/- 107.21 vs. 1,714.18 +/- 81.57 no. /mm)
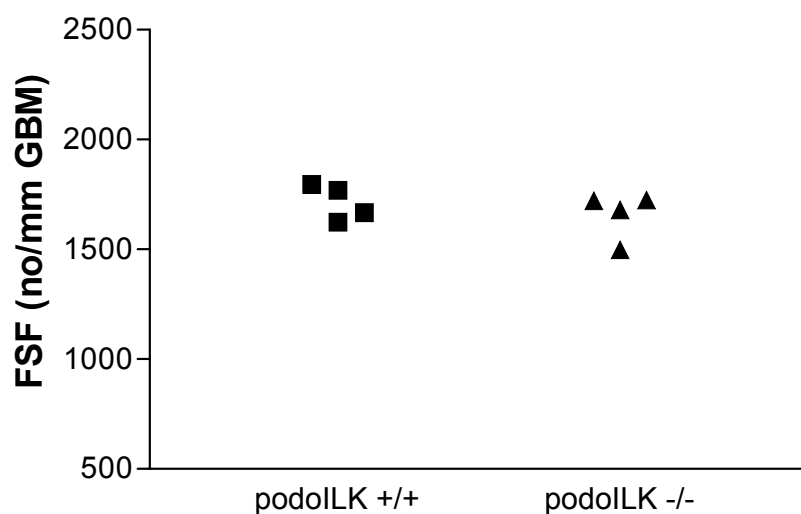

Figure 35: Determination of the filtration slit frequency in podoILK -/- mice.

Analysis of the filtration slit frequency of 3 weeks old animals with selective albuminuria. FSF was determined by counting the number of epithelial filtration slits and dividing that number by the length of the peripheral capillary wall at the epithelial interface. No significant difference was found in podoILK -/- compared to wild-type litter mates, n=4 in each group.

To further evaluate the status of the slit diaphragm, the expression levels and localization of two key SD components, nephrin and podocin, were evaluated in glomeruli from podoILK -/-. Steady state mRNA levels for both molecules did not show a significant difference in microdissected glomeruli from podoILK -/- mice to wild type littermates at 4 weeks of age. RT-PCR results demonstrated a significant decrease in nephrin expression at the age of week 12 weeks (Fig. 36) but in the case of podocin the expression remains same (Table 2). Immunofluorescence studies also demonstrated comparable signal intensities and distribution for both molecules (Fig. 37).
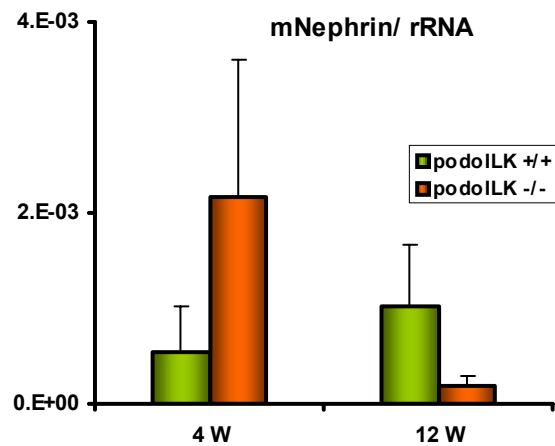
Figure 36: Real time RT-PCR quantification of mRNA expression of the nephrin gene.

The graph shows expression ratios to 18S rRNA. A significant decrease of nephrin was seen at 12 weeks of age in podoILK -/- mice.
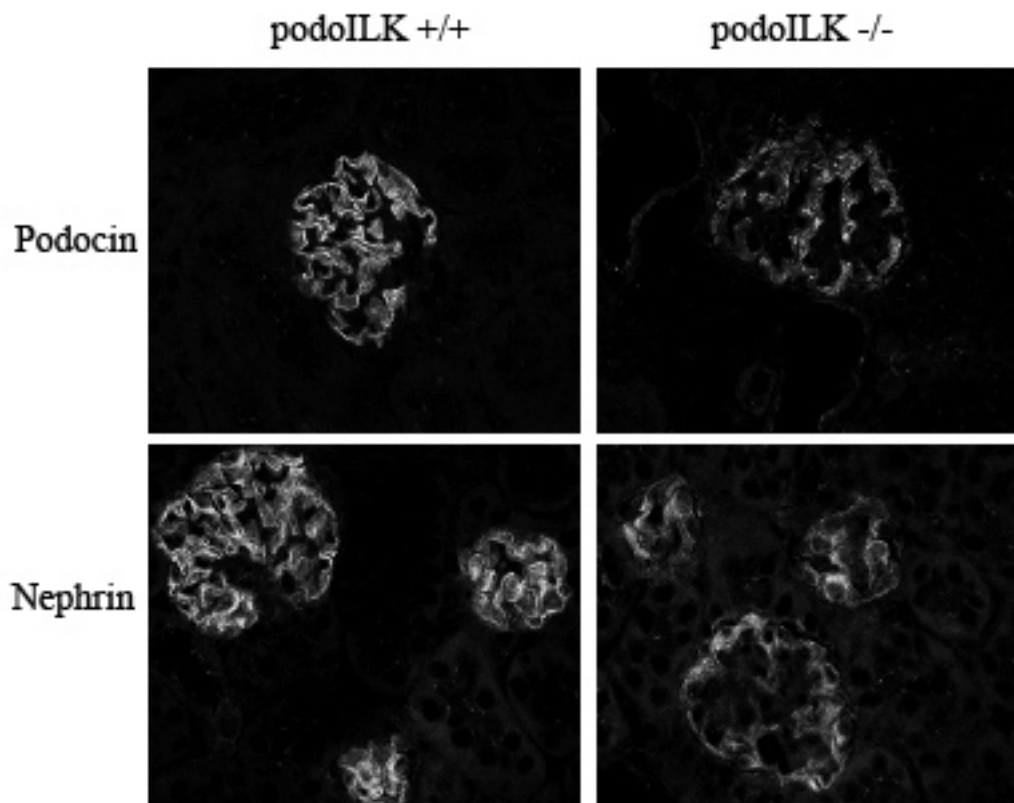
Figure 37: Slit membrane associated proteins in podoILK -/- mice.

In 4 week old animals, two key elements of the glomerular filtration barrier were analyzed for nephrin and podocin staining. Cryosections were incubated with the primary rabbit polyclonal antibody against nephrin or with the primary polyclonal anti-podocin both diluted 1:100, podocin and nephrin, were evaluated by immunofluorescences studies and showed comparable staining intensities and signal distribution along the GBM. The glomeruli showed a simplified lobular appearance as a consequence of mesangial expansion in the more severely affected glomeruli.

89

Discussion

5. <u>Discussion</u>

The glomerular podocyte is a terminally differentiated cell that lines the outer aspect of the glomerular basement membrane (GBM). It, therefore, forms the final barrier to protein loss, which explains why podocyte injury is typically associated with marked proteinuria. Podocytes are injured in many forms of human and experimental glomerular disease, including minimal change disease, focal segmental glomerulosclerosis, membranous glomerulopathy, diabetes mellitus, and lupus nephritis (Mundel and Shankland, 2002). Based on recent progress in molecular pathology podocytes have been linked to impaired formation of the slit function (Raats *et al.*, 2000; Reiser *et al.*, 2000a) and adhesive cell-cell interactions due to abnormalities in actin cytoskeleton (Smoyer *et al.*, 1997).

One such abnormality associated with the impaired podocyte function is a characteristic feature of the congenital nephritic syndrome of the Finnish type. A mRNA expression screen performed on human biopsy samples from a child population suffering from congenital nephritic syndrome of the Finnish type revealed marked induction of Integrin-liked kinase (Kretzler *et al.*, 2001). A role for ILK was therefore hypothesized in affecting the renal glomerular filtration barrier function. To elucidate the functional role of ILK in the glomerular filtration barrier, this study was designed. The deletion of the ILK gene from the podocytes in a tissue specific manner was performed using the Cre/Lox system.

To maintain an intact filtration barrier against the high transcapillary pressure gradient of the glomerulus an intimate molecular crosstalk between podocyte foot processes and the GBM is crucial (Kretzler, 2002). α3-/β1-Integrins are the main transmembrane matrix receptors of podocytes and collagen IV and laminins their GBM ligands. Integrins are the cell surface receptors that transduce signals from the GBM to the cell interior. They regulate cell function and matrix assembly via a protein complex associated with their cytoplasmic tail in focal adhesion plaques (Geiger *et al.*, 2001). Integrin linked kinase; an ankyrin repeat-containing Serine/Threonine kinase has emerged as a multifunctional protein in this complex at the cytoplasmatic domains of integrins. In cultured podocytes, ILK has been shown to orchestrate a wide array of functions, including focal adhesion plaque assembly (Kretzler *et al.*, 2001), F-actin cytoskeletal organization (Yang *et al.*, 1993; Kretzler *et al.*, 2001), membrane proximal initiation of signal transduction via Akt, GSK-3β and β-catenin (Kretzler *et al.*, 2001), regulating cell

phenotype and survival (Yang *et al.*, 1993; Kretzler *et al.*, 2001) and integrin binding affinity and avidity responsible for podocyte adhesion and extracellular matrix assembly (Yang *et al.*, 1993; Kretzler *et al.*, 2001).

As ILK levels have been found to be induced in progressive glomerular damage such as that characteristic of the nephritic syndrome of the Finnish type and in podocyte damage *in vivo* and *in vitro* (Hammes *et al.*, 2001; Kretzler *et al.*, 2001), the physiological role of ILK had to be addressed in the glomerular environment *in vivo*. Recent studies using genetic models have demonstrated a high degree of context dependency of ILK function. ILK deletion in Caenorhabditis elegans resulted in a phenotype resembling some aspects of α 1-integrin deletion underscoring ILK as a key adaptor between the cytoskeleton and integrins (Mackinnon *et al.*, 2002). A complete knock-out of ILK affects the ability to polarize and to generate the cytoskeleton in the epiblast, resulting in early embryonic lethality. Fibroblasts lacking ILK have been shown to poorly adhere to the ECM and showed defects in cell spreading, delayed formation of focal adhesion sites and stress fibers, and diminished proliferation rates (Sakai *et al.*, 2003). Tissue specific deletion of ILK in chondrocytes (Sakai *et al.*, 2003; Terpstra *et al.*, 2003) and endothelial cells in mice and zebra fish (Friedrich *et al.*, 2004) demonstrated key roles of ILK for intergrin-mediated cell adhesion and spreading, actin stress fiber formation, cell survival and proliferation (Sakai *et al.*, 2003; Terpstra *et al.*, 2003; Friedrich *et al.*, 2004).

5.1. <u>Development of mouse lines with podocyte specific deletion of ILK</u>

To evaluate ILK function in the glomerular context *in vivo*, a podocyte specific knockout mouse model was established using the Cre-Lox system. In this study, a mouse line bearing a targeting gene construct for the promoter region of Podocin (a protein almost exclusively located in podocytes) was generated. This line allowed the expression of the Cre-recombinase only in podocytes (Moeller, 2002). Likewise a second mouse line bearing the ILK gene flanked by two loxP sites was generated (Terpstra *et al.*, 2003). A crossing between these mouse lines yielded double transgenic mice in which the loxP-ILK gene had been specifically excised in their podocytes. This construct is known to activate the Cre-recombinase late in glomerular development during the capillary loop stage (Moeller *et al.*, 2003). In the present study, ILK excision was detectable at birth most likely in mature glomeruli found in the juxtaglomerular region of newborn mouse kidneys. At 2 weeks of age a loss of the ILK signal from podocyte foot

processes at the GBM could be shown with unchanged ILK expression in the mesangium. ILK mRNA levels were reduced by 76%, consistent with only mesangial ILK mRNA being detectable in the glomerular preparation. In contrast to the former cell type specific deletions, podoILK -/- mice did not show a developmental phenotype, most likely do to the timing of ILK excision in the late in development, but developed the first functional alteration (selective albuminuria) 2-3 weeks after birth. Albuminuria quickly progressed to non-selective proteinuria and classic progressive FSGS with terminal renal failure in all mice examined to date. This well-defined and easy to monitor onset of podocyte damage allowed the dissection of early events after ILK loss and to segregate them from late, unspecific lesions associated with FSGS.

5.2. <u>Effect of ILK deletion on the expression of slit diaphragm component proteins</u>

As glomerular filtration barrier loss has been linked to alterations in the slit diaphragm, this crucial unit of the filter was studied at disease onset. Ultrastructural and molecular analysis from podoILK -/- mice indicated an intact slit diaphragm complex. Several molecules have been shown to be crucial for an intact filtration barrier in humans and /or animal model systems. The expression of these molecules was assessed in the podoILK -/- mice, to define potential downstream consequences of ILK loss.

The SD complex is a modified adherent junction comprising of least four known transmembrane proteins: nephrin; NEPH1, which is structurally related to nephrin (Donoviel et al., 2001); P-cadherin (Reiser et al., 2000a); and FAT, a large cadherin homolog (Ciani et al., 2003). Mutations of the nephrin gene NPHS1 were identified by positional cloning as the pathogenic cause of the congenital nephrotic syndrome of the Finish type (CNF) In CNF a severe nephrotic sydrome is evident even in utero and is accompanied by the complete flattening of foot processes. Similarly, homozygous knockout mice generated by targeted inactivation of the nephrin gene fail to develop foot processes and are nephrotic (Kestila et al., 1998). Keeping in mind the crucial role of nephrin as a pathogenic factor related to nephropathy, in the present study nephrin mRNA expression levels were determined in young and adult mice lacking podoILK -/-. In the present study, no differences in the nephrin mRNA expression between the podoILK -/- mice as compared to the wild type mice were observed at disease onset. However, the expression of nephrin was found to be significantly reduced at mRNA levels in 12 week old podoILK -/- mice

as compared to the wild type mice.

Other crucial candidate genes that are known to affect the diaphragm complex assembly of podocytes, CD2AP, p-cadherin, podocin and ZO-1 were investigated in mice lacking ILK. These proteins are tightly associated and are embedded into lipid rafts at the slit diaphragm (Reiser *et al.*, 2002). Podocin may be critical for the stability of this complex by forming aggregates and lipid rafts. Intriguingly, its binding to nephrin at the lipid rafts dramatically activates the signalling capabilities of nephrin (Boute *et al.*, 2000). The scaffolding proteins ZO-1 and CD2AP form links with F-actin and may trap other yet unidentified proteins at the slit diaphragm complex. ZO-1 is another component of the slit complex and the loss of the ZO-1 at the slit has been associated with proteinuria (Schnabel *et al.*, 1990; Kawachi *et al.*, 1997), suggesting that it plays an important functional role. However in the present study, no change in their expression levels was observed in the podoILK -/- mice as compared to the wild type controls.

F-actin, is an important element of the podocyte cytoskeleton and localizes to the submembranous regions of podocyte foot processes (Drenckhahn and Franke, 1988). The α-actinin-4 molecule is an actin-filament cross-linking protein, the gene mutated in an autosomal dominant form of focal segmental glomerulosclerosis. The α-actinin-4 gene has widespread expression, but immunostaining of human kidney sections has revealed a glomerular podocyte location (Kaplan *et al.*, 2000). Although α-actinin-4 is less likely to be a component of the podocyte slit diaphragm, it may also play an important role in the integrity of podocyte foot processes and may be involved in cell motility. To study the biological role of α-actinin-4 further, Kos and colleagues (Kos *et al.*, 2003) generated an α-actinin-4 knockout mouse. Although there was some unexplained fetal/ perinatal loss of homozygote mice, a number of knockout mice survived, and most developed advanced glomerular disease with proteinuria, blebs in the GBM and foot process effacement by 10 weeks of age (Kos *et al.*, 2003).

The membrane at the foot processes' soles is attached to the actin meshwork via dystroclycan or via the integrin, talin, and paxillin complex. RT-PCR analysis of dystroglycan didn't reveal any difference between the podoILK -/- and wild type mice. The exact function of the dystroglycan complex at the soles of foot processes remains to be determined. However, based on findings in myocytes, the glomerular dystroglycan complex could provide an actin-directed positioning system by which podocytes actively control the exact spacing of matrix proteins and thus the porosity and permeability of the GBM The dystroglycan complex may serve as a regional organizer for membrane protein clusters in the sole of foot processes (Kerjaschki, 2001).

WT-1 is a zinc finger-containing transcription factor that is expressed in podocytes from the

capillary loop stage of development onwards. WT-1 knockout mice fail to form kidneys, which precludes the analysis of its role in glomerular development (Ly *et al.*, 2004). Presence of glomerular disease in patients and murine models of Denys-Drash syndrome (DDS) (Pelletier *et al.*, 1991; Natoli *et al.*, 2002), Frasier sydrome (Hammes *et al.*, 2001) were caused by specific mutations in WT-1, have clearly shown that WT-1 is required for podocyte function. In these experiments, the mice showed a reduction of WT-1 in RT-PCR analysis compared to the wild type in the later stage of unselective proteinuria.

Elements of the podocyte cytoskeleton were also found to be normally expressed in podocyte foot process without ultrastructural evidence of damage to the foot processes architecture at disease onset in podoILK -/- mice. In the present study at onset of albuminuria, no detachment of podocytes from the GBM was seen and tunnel staining did not reveal an increased positivity of podocytes in podoILK -/- at 3 and 4 weeks of age (data not shown), consistent with ILK not being essential for podocyte survival, cytoskeletal organization and matrix adhesion.

Synaptopodin is an unique actin-associated protein of glomerular podocytes and the telencephalic dendrites (Mundel and al). In both brain and kidney, *in vivo* and *in vitro*, synaptopodin gene expression is differentiation-dependent (Mundel *et al.*, 1997). Synaptopodin colocalizes with α-actinin in cultured podocytes and may be involved in the organization or regulation of a Z-disc equivalent in podocytes. In diseases with reversible foot process effacement such as minimal change disease and membranous glomerulopathy, synaptopodin expression in podocytes is preserved. In contrast, in collapsing idiopathic focal segmental glomerulsclerosis a loss of synaptopodin precedes the loss of foot processes and the actin cytoskeleton. The expression of synaptopodin commences at the capillary loop stage, i.e. the appearance of synaptopodin is linked to the formation of foot processes (Mundel *et al.*, 1997; Barisoni *et al.*, 1999). In this study the expression pattern of synaptopodin and α-actinin-4 was analyzed in podoILK -/- and control mice and diminished levels of synaptopodin and α-actinin-4 at a later disease stage was observed. This finding correlates with the data found in collapsing forms of FSGS. In FSGS in addition to the disappearance of processes associated with a loss of cytoskeletal elements, a disappearance of synaptopodin was noted (Barisoni *et al.*, 1999). These findings are consistent with the loss of synaptopodin preceding the dysregulation of the podocyte after ILK deletion.

Experiments with cultured cells suggested that synaptopodin plays a role in modulating the actin-based shape and motility of dendritic spines and podocyte foot processes (Mundel *et al.*, 1997). Synaptopodin knockout mice kidney structure did not reveal any obvious differences between podocytes of wild-type and synaptopodin knockout mice. But the lack of synaptopodin delays the

re-formation of the podocyte actin cytoskeleton *in vivo* and *in vitro* and synaptopodin specifically interacts with α-actinin. This interaction is functionally significant because synaptopodin bundles and elongates α-actinin-induced actin filaments (Asanuma *et al.*, 2005). From these data a direct relationship between synaptopodin and α-actini-4 was inferred.

Taken together, data from the present study shows a reduction of several podocyte specific proteins including nephrin, synaptopodin and α-actinin-4 levels after ILK deletion. These findings can be interpreted in two ways. They might suggest that ILK deletion leads to a loss of podocytes from a glomerulus and thereby reducing the mRNA levels of podocyte specific molecules in glomerular lysates. Alternatively, ILK loss might result directly in a reduced expression of synaptopodin which in turn leads to a reduction in α-actinin-4 and consequent alteration in the podocyte cytoskeleton.

5.3. <u>Effect of ILK on glomerular basement membrane</u>

Basement membranes are abundant specialized extracellular matrices in close vicinity to cells (Timpl and Brown, 1996). Major components of basement membranes are various forms of collagen IV and laminins, proteoglycans and small glycoproteins such as nidogen/entactin (Levidiotis and Power, 2005).

In the current study, first visible lesions consistently found at onset of albuminuria were GBM alteration. The GBM showed an increased diameter, followed by splitting and massive extension at later stages. The tubular basement membrane was not altered at this stage. Possible mechanism for this surprising GBM phenotype could be an increased matrix synthesis or decreased degradation, deposition of circulating proteins in the GBM or alterations in GBM assembly.

An analysis of the key components of the GBM did not demonstrate an increased concentration of GBM components at time of the onset of the lesions. This findings do not indicate an increased synthesis of matrix molecules or decreased production of matrix modifying enzymes, despite the fact that ILK had been reported to be involved in these processes in *in vitro* models (von Luttichau *et al.*, 2002). The significant induction of fibronectin during the later stages of progression in the podoILK -/- has been observed in several animal models and human diseases and might be part of an ILK independent scarring process (Van Vliet *et al.*, 2001).

Fibronectin can only assemble into a disulfide-linked pericellular network in cells which express activated integrins. Several reports have identified α5β1 as the first integrin which is able to

mediate fibronectin polymerisation (Mosher *et al.*, 1992). Yang et all, showed that other integrins can also assemble fibronectin (Yang *et al.*, 1993). Several studies have demonstrated that multiple integrins including α5β1, α3β1 and α5β3 integrins are involved in the regulation of fibronectin deposition into extracellular matrix. The ability of integrins to promote fibronectin matrix deposition is controlled by both the integrin activation state and the cytoskeletal interaction. As integrin activation and cytoskeletal interaction are regulated by integrin cytoplasmic domains, these studies suggest that intracellular proteins associated with the integrin cytoplasmic domains likely play important roles in the cellular regulation of fibronectin matrix assembly.

Our data suggest that fibronectin-binding integrins can assemble a fibronectin matrix when they are activated via ILK and interact with an intact actin cytoskeleton.

Fibronectin matrix production remained unchanged in ILK knock-down, but the integration of fibronectin into a complex, focal adhesion associated matrix was impaired. Potential mechanism of integrin mediated matrix adhesions are the unmasking of self-assembly sites in the fibronectin molecule by activated integrins, allowing spontaneous polymerization into densely packed fibers (Geiger *et al.*, 2001; Pankov and Yamada, 2002). Given a role for ILK in connecting integrins and actin cytoskeleton, it is likely, that ILK promotes the deposition of fibronectin into ECM by influencing the activation of integrins and/or by providing a molecular scaffold for the assembly of integrins that mediate fibronectin assembly and the actin cytoskeleton-associated proteins (Guo and Wu, 2002). Regardless of the mechanism involved, results from the current study establish that ILK is a crucial element in the cellular control of fibronectin deposition into the ECM.

A second alternative would be passive deposition of circulating molecules into the GBM. This is a frequent event in autoimmune renal disease, resulting in subendothelial or subepithelial immuncomplexes at the GBM (Kerjaschki *et al.*, 1989). However, immune complex deposits do show a typical ultrastructure not observed in the podoILK -/- mice. In addition, direct staining for immunoglobulins was not able to reveal a difference between controls and podoILK -/- GBM (data not shown).

An alternative explanation for the GBM phenotype could be an altered matrix with impaired integrin function (Velling *et al.*, 2002). Matrix molecules could be less densely packed, causing a broadened and split GBM parallel to the consequences of some of the collagen IV mutations in Alport syndrome (Hudson, 2004). Analysis of collagen IV α1 to α6 revealed no change between wild type and podoILK -/- mice in the earlier stage of microalbuminuria but a reduction of

collagen IV α3 to α5. The importance of collagen IV α3 through α5 chains to the proper function of the GBM is underscored by the effects of mutations in the genes that codes these chains (Antignac, 1995; Lemmink *et al.*, 1997). The most severe mutations cause Alport syndrome (hereditary glomerulonephritis) in humans (Barker *et al.*, 1990; Mochizuki *et al.*, 1994) and an analogous disease in dogs and knockout mice (Zheng *et al.*, 1994; Cosgrove *et al.*, 1996; Miner and Sanes, 1996). Alprt syndrome, an inherited nephropathy characterized by irregular thinning, thickening, and splitting of the GBM and progressive renal failure, is associated with mutations an any of the collagen IV α3, α4 and α5 genes. The GBM shows the loss of the α3- α4- α5- network and the persistence of the α1- α2- network (Gubler *et al.*, 1993). The abnormal composition of the collagen networks predisposes the GBM to events, such as proteolysis, that cause progressive deterioration and loss of function (Kalluri *et al.*, 1997). A particularly interesting aspect of Alport syndrome is that in most cases, the collagen α3 through α5 chains are all absent from the GBM, despite the fact that only one of the three chain genes harbors a mutation. However, this is perfectly consistent with the hypothesis that these chains are all part of the same collagen IV network in the GBM and that this network requires all three chains for proper assembly (Kashtan *et al.*, 1990; Hudson *et al.*, 1993; Tryggvason *et al.*, 1993).

In Alport syndrome, mutations in one of the collagen IV α3 to α5 chain genes prevent accumulation of all three of these chains. As a consequence, the collagen IV chain transition cannot occur in the GBM, and this leads to a retention of the α1 and α2 chains throughout the width of the GBM (Miner, 1999). Although these chains function properly early in life, they eventually fail to maintain the proper structure and function of the GBM, leading to the delayed-onset glomerulonephritis characteristic of Alport syndrome. An explanation of the GBM alteration may be the reduction of collagen α3 to α5. This results show that collagen IV α3 to α5 have an important role in the GBM that cannot be compensated for by other chains of the collagen IV complex. Several lines of evidence suggest that the absence of the whole α3- α4- α5- (IV) network is a consequence of a post-transcriptional co-regulation of the expression of these three chains, which either prevents the assembly of the α3- α4- α5- protomers, or produces defective protomers that are degraded or unable to assemble into supramolecular network (Boutaud *et al.*, 2000; Borza *et al.*, 2002).

Thickening of the GBM and expansion of the mesangial matrix in podoILK -/- mice reveal the diffuse nature of glomerulosclerosis associated with the onset of albuminuria. It has been shown in many studies that the collagen IV α3 through α5 chains, laminin, and fibronectin contribute to the thickened GBM, whereas the α1, α2 chains of collagen IV, laminin and fibronectin comprise

the expanded mesangium. The podoILK -/- mice show reduction in the expression of α3-α5 chains of collagen IV at late stages of disease. This might suggest that ILK may be required to regulate the expression of this collagen. Alternatively, loss of podocytes might result in lower expression levels of podocyte gene products in the microdissected glomeruli. Further, expression levels of other basement membrane components not produce by podocytes alone, such as perlecan, laminin, and nidogen, were found to be unaltered.

5.4. <u>Podocyte specific effects as a result of ILK deletion in mice</u>

Podocytes are the prime source of the GBM in the adult glomerulus (Miner, 1999) and are crucial for GBM dynamics and maintenance in health and disease (Martin *et al.*, 1998; Miner, 1999). In *in vitro* systems, ILK has been implicated in matrix assembly via modulation of integrin function by altering focal contact structure, integrin activity state and cell migration (Wagenknecht *et al.*, 1997; Wu *et al.*, 1998b; Hammes *et al.*, 2001; Attwell *et al.*, 2003; Friedrich *et al.*, 2004; Vouret-Craviari *et al.*, 2004). ILK depletion in endothelial cells via RNA interference impaired the ability to recruit α5-β1-integrins to fibrillar adhesions (as defined by Geiger 2001) and the maturation of the adhesions to competent matrix forming structures (Vouret-Craviari *et al.*, 2004).

After ILK knock-down in endothelial cells, an increased adhesion and reduced migration of ILK depleted cells was considered to be an additionally mechanism to impair matrix assembly. In analogy to the studies in endothelial cells, ILK function has been found to positively correlate with podocyte matrix adhesion (Kretzler *et al.*, 2001). Elegant studies have demonstrated the high degree of mobility of podocyte foot processes moving as mobile structures across the GBM (Seiler *et al.*, 1975). Podocyte migration can be studied *in vitro* and cathepsin L, a matrix modifying enzyme, has been implicated in this process (Reiser *et al.*, 2004). Inhibiting ILK activity or expression is known to inhibit cell migration (Attwell *et al.*, 2003). Although the precise mechanism for how ILK regulates cell migration remains to be determined, recent studies implicate the activation of small GTPases RAC and CDC42. In addition, absence of ILK or inhibition of its kinase activity is known to inhibit RAC (Mongroo *et al.*, 2004) and CDC42 (N. Filipenko and S. Dedhar, unpublished observation). In another study, ILK knockdown by RNAi in bovine aortic endothelial cells resulted in the inhibition of endothelial-cell migration and capillary formation. ILK was shown to regulate vascular network formation by directing the assembly of integrin-dependent matrix forming adhesions (Vouret-Craviari *et al.*, 2004). Muranyi

and co-workers showed in smooth muscle cells, that ILK can stimulate cell motility by activating the cellular contractile machinery through its ability to directly phosphorylate myosin light chain (MLC), and through inactivating the myosin phosphatase target subunit, leading to further stimulation of MLC phosphorylation (Muranyi *et al.*, 2002). It has been postulated that foot processes have a certain motility, which allows them to move slowly on the GBM along the outer surface of the capillaries. As a consequence of these movements, the association of GBM areas with filtration slit and sole plates of foot processes would constantly change, thereby facilitating the cleansing of the glomerular filter (Mundel, 1998).

The hypothesis of GBM matrix assembly defect in podoILK -/- podocytes is exquisitely difficult to test. The only indirect evidence of altered integrin function in the ILK deficient glomeruli could be an altered integrin distribution. α3-Integrins was found to be present in a more granular pattern in podoILK -/- glomeruli compared to all other GBM associated molecules studied at the micro-albuminuric stage of the disease.

Interestingly, using a small molecular ILK kinase inhibitor preliminary data indicates reduced migratory ability of differentiated cultured podocytes in transfilter migration assays after ILK inhibition (own unpublished observation).

This finding together with the altered GBM in podoILK -/- mice, suggests that ILK are involved in either actively organizing or, at least, in maintaining the structural integrity of basement membranes. The role of ILK in the assembly or maintenance of ECM matrices has significant implications. A number of ECM proteins bind to matrices which are assembled by ILK and defects in ECM assembly could consequently also result in abnormal deposition of molecules such as fibronectin and collagen.

Taken together, this study clearly establishes that cell signaling is a major function of the podocyte, and suggests ways in which environmental cues from the glomerulus, such as changes in matrix composition may effect changes in the complete unit of the filtration barrier function.

5.5. <u>Alterations in α3β1 functions in absence of ILK</u>

The α3β1 integrin is the major ECM receptor expressed by podocytes along the GBM (Korhonen *et al.*, 1990; Patey *et al.*, 1994). It provides a dynamic link between cell and matrix, which allows a link to actin cytoskeleton in the foot process. α3β1 integrin was originally characterized as a promiscuous receptor, binding collagen, fibronectin, laminin, and entactin/nidogen (Elices *et al.*,

1991; Dedhar *et al.*, 1992; Pattaramalai *et al.*, 1996). More recent studies have demonstrated that although ECM components might be weak ligands, α3β1 binds with much higher affinity to isoforms of laminin, including laminin-5 and laminin-10/11 (Delwel *et al.*, 1994; Kikkawa *et al.*, 1998). In maturing glomeruli, α3β1 is highly expressed in GBM (Korhonen *et al.*, 1990; Rahilly and Fleming, 1992) and is essential for maturation of podocytes, α3-integrin null mice demonstrate foot process effacement at birth and an immature GBM (kreidberg, 1996 alpha1). Likewise the knockouts of s-laminin/ laminin- β2 show a similar phenotype (Noakes *et al.*, 1995). These facts raise an important question: how does GBM/ receptor interaction affects podocyte morphology and cell proliferation? Podocytes deficient in α3β1 integrin appear unable to assemble mature foot processes, and form instead, flattened cytoplasmic projections from the podocyte cell body to the GBM (Kreidberg *et al.*, 1996). The lack of formation of mature foot processes in α3β1-integrin–deficient podocytes suggests that signals transduced by this integrin are essential for triggering the cytoskeletal rearrangements required to assemble and maintain foot process structure (Wang *et al.*, 1999). α3β1 is normally localized in FSGS and other glomerular diseases in which podocytes are extensively flattened, suggesting that α3β1 integrin constitutes stable, static bonds between podocytes and the GBM. Studies have shown that podocytes α3β1 associates on its cytoplasmic side with paxilin, talin, and vinculin (Drenckhahn and Franke, 1988), which mediate its connection to the actin cytoskeleton. It has been demonstrated that integrin linked kinase monitors and influences the state of activity of the α3β1 integrin and serves a signaling function (Kretzler *et al.*, 2001)**.**

As α3β1 deficient podocytes appear to remain adherent to the basement membrane along their entire length of contact, the concept that integrins are simple adhesion receptors is oversimplified. Instead, it may be more appropriate to consider integrins as receptors transducing signals on contact with the ECM that elicit specific responses such as adhesion, migration, filopodial extension and, in the case of podocytes, foot processes assembly. Importantly, all of these responses involve cytoskeletal rearrangement, and there is an emerging understanding of how integrin-ECM interactions affect cytoskeletal assembly.

ILK deletion has a diverse array of effects via interactions with several molecules important for normal functioning of the podocytes.

5.6. <u>Kinase activity of ILK</u>

ILK was described in 1995 as a Ser/Thr kinase that binds to the cytoplasmic tails of β1, β2 and β3- integrin subunits (Dedhar *et al.*, 1999). It was suggested that ILK activation might be crucial for the stimulation of various integrin signalling pathways. ILK was shown to induce phosphorylation of the protein kinase PKB/Akt and GSK-3β in cells overexpressing ILK (Delcommenne *et al.*, 1998). PKB/Akt is a Ser/Thr kinase implicated in cell proliferation, survival and growth factor signaling. GSK-3β is a negative regulator of Wnt signaling that is inactivated by phosphorylation mediated by Wnt signals (Cohen and Frame, 2001) or ILK. This inactivation leads to the stabilization and elevation of β-catenin levels and translocation into the nucleus, where β-catenin interacts with Lef-1/Tcf, leading to the activation of gene expression including cyclin D1 and c-myc. In the present study, immunohistochemial staining of kidney sections with an anti-GSK-3β reveals no difference in the GSK-3β expression in podoILK -/- mice as compared to wild type controls (data not shown). This observation is further supported by another study performed by Grashoff et al. A condrocyte-specific deletion *in vivo* of ILK in mice did not affect the phosphorylation levels of PKB/Akt and GSK-3β (Sakai *et al.*, 2003). In addition to this, isolated macrophages from the ILK knockout mice showed not only specific inhibition of PKB/Akt on serine 473 phosphorylation and a down regulation of cyclin D1 expression, but also showed inhibition of GSK-3β phosphorylation by the ILK-PKB/Akt pathway (Troussard *et al.*, 2003).

In addition to its signaling properties as a kinase in the regulation of PKB/Akt, GSK-3 β and cyclin D1, ILK also functions as an adaptor protein in coupling integrins to the actin cytoskeleton. In our study only the kinase domain was deleted while, the adaptor domain of ILK was left intact. Despite the presence of the adaptor sequence a down regulation of proteins of the actin cytoskeleton such as α-actinin 4 was found in the current study. It known that ILK can interact with paxilin at the kinase domain and this interaction may be responsible for the localisation of ILK to the focal adhesion plaques (Wu and Dedhar, 2001). Recent genetic data from Drosophila and C. elegans (Zervas *et al.*, 2001) provide strong support for an essential role for ILK in the regulation of cell adhesion and spreading. The observations from the present study reveals that ILK deletion in podocytes leads to a defect in their attachment to the GBM providing further support for an essential role of ILK in the regulation of cell attachment and spreading on extracellular matrix. The disorganization of the foot processes in the podoILK -/- mice may be a reflection of these altered cell attachment and spreading properties. Despite of this fact, flies as well as worms expressing an inactive kinase ILK gene are normal, suggesting no role of the

kinase activity of ILK in these systems (Zervas *et al.*, 2001). As mentioned above, the activation of cyclins and cyclin-dependent kinases (cdc), the reduction of E-cadherin expression, stabilisation of β-catenin, and the formation of Lef-1/Tcf- β-catenin complexes are dependant on ILK expression, in our study we did not examine the expression of these genes if they are affected after ILK deletion in podocyte or not. An explanation of the phenotype that we observed could be due to an alteration of the gene expression. Recent biochemical studies *in vitro* are consistent with ILK being rather an adaptor than a kinase and may help to recruit a kinase into a multiprotein complex that phosphorylates PKB/Akt on Ser 473 (Lynch *et al.*, 1999; Hill *et al.*, 2002). However, this issue remains controversial in the field.

5.7. <u>Overexpressionfailure of ILK</u>

ILK has been shown to be involved in the regulation of a number of integrin-mediated processes that include cell adhesion, cell shape changes, gene expression, and ECM deposition (Wu *et al.*, 1998a). Recent studies have implicated ILK dysregulation in the development of several chronic glomerular diseases. For instance, using an unbiased mRNA expression screening approach, ILK was identified as a candidate downstream effector in proteinuria in patients with congenital nephritic syndrome (Kretzler *et al.*, 2001). Overexpression of ILK is also observed in glomerular podocytes in two murine proteinuria models (Wanke *et al.*, 1992; Schadde *et al.*, 2000). Such alteration in ILK abundance is associated with progressive FSGS (Kretzler *et al.*, 2001). Our aim was to confirm this finding by *in vivo* overexpression of ILK in mice, and if its overexpression can primarily lead to induction of renal disease.

In order to test the influence of ILK overexpression on kidney function *in vivo*, a similar strategy as used for podocyte-specific ILK deletion was adopted. To address this issue, a construct with the podocin promoter was employed for which only an expression of LacZ cassette in podocyte was demonstrated (Moeller *et al.*, 2003). This construct was modified such that podocin promoter and the ILK gene were coupled to the EGF gene. The construct so obtained was then microinjected in mice to generate a line overexpressing the ILK gene. 3 mice lines which revealing genomic integration of ILK were analysed of which one line expressed ILK mRNA at higher levels as compared to controls (data not shown). However, it was not possible to detect the GFP-tagged ILK protein by western blot in kidney lysates or by immunofluoerscence in tissue sections. This mouse line also failed to show any features of a renal disease phenotype throughout its lifespan. The failure of this mouse line to show any disease phenotype could be attributed to several factors that influence whether a promoter/transgene construct will express (produce the

appropriate mRNA and protein) in transgenic mice. The promoters that are used must be known to function appropriately *in vivo* (*in vitro* function does not always guarantee this). A possibility that transgene constructs may have accumulated mutations during cloning (especially if PCR was involved) cannot be ignored. Perhaps the most important consideration has to do with the trangene's insertion site in the mouse genome. At many chromosomal locations, transgenes may be transcriptionally silent. At others they may express, but with a tissue- and temporal specificity that is not identical to what has previously been seen with the same promoter construct. The intrinsic ability of a promoter construct to drive transgene expression reliably and with faithful tissue specificity also varies from promoter to promoter, for reasons that are not well understood. One of the most critical steps in making transgenic mice is preparing the DNA for microinjection. Poorly prepared DNA can be toxic to the ovum and contaminants can clog the injection needle, which typically have inside diameters of 0.5 microns at the tip.

It would be interesting to show, that both loss of function and gain of function mutations in integrin linked kinase lead to glomerular disease, and further studies following this strategy are underway.

Summary

6. <u>Summary</u>

For many years the attention of researchers was focused on the glomerular besement membrane (GBM) or extraglomerular factors being responsible for increased glomerular permeability. However, recent evidence suggests that the primary defect might be at the level of the podocyte, the glomerular visceral epithelial cell. Glomerular podocyte function is essential for the maintenance of the glomerular filtration barrier. Podocytes injury leads to a cascade of events starting from detachment from the GBM, and hence denuded GBM leading to misdirected filtration of protein. Injury to the podocyte can occur in many immune and non-immune renal diseases. Podocyte injury or structural inherited defects are increasingly implicated in the occurrence of glomerular proteinuria. In this light it is believed that alterations in podocyte cell-cell and cell-matrix contacts are key events in progressive glomerular failure. Integrin-linked kinase (ILK) has been found to be a key molecule that may play a role in alteration of podocyte structure and function. Thus it was hypothesized that lack of ILK would lead to disruption of podocyte cell matrix interaction and thus compromised renal function. However, as ILK deletion results in early embryonic lethality, podocyte specific ILK knock-outs had to be generated to evaluate ILK function *in vivo*. Crossing of 2.5P-Cre mice, expressing Cre-recombinase under the control of podocin promoter in a podocyte specific manner, with ILK-floxed mice resulted in kidney specific ILK inactivation. ILK loss was confirmed by subsequent loss of podocyte ILK staining in bitransgenic mice homozygous for the floxed ILK allele (podoILK -/-). PodoILK -/- mice were found to appear normal at birth, but developed progressive filtration barrier failure and died while suffering from terminal renal failure at a mean age of 19 weeks. Kidneys from these mice revealed a classic progressive focal segmental glomerulosclerosis. The first ultrastructural lesion seen at onset of albuminuria was a 23% GBM diameter increase in orthogonal intercepts, resulting in a broadened and split GBM, while foot processes architecture and slit diaphragms remained intact. However, no significant reduction in the mRNA or protein levels of slit-membrane molecules (podocin and nephrin), key GBM components (fibronectin, laminins and collagen IV isoforms) or podocyte matrix receptors (α3-/β1-integrine and dystroglycan) could be demonstrated at onset of albuminuria. α3-Integrins were found in granular pattern along the GBM, consistent with altered integrin function podoILK -/- mice.

In conclusion, podocyte specific ILK deletion resulted in a striking GBM phenotype followed by progressive glomerulosclerosis. As the key components of the GBM are expressed at comparable levels to controls, an alteration in matrix assembly subsequent to ILK deletion appears to be an attractive hypothesis for the phenotype observed. Further podocyte-specific ILK-deletion in mice led to cytoskeletal disruptions and alterations in podocyte cell-cell and cell-matrix contacts that are key events in progressive glomerular failure.

Zusammenfassung

7. <u>Zusammenfassung</u>

Die glomeruläre Filtrationseinheit ist die entscheidende Struktur um ein Protein-freies Ultrafiltrat zu generieren. Zytoskeletale Störungen und Veränderungen in Podozyten Zell-Zell- und Zell-Matrix-Kontakten spielen eine Schlüsselrolle bei der Entwicklung progressiver glomerulärer Alterationen, die zum Nierenversagen führen. Integrin-linked kinase (ILK) ist mit $\alpha3/\beta1$ Integrinen assoziiert und in die Podozyten-Zell-Matrix-Interaktion involviert. ILK ist bei Patienten und in Mausmodellen mit schwerer Proteinuria induziert. Um die funktionelle Rolle der ILK zu evaluieren, wurde eine Podozyten spezifische ILK Knock-out Maus generiert.

Da die ILK Knock-out Mäuse früh embryonal lethal sind, wurde eine Mauslinie, die die Cre-Recombinase unter der Kontrolle des Podocin-Promoter exprimiert, mit einer ILK-floxed Mausline gekreuzt, um eine spezifische ILK-Deletion in Podozyten hervorzurufen. Die genomische Exzision der mit loxP-Erkennungsstellen für die Cre-Rekombinase flankierten („gefloxt") ILK-Sequenz wurde mittels PCR nachgewiesen und anschließend das Fehlen des ILK-Proteins in den Podozyten mittels Immunfluoreszenz bestätigt. Podocin Cre-ILK-loxP Mäuse wurden mit einen intakten Filtrationseinheit geboren. Im Alter von 3 Wochen fand sich bei podoILK -/- Mäusen eine selektive Albuminurie und eine geringgradige Vergrößerung von einzelnen Podozyten insbesondere der juxtamedullären Glomerula im Vergleich zu Wildtyp-Mäusen. Morphometrische Analysen konnten eine signifikante Verbreitung der glomerulären Basalmembran nachweisen. Die glomerulären Veränderungen von podoILK -/- Mäusen umfassten eine Vergrößerung von Podozyten, segmentale Mesangiumexpansionen mit Matrixvermehrung und Kapillardilatation sowie Podozyten-Retraktion. In der achten Lebenswochen zeigen die Tiere eine massive Proteinuria, eine fokal-segmentale Glomerulosklerose und eine tubulär-interstitial Fibrose zusammen mit laborchemischen Parametern des terminalen Nierenversagens. Molekularen Analysen wiesen eine Reduktion der Kollagen IV $\alpha3$- 5 Ketten, sowie von Nephrin und WT-1 mRNA Spiegeln nach. Integrin $\alpha3$ zeigt bei unveränderten Proteinspiegeln eine Relokalization innerhalb der Podozyten. In der Phase des progressiven Nierenversagens konnte eine Überexpression der Matrix-Molekülen, z.B. Fibronektin, nachgewiesen werden. Diese Daten weisen auf eine Schlüsselrolle der ILK für die Podozyten – GBM Interaktion nach. Als möglicher Mechanism ist hierbei ein Defekt im integrinabhängigen Matrixaufbau zu diskutieren.

Literature

8. <u>Literature</u>

Akhtar, M., and Al Mana, H. (2004). Molecular basis of proteinuria. Adv Anat Pathol *11*, 304-309.

Andrews, P.M. (1981). Investigations of cytoplasmic contractile and cytoskeletal elements in the kidney glomerulus. Kidney Int *20*, 549-562.

Antignac, C. (1995). Molecular genetics of basement membranes: the paradigm of Alport syndrome. Kidney Int Suppl *49*, S29-33.

Asanuma, K., Kim, K., Oh, J., Giardino, L., Chabanis, S., Faul, C., Reiser, J., and Mundel, P. (2005). Synaptopodin regulates the actin-bundling activity of alpha-actinin in an isoform-specific manner. J Clin Invest *115*, 1188-1198.

Attwell, S., Mills, J., Troussard, A., Wu, C., and Dedhar, S. (2003). Integration of cell attachment, cytoskeletal localization, and signaling by integrin-linked kinase (ILK), CH-ILKBP, and the tumor suppressor PTEN. Mol Biol Cell *14*, 4813-4825.

Attwell, S., Roskelley, C., and Dedhar, S. (2000). The integrin-linked kinase (ILK) suppresses anoikis. Oncogene *19*, 3811-3815.

Barisoni, L., Kriz, W., Mundel, P., and D'Agati, V. (1999). The dysregulated podocyte phenotype: a novel concept in the pathogenesis of collapsing idiopathic focal segmental glomerulosclerosis and HIV-associated nephropathy. J Am Soc Nephrol *10*, 51-61.

Barisoni, L., and Mundel, P. (2003). Podocyte biology and the emerging understanding of podocyte diseases. Am J Nephrol *23*, 353-360.

Barker, D.F., Hostikka, S.L., Zhou, J., Chow, L.T., Oliphant, A.R., Gerken, S.C., Gregory, M.C., Skolnick, M.H., Atkin, C.L., and Tryggvason, K. (1990). Identification of mutations in the COL4A5 collagen gene in Alport syndrome. Science *248*, 1224-1227.

Borza, D.B., Bondar, O., Todd, P., Sundaramoorthy, M., Sado, Y., Ninomiya, Y., and Hudson, B.G. (2002). Quaternary organization of the goodpasture autoantigen, the alpha 3(IV) collagen chain. Sequestration of two cryptic autoepitopes by intrapromoter interactions with the alpha4 and alpha5 NC1 domains. J Biol Chem *277*, 40075-40083.

Boutaud, A., Borza, D.B., Bondar, O., Gunwar, S., Netzer, K.O., Singh, N., Ninomiya, Y., Sado, Y., Noelken, M.E., and Hudson, B.G. (2000). Type IV collagen of the glomerular basement membrane. Evidence that the chain specificity of network assembly is encoded by the noncollagenous NC1 domains. J Biol Chem *275*, 30716-30724.

Boute, N., Gribouval, O., Roselli, S., Benessy, F., Lee, H., Fuchshuber, A., Dahan, K., Gubler, M.C., Niaudet, P., and Antignac, C. (2000). NPHS2, encoding the glomerular protein podocin, is mutated in autosomal recessive steroid-resistant nephrotic syndrome. Nat Genet *24*, 349-354.

Braden, G.L., Mulhern, J.G., O'Shea, M.H., Nash, S.V., Ucci, A.A., Jr., and Germain, M.J.

(2000). Changing incidence of glomerular diseases in adults. Am J Kidney Dis *35*, 878-883.

Brakebusch, C., Bouvard, D., Stanchi, F., Sakai, T., and Fassler, R. (2002). Integrins in invasive growth. J Clin Invest *109*, 999-1006.

Bravou, V., Klironomos, G., Papadaki, E., Stefanou, D., and Varakis, J. (2003). Integrin-linked kinase (ILK) expression in human colon cancer. Br J Cancer *89*, 2340-2341.

Brinster, R.L., and Palmiter, R.D. (1984). Introduction of genes into the germ line of animals. Harvey Lect *80*, 1-38.

Buchholz, F., Angrand, P.O., and Stewart, A.F. (1998). Improved properties of FLP recombinase evolved by cycling mutagenesis. Nat Biotechnol *16*, 657-662.

Ciani, L., Patel, A., Allen, N.D., and ffrench-Constant, C. (2003). Mice lacking the giant protocadherin mFAT1 exhibit renal slit junction abnormalities and a partially penetrant cyclopia and anophthalmia phenotype. Mol Cell Biol *23*, 3575-3582.

Cohen, P., and Frame, S. (2001). The renaissance of GSK3. Nat Rev Mol Cell Biol *2*, 769-776.

Cosgrove, D., Meehan, D.T., Grunkemeyer, J.A., Kornak, J.M., Sayers, R., Hunter, W.J., and Samuelson, G.C. (1996). Collagen COL4A3 knockout: a mouse model for autosomal Alport syndrome. Genes Dev *10*, 2981-2992.

Cuthbertson, R.A., and Klintworth, G.K. (1988). Transgenic mice--a gold mine for furthering knowledge in pathobiology. Lab Invest *58*, 484-502.

Dai, D.L., Makretsov, N., Campos, E.I., Huang, C., Zhou, Y., Huntsman, D., Martinka, M., and Li, G. (2003). Increased expression of integrin-linked kinase is correlated with melanoma progression and poor patient survival. Clin Cancer Res *9*, 4409-4414.

Dawid, I.B., Breen, J.J., and Toyama, R. (1998). LIM domains: multiple roles as adapters and functional modifiers in protein interactions. Trends Genet *14*, 156-162.

Dedhar, S., Jewell, K., Rojiani, M., and Gray, V. (1992). The receptor for the basement membrane glycoprotein entactin is the integrin alpha 3/beta 1. J Biol Chem *267*, 18908-18914.

Dedhar, S., Williams, B., and Hannigan, G. (1999). Integrin-linked kinase (ILK): a regulator of integrin and growth-factor signalling. Trends Cell Biol *9*, 319-323.

Delcommenne, M., Tan, C., Gray, V., Rue, L., Woodgett, J., and Dedhar, S. (1998). Phosphoinositide-3-OH kinase-dependent regulation of glycogen synthase kinase 3 and protein kinase B/AKT by the integrin-linked kinase. Proc Natl Acad Sci U S A *95*, 11211-11216.

Delwel, G.O., de Melker, A.A., Hogervorst, F., Jaspars, L.H., Fles, D.L., Kuikman, I., Lindblom, A., Paulsson, M., Timpl, R., and Sonnenberg, A. (1994). Distinct and overlapping ligand specificities of the alpha 3A beta 1 and alpha 6A beta 1 integrins: recognition of laminin isoforms. Mol Biol Cell *5*, 203-215.

Deng, J.T., Van Lierop, J.E., Sutherland, C., and Walsh, M.P. (2001). Ca2+-independent smooth muscle contraction. a novel function for integrin-linked kinase. J Biol Chem *276*, 16365-16373.

Denny, P., and Justice, M.J. (2000). Mouse as the measure of man? Trends Genet *16*, 283-287.

Donoviel, D.B., Freed, D.D., Vogel, H., Potter, D.G., Hawkins, E., Barrish, J.P., Mathur, B.N., Turner, C.A., Geske, R., Montgomery, C.A., Starbuck, M., Brandt, M., Gupta, A., Ramirez-Solis, R., Zambrowicz, B.P., and Powell, D.R. (2001). Proteinuria and perinatal lethality in mice lacking NEPH1, a novel protein with homology to NEPHRIN. Mol Cell Biol *21*, 4829-4836.

Drenckhahn, D., and Franke, R.P. (1988). Ultrastructural organization of contractile and cytoskeletal proteins in glomerular podocytes of chicken, rat, and man. Lab Invest *59*, 673-682.

Dymecki, S.M. (1996). Flp recombinase promotes site-specific DNA recombination in embryonic stem cells and transgenic mice. Proc Natl Acad Sci U S A *93*, 6191-6196.

Eddy, A.A., and Schnaper, H.W. (1998). The nephrotic syndrome: from the simple to the complex. Semin Nephrol *18*, 304-316.

Elices, M.J., Urry, L.A., and Hemler, M.E. (1991). Receptor functions for the integrin VLA-3: fibronectin, collagen, and laminin binding are differentially influenced by Arg-Gly-Asp peptide and by divalent cations. J Cell Biol *112*, 169-181.

Endlich, K., Kriz, W., and Witzgall, R. (2001). Update in podocyte biology. Curr Opin Nephrol Hypertens *10*, 331-340.

Friedrich, E.B., Liu, E., Sinha, S., Cook, S., Milstone, D.S., MacRae, C.A., Mariotti, M., Kuhlencordt, P.J., Force, T., Rosenzweig, A., St-Arnaud, R., Dedhar, S., and Gerszten, R.E. (2004). Integrin-linked kinase regulates endothelial cell survival and vascular development. Mol Cell Biol *24*, 8134-8144.

Gassmann, M., and Hennet, T. (1998). From Genetically Altered Mice to Integrative Physiology. News Physiol Sci *13*, 53-57.

Geiger, B., Bershadsky, A., Pankov, R., and Yamada, K.M. (2001). Transmembrane crosstalk between the extracellular matrix--cytoskeleton crosstalk. Nat Rev Mol Cell Biol *2*, 793-805.

Ghiggeri, G.M., Carraro, M., and Vincenti, F. (2004). Recurrent focal glomerulosclerosis in the era of genetics of podocyte proteins: theory and therapy. Nephrol Dial Transplant *19*, 1036-1040.

Graff, J.R., Deddens, J.A., Konicek, B.W., Colligan, B.M., Hurst, B.M., Carter, H.W., and Carter, J.H. (2001). Integrin-linked kinase expression increases with prostate tumor grade. Clin Cancer Res *7*, 1987-1991.

Gubler, M.C., Antignac, C., Deschenes, G., Knebelmann, B., Hors-Cayla, M.C., Grunfeld, J.P., Broyer, M., and Habib, R. (1993). Genetic, clinical, and morphologic heterogeneity in Alport's syndrome. Adv Nephrol Necker Hosp *22*, 15-35.

Gundersen, H.J., and Osterby, R. (1977). Glomerular size and structure in diabetes mellitus. II. Late abnormalities. Diabetologia *13*, 43-48.

Guo, L., and Wu, C. (2002). Regulation of fibronectin matrix deposition and cell proliferation by the PINCH-ILK-CH-ILKBP complex. Faseb J *16*, 1298-1300.

Haltia, A., Solin, M., Luimula, P., Kretzler, M., and Holthofer, H. (1999). mRNA differential

display analysis of nephrotic kidney glomeruli. Exp Nephrol *7*, 52-58.

Hammes, A., Guo, J.K., Lutsch, G., Leheste, J.R., Landrock, D., Ziegler, U., Gubler, M.C., and Schedl, A. (2001). Two splice variants of the Wilms' tumor 1 gene have distinct functions during sex determination and nephron formation. Cell *106*, 319-329.

Hanks, S.K., and Quinn, A.M. (1991). Protein kinase catalytic domain sequence database: identification of conserved features of primary structure and classification of family members. Methods Enzymol *200*, 38-62.

Haslam, R.J., Koide, H.B., and Hemmings, B.A. (1993). Pleckstrin domain homology. Nature *363*, 309-310.

Hill, M.M., Feng, J., and Hemmings, B.A. (2002). Identification of a plasma membrane Raft-associated PKB Ser473 kinase activity that is distinct from ILK and PDK1. Curr Biol *12*, 1251-1255.

Hoess, R., Abremski, K., Irwin, S., Kendall, M., and Mack, A. (1990). DNA specificity of the Cre recombinase resides in the 25 kDa carboxyl domain of the protein. J Mol Biol *216*, 873-882.

Hudson, B.G. (2004). The molecular basis of Goodpasture and Alport syndromes: beacons for the discovery of the collagen IV family. J Am Soc Nephrol *15*, 2514-2527.

Hudson, B.G., Reeders, S.T., and Tryggvason, K. (1993). Type IV collagen: structure, gene organization, and role in human diseases. Molecular basis of Goodpasture and Alport syndromes and diffuse leiomyomatosis. J Biol Chem *268*, 26033-26036.

Huttunen, N.P. (1976). Congenital nephrotic syndrome of Finnish type. Study of 75 patients. Arch Dis Child *51*, 344-348.

Hynes, R.O. (1992). Integrins: versatility, modulation, and signaling in cell adhesion. Cell *69*, 11-25.

Ingber, D.E., Dike, L., Hansen, L., Karp, S., Liley, H., Maniotis, A., McNamee, H., Mooney, D., Plopper, G., Sims, J., and et al. (1994). Cellular tensegrity: exploring how mechanical changes in the cytoskeleton regulate cell growth, migration, and tissue pattern during morphogenesis. Int Rev Cytol *150*, 173-224.

Juliano, R.L. (1994). Integrin signals and tumor growth control. Princess Takamatsu Symp *24*, 118-124.

Kalluri, R., Shield, C.F., Todd, P., Hudson, B.G., and Neilson, E.G. (1997). Isoform switching of type IV collagen is developmentally arrested in X-linked Alport syndrome leading to increased susceptibility of renal basement membranes to endoproteolysis. J Clin Invest *99*, 2470-2478.

Kaplan, J.M., Kim, S.H., North, K.N., Rennke, H., Correia, L.A., Tong, H.Q., Mathis, B.J., Rodriguez-Perez, J.C., Allen, P.G., Beggs, A.H., and Pollak, M.R. (2000). Mutations in ACTN4, encoding alpha-actinin-4, cause familial focal segmental glomerulosclerosis. Nat Genet *24*, 251-256.

Kashtan, C.E., Kleppel, M.M., Butkowski, R.J., Michael, A.F., and Fish, A.J. (1990). Alport syndrome, basement membranes and collagen. Pediatr Nephrol *4*, 523-532.

Kawachi, H., Koike, H., Kurihara, H., Yaoita, E., Orikasa, M., Shia, M.A., Sakai, T., Yamamoto, T., Salant, D.J., and Shimizu, F. (2000). Cloning of rat nephrin: expression in developing glomeruli and in proteinuric states. Kidney Int *57*, 1949-1961.

Kawachi, H., Kurihara, H., Topham, P.S., Brown, D., Shia, M.A., Orikasa, M., Shimizu, F., and Salant, D.J. (1997). Slit diaphragm-reactive nephritogenic MAb 5-1-6 alters expression of ZO-1 in rat podocytes. Am J Physiol *273*, F984-993.

Kerjaschki, D. (2001). Caught flat-footed: podocyte damage and the molecular bases of focal glomerulosclerosis. J Clin Invest *108*, 1583-1587.

Kerjaschki, D., Ojha, P.P., Susani, M., Horvat, R., Binder, S., Hovorka, A., Hillemanns, P., and Pytela, R. (1989). A beta 1-integrin receptor for fibronectin in human kidney glomeruli. Am J Pathol *134*, 481-489.

Kestila, M., Lenkkeri, U., Mannikko, M., Lamerdin, J., McCready, P., Putaala, H., Ruotsalainen, V., Morita, T., Nissinen, M., Herva, R., Kashtan, C.E., Peltonen, L., Holmberg, C., Olsen, A., and Tryggvason, K. (1998). Positionally cloned gene for a novel glomerular protein--nephrin--is mutated in congenital nephrotic syndrome. Mol Cell *1*, 575-582.

Kierszenbaum, L.A. (2002). Histology and cell biology. Elsevier USA.

Kikkawa, Y., Sanzen, N., and Sekiguchi, K. (1998). Isolation and characterization of laminin-10/11 secreted by human lung carcinoma cells. laminin-10/11 mediates cell adhesion through integrin alpha3 beta1. J Biol Chem *273*, 15854-15859.

Kiss, E., Muranyi, A., Csortos, C., Gergely, P., Ito, M., Hartshorne, D.J., and Erdodi, F. (2002). Integrin-linked kinase phosphorylates the myosin phosphatase target subunit at the inhibitory site in platelet cytoskeleton. Biochem J *365*, 79-87.

Korhonen, M., Ylanne, J., Laitinen, L., and Virtanen, I. (1990). The alpha 1-alpha 6 subunits of integrins are characteristically expressed in distinct segments of developing and adult human nephron. J Cell Biol *111*, 1245-1254.

Kos, C.H., Le, T.C., Sinha, S., Henderson, J.M., Kim, S.H., Sugimoto, H., Kalluri, R., Gerszten, R.E., and Pollak, M.R. (2003). Mice deficient in alpha-actinin-4 have severe glomerular disease. J Clin Invest *111*, 1683-1690.

Kreidberg, J.A., Donovan, M.J., Goldstein, S.L., Rennke, H., Shepherd, K., Jones, R.C., and Jaenisch, R. (1996). Alpha 3 beta 1 integrin has a crucial role in kidney and lung organogenesis. Development *122*, 3537-3547.

Kretzler, M. (2002). Regulation of adhesive interaction between podocytes and glomerular basement membrane. Microsc Res Tech *57*, 247-253.

Kretzler, M., Teixeira, V.P., Unschuld, P.G., Cohen, C.D., Wanke, R., Edenhofer, I., Mundel, P., Schlondorff, D., and Holthofer, H. (2001). Integrin-linked kinase as a candidate downstream effector in proteinuria. Faseb J *15*, 1843-1845.

Kritz, H., Underwood, S.R., and Sinzinger, H. (1996a). Imaging of atherosclerosis (Part I). Wien Klin Wochenschr *108*, 87-97.

Kritz, H., Underwood, S.R., and Sinzinger, H. (1996b). Imaging of atherosclerosis (Part II). Wien

Klin Wochenschr *108*, 123-132.

Kwan, K.M. (2002). Conditional alleles in mice: practical considerations for tissue-specific knockouts. Genesis *32*, 49-62.

Lawlor, M.A., and Alessi, D.R. (2001). PKB/Akt: a key mediator of cell proliferation, survival and insulin responses? J Cell Sci *114*, 2903-2910.

Lemmink, H.H., Schroder, C.H., Monnens, L.A., and Smeets, H.J. (1997). The clinical spectrum of type IV collagen mutations. Hum Mutat *9*, 477-499.

Levidiotis, V., and Power, D.A. (2005). New insights into the molecular biology of the glomerular filtration barrier and associated disease. Nephrology (Carlton) *10*, 157-166.

Li, F., Liu, J., Mayne, R., and Wu, C. (1997). Identification and characterization of a mouse protein kinase that is highly homologous to human integrin-linked kinase. Biochim Biophys Acta *1358*, 215-220.

Li, F., Zhang, Y., and Wu, C. (1999). Integrin-linked kinase is localized to cell-matrix focal adhesions but not cell-cell adhesion sites and the focal adhesion localization of integrin-linked kinase is regulated by the PINCH-binding ANK repeats. J Cell Sci *112 (Pt 24)*, 4589-4599.

Lux, S.E., John, K.M., and Bennett, V. (1990). Analysis of cDNA for human erythrocyte ankyrin indicates a repeated structure with homology to tissue-differentiation and cell-cycle control proteins. Nature *344*, 36-42.

Ly, J., Alexander, M., and Quaggin, S.E. (2004). A podocentric view of nephrology. Curr Opin Nephrol Hypertens *13*, 299-305.

Lynch, D.K., Ellis, C.A., Edwards, P.A., and Hiles, I.D. (1999). Integrin-linked kinase regulates phosphorylation of serine 473 of protein kinase B by an indirect mechanism. Oncogene *18*, 8024-8032.

Mackinnon, A.C., Qadota, H., Norman, K.R., Moerman, D.G., and Williams, B.D. (2002). C. elegans PAT-4/ILK functions as an adaptor protein within integrin adhesion complexes. Curr Biol *12*, 787-797.

Malakoff, D. (2000). The rise of the mouse, biomedicine's model mammal. Science *288*, 248-253.

Martin, J., Steadman, R., Knowlden, J., Williams, J., and Davies, M. (1998). Differential regulation of matrix metalloproteinases and their inhibitors in human glomerular epithelial cells in vitro. J Am Soc Nephrol *9*, 1629-1637.

Mayer, B.J., Ren, R., Clark, K.L., and Baltimore, D. (1993). A putative modular domain present in diverse signaling proteins. Cell *73*, 629-630.

Miner, J.H. (1999). Renal basement membrane components. Kidney Int *56*, 2016-2024.

Miner, J.H., Patton, B.L., Lentz, S.I., Gilbert, D.J., Snider, W.D., Jenkins, N.A., Copeland, N.G., and Sanes, J.R. (1997). The laminin alpha chains: expression, developmental transitions, and chromosomal locations of alpha1-5, identification of heterotrimeric laminins 8-11, and cloning of a novel alpha3 isoform. J Cell Biol *137*, 685-701.

Miner, J.H., and Sanes, J.R. (1994). Collagen IV alpha 3, alpha 4, and alpha 5 chains in rodent basal laminae: sequence, distribution, association with laminins, and developmental switches. J Cell Biol *127*, 879-891.

Miner, J.H., and Sanes, J.R. (1996). Molecular and functional defects in kidneys of mice lacking collagen alpha 3(IV): implications for Alport syndrome. J Cell Biol *135*, 1403-1413.

Mochizuki, T., Lemmink, H.H., Mariyama, M., Antignac, C., Gubler, M.C., Pirson, Y., Verellen-Dumoulin, C., Chan, B., Schroder, C.H., Smeets, H.J., and et al. (1994). Identification of mutations in the alpha 3(IV) and alpha 4(IV) collagen genes in autosomal recessive Alport syndrome. Nat Genet *8*, 77-81.

Moeller, M.J., Sanden, S.K., Soofi, A., Wiggins, R.C., and Holzman, L.B. (2002). Two gene fragments that direct podocyte-specific expression in transgenic mice. J Am Soc Nephrol *13*, 1561-1567.

Moeller, M.J., Sanden, S.K., Soofi, A., Wiggins, R.C., and Holzman, L.B. (2003). Podocyte-specific expression of cre recombinase in transgenic mice. Genesis *35*, 39-42.

Mongroo, P.S., Johnstone, C.N., Naruszewicz, I., Leung-Hagesteijn, C., Sung, R.K., Carnio, L., Rustgi, A.K., and Hannigan, G.E. (2004). Beta-parvin inhibits integrin-linked kinase signaling and is downregulated in breast cancer. Oncogene *23*, 8959-8970.

Morimoto, A.M., Tomlinson, M.G., Nakatani, K., Bolen, J.B., Roth, R.A., and Herbst, R. (2000). The MMAC1 tumor suppressor phosphatase inhibits phospholipase C and integrin-linked kinase activity. Oncogene *19*, 200-209.

Mosher, D.F., Sottile, J., Wu, C., and McDonald, J.A. (1992). Assembly of extracellular matrix. Curr Opin Cell Biol *4*, 810-818.

Mundel, P. (1998). [Synaptopodin: an actin-associated protein of telencephalic dendrites and of podocytes in the kidney glomerulus]. Ann Anat *180*, 391-392.

Mundel, P., Gilbert, P., and Kriz, W. (1991). Podocytes in glomerulus of rat kidney express a characteristic 44 KD protein. J Histochem Cytochem *39*, 1047-1056.

Mundel, P., Heid, H.W., Mundel, T.M., Kruger, M., Reiser, J., and Kriz, W. (1997). Synaptopodin: an actin-associated protein in telencephalic dendrites and renal podocytes. J Cell Biol *139*, 193-204.

Mundel, P., and Kriz, W. (1995). Structure and function of podocytes: an update. Anat Embryol (Berl) *192*, 385-397.

Mundel, P., and Shankland, S.J. (1999). Glomerular podocytes and adhesive interaction with glomerular basement membrane. Exp Nephrol *7*, 160-166.

Mundel, P., and Shankland, S.J. (2002). Podocyte biology and response to injury. J Am Soc Nephrol *13*, 3005-3015.

Muranyi, A., MacDonald, J.A., Deng, J.T., Wilson, D.P., Haystead, T.A., Walsh, M.P., Erdodi, F., Kiss, E., Wu, Y., and Hartshorne, D.J. (2002). Phosphorylation of the myosin phosphatase target subunit by integrin-linked kinase. Biochem J *366*, 211-216.

Natoli, T.A., Liu, J., Eremina, V., Hodgens, K., Li, C., Hamano, Y., Mundel, P., Kalluri, R., Miner, J.H., Quaggin, S.E., and Kreidberg, J.A. (2002). A mutant form of the Wilms' tumor suppressor gene WT1 observed in Denys-Drash syndrome interferes with glomerular capillary development. J Am Soc Nephrol *13*, 2058-2067.

Ninomiya, Y., Kagawa, M., Iyama, K., Naito, I., Kishiro, Y., Seyer, J.M., Sugimoto, M., Oohashi, T., and Sado, Y. (1995). Differential expression of two basement membrane collagen genes, COL4A6 and COL4A5, demonstrated by immunofluorescence staining using peptide-specific monoclonal antibodies. J Cell Biol *130*, 1219-1229.

Noakes, P.G., Miner, J.H., Gautam, M., Cunningham, J.M., Sanes, J.R., and Merlie, J.P. (1995). The renal glomerulus of mice lacking s-laminin/laminin beta 2: nephrosis despite molecular compensation by laminin beta 1. Nat Genet *10*, 400-406.

Novak, A., Hsu, S.C., Leung-Hagesteijn, C., Radeva, G., Papkoff, J., Montesano, R., Roskelley, C., Grosschedl, R., and Dedhar, S. (1998). Cell adhesion and the integrin-linked kinase regulate the LEF-1 and beta-catenin signaling pathways. Proc Natl Acad Sci U S A *95*, 4374-4379.

Pankov, R., and Yamada, K.M. (2002). Fibronectin at a glance. J Cell Sci *115*, 3861-3863.

Patey, N., Halbwachs-Mecarelli, L., Droz, D., Lesavre, P., and Noel, L.H. (1994). Distribution of integrin subunits in normal human kidney. Cell Adhes Commun *2*, 159-167.

Pattaramalai, S., Skubitz, K.M., and Skubitz, A.P. (1996). A novel recognition site on laminin for the alpha 3 beta 1 integrin. Exp Cell Res *222*, 281-290.

Pelletier, J., Bruening, W., Kashtan, C.E., Mauer, S.M., Manivel, J.C., Striegel, J.E., Houghton, D.C., Junien, C., Habib, R., Fouser, L., and et al. (1991). Germline mutations in the Wilms' tumor suppressor gene are associated with abnormal urogenital development in Denys-Drash syndrome. Cell *67*, 437-447.

Persad, S., Attwell, S., Gray, V., Mawji, N., Deng, J.T., Leung, D., Yan, J., Sanghera, J., Walsh, M.P., and Dedhar, S. (2001). Regulation of protein kinase B/Akt-serine 473 phosphorylation by integrin-linked kinase: critical roles for kinase activity and amino acids arginine 211 and serine 343. J Biol Chem *276*, 27462-27469.

Pozzi, A., and Zent, R. (2003). Integrins: sensors of extracellular matrix and modulators of cell function. Nephron Exp Nephrol *94*, e77-84.

Raats, C.J., van den Born, J., Bakker, M.A., Oppers-Walgreen, B., Pisa, B.J., Dijkman, H.B., Assmann, K.J., and Berden, J.H. (2000). Expression of agrin, dystroglycan, and utrophin in normal renal tissue and in experimental glomerulopathies. Am J Pathol *156*, 1749-1765.

Radeva, G., Petrocelli, T., Behrend, E., Leung-Hagesteijn, C., Filmus, J., Slingerland, J., and Dedhar, S. (1997). Overexpression of the integrin-linked kinase promotes anchorage-independent cell cycle progression. J Biol Chem *272*, 13937-13944.

Rahilly, M.A., and Fleming, S. (1992). Differential expression of integrin alpha chains by renal epithelial cells. J Pathol *167*, 327-334.

Rearden, A. (1994). A new LIM protein containing an autoepitope homologous to "senescent cell antigen". Biochem Biophys Res Commun *201*, 1124-1131.

Reiser, J., Kriz, W., Kretzler, M., and Mundel, P. (2000a). The glomerular slit diaphragm is a modified adherens junction. J Am Soc Nephrol *11*, 1-8.

Reiser, J., Oh, J., Shirato, I., Asanuma, K., Hug, A., Mundel, T.M., Honey, K., Ishidoh, K., Kominami, E., Kreidberg, J.A., Tomino, Y., and Mundel, P. (2004). Podocyte migration during nephrotic syndrome requires a coordinated interplay between cathepsin L and alpha3 integrin. J Biol Chem *279*, 34827-34832.

Reiser, J., Pixley, F.J., Hug, A., Kriz, W., Smoyer, W.E., Stanley, E.R., and Mundel, P. (2000b). Regulation of mouse podocyte process dynamics by protein tyrosine phosphatases rapid communication. Kidney Int *57*, 2035-2042.

Reiser, J., von Gersdorff, G., Simons, M., Schwarz, K., Faul, C., Giardino, L., Heider, T., Loos, M., and Mundel, P. (2002). Novel concepts in understanding and management of glomerular proteinuria. Nephrol Dial Transplant *17*, 951-955.

Ryding, A.D., Sharp, M.G., and Mullins, J.J. (2001). Conditional transgenic technologies. J Endocrinol *171*, 1-14.

Sakai, T., Li, S., Docheva, D., Grashoff, C., Sakai, K., Kostka, G., Braun, A., Pfeifer, A., Yurchenco, P.D., and Fassler, R. (2003). Integrin-linked kinase (ILK) is required for polarizing the epiblast, cell adhesion, and controlling actin accumulation. Genes Dev *17*, 926-940.

Sasaki, T., Mann, K., Miner, J.H., Miosge, N., and Timpl, R. (2002). Domain IV of mouse laminin beta1 and beta2 chains. Eur J Biochem *269*, 431-442.

Schadde, E., Kretzler, M., Banas, B., Luckow, B., Assmann, K., and Schlondorff, D. (2000). Expression of chemokines and their receptors in nephrotoxic serum nephritis. Nephrol Dial Transplant *15*, 1046-1053.

Schnabel, E., Anderson, J.M., and Farquhar, M.G. (1990). The tight junction protein ZO-1 is concentrated along slit diaphragms of the glomerular epithelium. J Cell Biol *111*, 1255-1263.

Schuler, F., and Sorokin, L.M. (1995). Expression of laminin isoforms in mouse myogenic cells in vitro and in vivo. J Cell Sci *108 (Pt 12)*, 3795-3805.

Schwartz, M.A., Schaller, M.D., and Ginsberg, M.H. (1995). Integrins: emerging paradigms of signal transduction. Annu Rev Cell Dev Biol *11*, 549-599.

Seiler, M.W., Venkatachalam, M.A., and Cotran, R.S. (1975). Glomerular epithelium: structural alterations induced by polycations. Science *189*, 390-393.

Shih, N.Y., Li, J., Karpitskii, V., Nguyen, A., Dustin, M.L., Kanagawa, O., Miner, J.H., and Shaw, A.S. (1999). Congenital nephrotic syndrome in mice lacking CD2-associated protein. Science *286*, 312-315.

Shirato, I., Sakai, T., Kimura, K., Tomino, Y., and Kriz, W. (1996). Cytoskeletal changes in podocytes associated with foot process effacement in Masugi nephritis. Am J Pathol *148*, 1283-1296.

Smoyer, W.E., Mundel, P., Gupta, A., and Welsh, M.J. (1997). Podocyte alpha-actinin induction precedes foot process effacement in experimental nephrotic syndrome. Am J Physiol *273*, F150-

157.

Somlo, S., and Mundel, P. (2000). Getting a foothold in nephrotic syndrome. Nat Genet *24*, 333-335.

St John, P.L., and Abrahamson, D.R. (2001). Glomerular endothelial cells and podocytes jointly synthesize laminin-1 and -11 chains. Kidney Int *60*, 1037-1046.

Sternberg, N., Sauer, B., Hoess, R., and Abremski, K. (1986). Bacteriophage P1 cre gene and its regulatory region. Evidence for multiple promoters and for regulation by DNA methylation. J Mol Biol *187*, 197-212.

Tan, C., Costello, P., Sanghera, J., Dominguez, D., Baulida, J., de Herreros, A.G., and Dedhar, S. (2001). Inhibition of integrin linked kinase (ILK) suppresses beta-catenin-Lef/Tcf-dependent transcription and expression of the E-cadherin repressor, snail, in APC-/- human colon carcinoma cells. Oncogene *20*, 133-140.

Terpstra, L., Prud'homme, J., Arabian, A., Takeda, S., Karsenty, G., Dedhar, S., and St-Arnaud, R. (2003). Reduced chondrocyte proliferation and chondrodysplasia in mice lacking the integrin-linked kinase in chondrocytes. J Cell Biol *162*, 139-148.

Timpl, R., and Brown, J.C. (1996). Supramolecular assembly of basement membranes. Bioessays *18*, 123-132.

Tisher, C.C., Madsen, K.M., and Verlander, J.W. (1991). Structural adaptation of the collecting duct to acid-base disturbances. Contrib Nephrol *95*, 168-177.

Troussard, A.A., Mawji, N.M., Ong, C., Mui, A., St -Arnaud, R., and Dedhar, S. (2003). Conditional knock-out of integrin-linked kinase demonstrates an essential role in protein kinase B/Akt activation. J Biol Chem *278*, 22374-22378.

Tryggvason, K., and Wartiovaara, J. (2001). Molecular basis of glomerular permselectivity. Curr Opin Nephrol Hypertens *10*, 543-549.

Tryggvason, K., Zhou, J., Hostikka, S.L., and Shows, T.B. (1993). Molecular genetics of Alport syndrome. Kidney Int *43*, 38-44.

van der Weyden, L., Adams, D.J., and Bradley, A. (2002). Tools for targeted manipulation of the mouse genome. Physiol Genomics *11*, 133-164.

Van Vliet, A., Baelde, H.J., Vleming, L.J., de Heer, E., and Bruijn, J.A. (2001). Distribution of fibronectin isoforms in human renal disease. J Pathol *193*, 256-262.

Velling, T., Risteli, J., Wennerberg, K., Mosher, D.F., and Johansson, S. (2002). Polymerization of type I and III collagens is dependent on fibronectin and enhanced by integrins alpha 11beta 1 and alpha 2beta 1. J Biol Chem *277*, 37377-37381.

von Luttichau, I., Djafarzadeh, R., Henger, A., Cohen, C.D., Mojaat, A., Jochum, M., Ries, C., Nelson, P.J., and Kretzler, M. (2002). Identification of a signal transduction pathway that regulates MMP-9 mRNA expression in glomerular injury. Biol Chem *383*, 1271-1275.

Vouret-Craviari, V., Boulter, E., Grall, D., Matthews, C., and Van Obberghen-Schilling, E. (2004). ILK is required for the assembly of matrix-forming adhesions and capillary

morphogenesis in endothelial cells. J Cell Sci *117*, 4559-4569.

Wagenknecht, B., Gulbins, E., Lang, F., Dichgans, J., and Weller, M. (1997). Lipoxygenase inhibitors block CD95 ligand-mediated apoptosis of human. FEBS Lett *409*, 17-23.

Wang, Z., Symons, J.M., Goldstein, S.L., McDonald, A., Miner, J.H., and Kreidberg, J.A. (1999). (Alpha)3(beta)1 integrin regulates epithelial cytoskeletal organization. J Cell Sci *112 (Pt 17)*, 2925-2935.

Wanke, R., Wolf, E., Hermanns, W., Folger, S., Buchmuller, T., and Brem, G. (1992). The GH-transgenic mouse as an experimental model for growth research: clinical and pathological studies. Horm Res *37 Suppl 3*, 74-87.

Weibel, E.R., and Gomez, D.M. (1962). A principle for counting tissue structures on random sections. J Appl Physiol *17*, 343-348.

Whiteside, C.I., Cameron, R., Munk, S., and Levy, J. (1993). Podocytic cytoskeletal disaggregation and basement-membrane detachment in puromycin aminonucleoside nephrosis. Am J Pathol *142*, 1641-1653.

Wu, C., and Dedhar, S. (2001). Integrin-linked kinase (ILK) and its interactors: a new paradigm for the coupling of extracellular matrix to actin cytoskeleton and signaling complexes. J Cell Biol *155*, 505-510.

Wu, C., Keightley, S.Y., Leung-Hagesteijn, C., Radeva, G., Coppolino, M., Goicoechea, S., McDonald, J.A., and Dedhar, S. (1998a). Integrin-linked protein kinase regulates fibronectin matrix assembly, E-cadherin expression, and tumorigenicity. J Biol Chem *273*, 528-536.

Wu, C., Keightley, S.Y., Leung-Hagestein, C., Radeva, G., Coppolino, M., Goicoechea, S., McDonald, J.A., and Dedhar, S. (1998b). Integrin-linked protein kinase regulates fibronectin matrix assembly, E-cadherin expression, and tumorigenicity. JBC *273*, 528-536.

Yamaji, S., Suzuki, A., Sugiyama, Y., Koide, Y., Yoshida, M., Kanamori, H., Mohri, H., Ohno, S., and Ishigatsubo, Y. (2001). A novel integrin-linked kinase-binding protein, affixin, is involved in the early stage of cell-substrate interaction. J Cell Biol *153*, 1251-1264.

Yang, J.T., Rayburn, H., and Hynes, R.O. (1993). Embryonic mesodermal defects in alpha 5 integrin-deficient mice. Development *119*, 1093-1105.

Yoganathan, N., Yee, A., Zhang, Z., Leung, D., Yan, J., Fazli, L., Kojic, D.L., Costello, P.C., Jabali, M., Dedhar, S., and Sanghera, J. (2002). Integrin-linked kinase, a promising cancer therapeutic target: biochemical and biological properties. Pharmacol Ther *93*, 233-242.

Yuan, H., Takeuchi, E., and Salant, D.J. (2002a). Podocyte slit-diaphragm protein nephrin is linked to the actin cytoskeleton. Am J Physiol Renal Physiol *282*, F585-591.

Yuan, H., Takeuchi, E., Taylor, G.A., McLaughlin, M., Brown, D., and Salant, D.J. (2002b). Nephrin dissociates from actin, and its expression is reduced in early experimental membranous nephropathy. J Am Soc Nephrol *13*, 946-956.

Zervas, C.G., Gregory, S.L., and Brown, N.H. (2001). Drosophila integrin-linked kinase is required at sites of integrin adhesion to link the cytoskeleton to the plasma membrane. J Cell Biol

152, 1007-1018.

Zheng, K., Thorner, P.S., Marrano, P., Baumal, R., and McInnes, R.R. (1994). Canine X chromosome-linked hereditary nephritis: a genetic model for human X-linked hereditary nephritis resulting from a single base mutation in the gene encoding the alpha 5 chain of collagen type IV. Proc Natl Acad Sci U S A *91*, 3989-3993.

Acknowledgements

Acknowledgments

I am thankful to God for blessing me with ability to carry out my doctoral work. I am truly grateful to the graduierten collegue vasculaere biologie 437 for supporting this work. I would like to thank PD. Dr. Matthias Kretzler for providing the opportunity to work in the Department Klinische Biochemie, Klinikum Innenstadt, LMU, Munich and for his assistance during the thesis. I also thank PD. Dr. Angelika Böttger for providing me an opportunity, supporting me and for representing this work at the faculty. I would like to thank Prof. Detlef Schlöndorf who inspired me by his wealth of knowledge and in-depth understanding of the subject of research.

I thank Prof. Rüdiger Wanke for many dedicated discussions and timely suggestions as well as Dr. Nadja Herbach for her help and performing qualitative and quantitative histologic and electron microscopic analyses and immunohitochemistry. I am thankfull to Prof. Maria Pia Rastaldi and Prof. Jeff Miner for performing the immunofluorescense stainings.

I wish to thank Anne Henger, Simone Blattner and Anissa Boucherot for their co-operation during my research term during this project. I also wish to thank Ilka Eddenhofer for her assistance for animal care and to support me by routine analyses during this project. I also wish to thank Sandra Irrgang, Karin Fracht and Ingrid Bayer for their technical support.

I thank Javid Wani for being a good friend and well-wisher and for careful reading my thesis. I also thank Prashant S. Patole for critically reviewing the thesis and for his invaluable assistance. I extand my gratitude to Dr. Pankaj Goyal for his expert help in editing the thesis.

I am grateful to Bruno Luckow for extending a helping hand as a when needed in general laboratory procedures. Further, my colleagues at AG Klinische biochemie have been very helpful in the lab and providing a coherent work atmosphere.

Finally, I specially thank my mother for her love, encouragement and support without which I nothing of this would be possible.

Curriculum Vitae

Curriculum vitae

Personal details

Name: Chiraz El- Aouni

Sex: female

Date of birth: 09.05.1974 Sousse/ Tunisia

Nationality: Tunesian

Material status: single

Career profile

09.1979 – 07.1985   Primary School in Ben Guerdene, Tunesia

09.1985 – 06. 1992   Secondary School in Ben Guerdene, Tunesia

10.1993 – 09. 1994   German language course in Bremen, Germany

10.1994 – 07.2001   Biology study, University of Bremen, Germany

03. 2002 – 02. 2006   Ph.D. at the Medical Policlinic, Ludwig-Maximilians University, Munich, Germany, Dissertation: ILK deletion using transgenic mice.

Conferences attended and Poster presentations

1. Satellite symposium to the "World Congres of Nephrology" in Kloster Seon Germany, August 2003.

2. "Podocyte specific deletion of Integrin-linked kinase results in progressive glomerular filtration barrier failure". Adhesion meeting 2005, podosomes - invadopodia - focal adhesions, München, April 28 - 30, Deutschland (poster presentation).

3. "Podozyten-spezifische Deletion der Integrin-linked Kinase induziert ein progredientes glomeruläres Filtrationsversagen". 20 Juni 2005, Followsnight des Nephrologischen Forrums München (oral presentation), 1st price awarded from all competing candidates.

4. "Podozytenspezifische Deletion der Integrin-linked Kinase führt zum progredienten Verlust der glomerulären Filtrationsbarriere". 36. Kongress der Gesellschaft für Nephrologie / 38.

Jahrestagung der Deutschen Arbeitsgemeinschaft für Klinische Nephrologie, Saarbrücken, Deutschland (oral presentation).

5. "Glomerular podocyte specific deletion of integrin-linked-kinase results in severe Basement membrane alterations, progressive glomerulosclerosis and renal scaring". 2nd International Meeting on Epithelial-Mesenchymal Transition, EMT 2005 October 1-3, 2005, Vancouver, British Columbia, Canada (poster presentation).

6. "Podocyte specific deletion of Integrin-linked kinase results in severe glomerular basement membrane alterations and progressive glomerulosclerosis". Annual Meeting of the American Society of Nephrology, November 10, 2005, Philadelphia, USA.

Awards

1st Award Fellowsnight, Nephrologisches Forum Muenchen 2005

Publications

1. Does conventional cytogenetics detect the real frequency of 19q13 aberrations in benign thyroid lesions? A survey of 38 cases. Cancer Genet Cytogenet. 2003 Oct 1; 146(1):70-2.

Meiboom M, Belge G, Bol S, **El-Aouni C**, Schoenmakers EF, Bullerdiek J.

2. Podocyte-specific deletion of Integrin-linked kinase results in severe glomerular basement membrane alterations and progressive glomerulosclerosis. J Am Soc Nephrol. 2006 May; 17(5):1334-44. Epub 2006 Apr 12.

Chiraz El-Aouni, Nadja Herbach, Simone M. Blattner, Anna Henger, Maria P. Rastaldi, George Jarad, Jeffrey H. Miner, Marcus J. Moeller, Rene St-Arnaud, Shoukat Dedhar, Lawrence B. Holzman, Ruediger Wanke, and Matthias Kretzler.